AD-A112 104 TEXAS UNIV AT DALLAS RICHARDSON CENTER FOR QUANTUM E--ETC F/G 20/5
BLUE-GREEN LASER OUTPUT FROM N(+2) AND XEF.(U)
DEC 81 C B COLLINS N00014-77-C-0168
UNCLASSIFIED UTDCQE-ML-07 NL

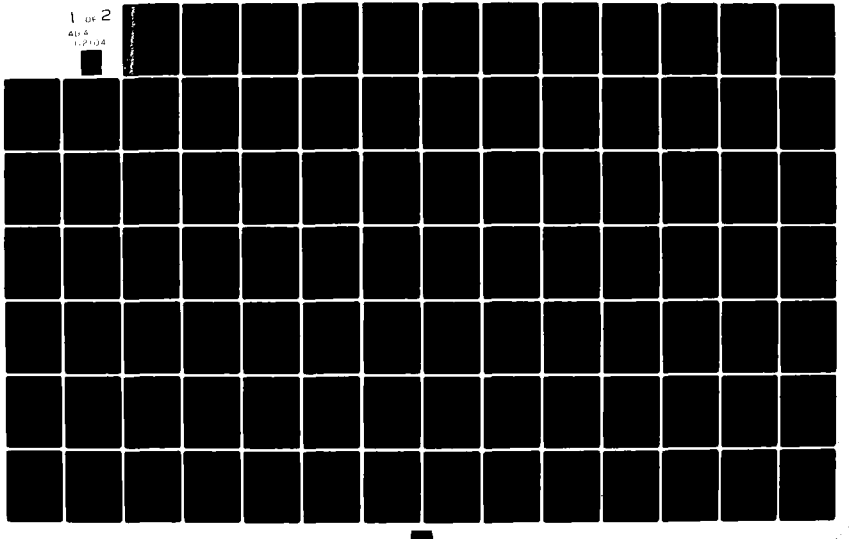

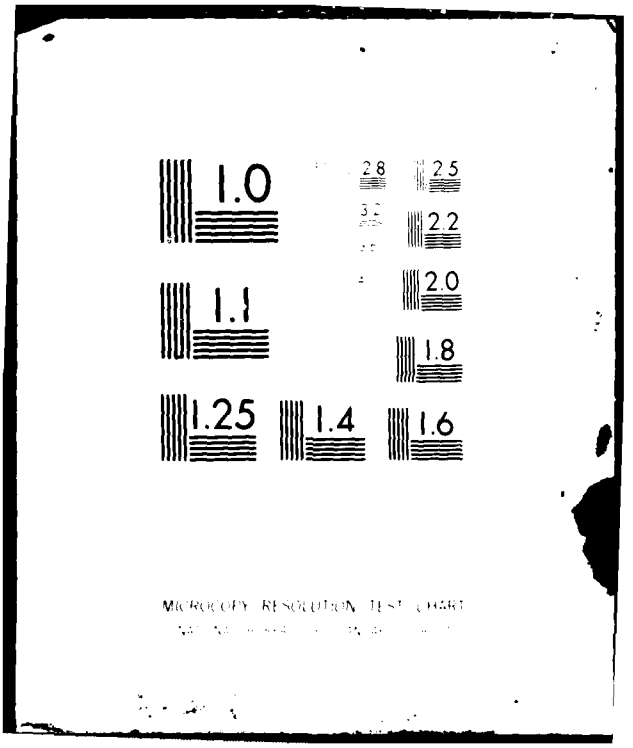
1.0
2.8
2.5
3.2
2.2
2.0
1.1
1.8
1.25
1.4
1.6
MICROCOPY RESOLUTION TEST CHART

(12)

BLUE-GREEN LASER OUTPUT from N_2^+ and XeF

by

C.B. COLLINS

Final Technical Report
UTDCQE-ISL-67
Prepared for
Office of Naval Research
Department of the Navy
December 1981

SECURITY CLASSIFICATION OF THIS PAGE (When Data Entered)

REPORT DOCUMENTATION PAGE	READ INSTRUCTIONS BEFORE COMPLETING FORM
1. REPORT NUMBER: UTDCQE ML-07	2. GOVT ACCESSION NO.: AD-A112 164
	3. RECIPIENT'S CATALOG NUMBER:
4. TITLE (and Subtitle): BLUE GREEN LASER OUTPUT FROM N_2^+ AND XeF	5. TYPE OF REPORT & PERIOD COVERED: Final 1/1/77 to 10/31/81
	6. PERFORMING ORG. REPORT NUMBER:
7. AUTHOR(s): C. B. Collins	8. CONTRACT OR GRANT NUMBER(s): N00014-77-C-0168
9. PERFORMING ORGANIZATION NAME AND ADDRESS: The University of Texas at Dallas, P.O. Box 688, Richardson, Texas 75080.	10. PROGRAM ELEMENT, PROJECT, TASK AREA & WORK UNIT NUMBERS: NR 395-601 421
11. CONTROLLING OFFICE NAME AND ADDRESS: Office of Naval Research, Physics Program Office, Arlington, VA 22217.	12. REPORT DATE: 12/30/81
	13. NUMBER OF PAGES: 170
14. MONITORING AGENCY NAME & ADDRESS(if different from Controlling Office)	15. SECURITY CLASS. (of this report): Unclassified
	15a. DECLASSIFICATION/DOWNGRADING SCHEDULE

16. DISTRIBUTION STATEMENT (of this Report)

Approved for public release; distribution unlimited.

17. DISTRIBUTION STATEMENT (of the abstract entered in Block 20, if different from Report)

18. SUPPLEMENTARY NOTES

19. KEY WORDS (Continue on reverse side if necessary and identify by block number)

Blue-green laser
Charge transfer laser
Helium nitrogen laser

20. ABSTRACT (Continue on reverse side if necessary and identify by block number)

The objective of this work was to determine the feasibility of developing, first the helium nitrogen charge transfer laser, and later the XeF laser into efficient scalable devices excited by preionized discharges for the production of blue-green outputs. The performance and scalability of the N_2^+ laser pumped by charge transfer from He_2^+ was determined in such a discharge environment. The gain and saturation

cont. next pg.

DD FORM 1 JAN 73 1473 EDITION OF 1 NOV 65 IS OBSOLETE

SECURITY CLASSIFICATION OF THIS PAGE (When Data Entered)

..Cont..

parameters were measured and a regenerative amplifier capable of operation at 470.9 nm was constructed. A traveling wave device was built which at 427 nm produced peak powers of 5 MW in the forward direction and which had a front-to-back ratio of 10,000 to 1 for the pulse energies. Efforts were made to apply that technology to the problem of switching the output from a XeF laser into the C→A transition at 480 nm. Gain and saturation parameters were examined and it was found that the relative gains between the stronger UV transition and the blue-green transition were greater than 30 to 1. These results implied that the blue-green transition of XeF was too weak to support the development of any practical device pumped by a preionized discharge.

ON THE COVER IS A COMPUTER RECONSTRUCTION OF THE SPECTRUM OF THE BLUE-GREEN OUTPUT FROM THE HELIUM NITROGEN LASER AT 470.9 NM.

On the scale of this representation the full width of the cover is equivalent to 0.1 nm.

Approved for public release; distribution unlimited.

FINAL TECHNICAL REPORT[†,††]

BLUE-GREEN LASER OUTPUT FROM N_2^+ AND XeF

Item A002

Period Ending: 31 October 1981

Contract Number N00014-77-C-0168

Principal Investigator: Carl B. Collins
Center for Quantum Electronics
The University of Texas at Dallas
P.O. Box 688
Richardson, Texas 75080
(214) 690-2863

Contractor: The University of Texas at Dallas
P.O. Box 688
Richardson, Texas 75080

Scientific Officer: Director, Physics Programs
Physical Sciences Division
Office of Naval Research
Department of the Navy
800 N. Quincy Street
Arlington, Virginia 22217

Effective Date of Contract: 1 January 1977

Expiration Date of Contract: 31 October 1981

Amount of Contract: $285,000

Sponsored by
Office of Naval Research

[†]The views and conclusions contained in this document are those of the authors and should not be interpreted as necessarily representing the official policies, either expressed or implied, of the Office of Naval Research or of any agency of the U.S. Government.

CONTENTS

TECHNICAL REPORT SUMMARY

This final report describes activities undertaken within the general program for the development of an efficient, scalable blue-green laser excited by a fast pulsed electrical discharge. The objectives of this specific contract were to determine the feasibilities of developing, first the helium-nitrogen charge transfer laser, and, later the XeF laser into such a device. More specifically, the focus of this research began with the task of characterizing the performance and scalability of the N_2^+ laser pumped by charge transfer from He_2^+ in a discharge environment. After accomplishing this goal, a logical continuation of interest emphasized the study of the means for switching the output from the strong transition in the violet to the weaker transition at 470.9 nm. Difficulties which are now fully understood prevented this in systems excited purely by preionized discharges, but the switching was successfully demonstrated in a regenerative amplifier pumped directly by e-beam excitation.

The course of the first phase of this contract research was rich in discovery. The wealth of scientific detail resulting from this work has been reported in nine journal articles, copies of which form the main part of this report. One of these, an invited review article for the IEEE Journal of Quantum Electronics provides a particularly comprehensive insight into the N_2^+ laser pumped by charge transfer from He_2^+. This system was shown to have a figure-of-merit in terms of efficiency and scalability that, surprisingly, approaches one-half of that of the best inert gas halide lasers. Previously, differences in performances of an order-of-magnitude had been expected. In fact, there are some unique features to the charge transfer system which could make it even superior in some applications, but unfortunately, not in the production of blue-green output.

In a final phase of investigation the principles taught by the charge transfer work were applied to the XeF system. As was well known, that system had the potential for output in the blue-green. Because of collisional mixing of the upper laser levels, both UV and blue-green transitions in XeF, in effect, had a common initial state and two possible lower levels. In the charge transfer system there had actually been only a single upper level, and in both cases the desirable transition was the weaker of the two possibilities.

The excitation system and optical techniques refined in the first phase of the research with the analogous helium nitrogen system were adapted to the XeF problem. An amplifier with a maximal gain-pathlength product was arranged, the UV output was inhibited to avoid a competitive saturation of the blue-green gain by the development of UV superfluorescence and an apparently definitive experiment was conducted. The critical parameter to successful switching of the output into the weaker transition was the intrinsic gain ratio between strong and weak transitions which was unknown at that time. Had it been no less favorable than 20:1, blue-green output would have been obtained and feasibility would have been proven. The test was successfully conducted with a clear negative result indicating a very unfavorable gain ratio of UV to blue-green in excess of 20:1. The inescapable conclusion is that the blue-green transition of XeF is too weak with respect to the competing UV transition to support the development of any practical device pumped by a preionized discharge.

As is often the case with even a negative result, it seems that the successes of the work supported by this contract go beyond the simple elimination of a "blind alley." The development and characterization of

the analogous helium nitrogen laser produced a system and a technology that hold much promise for other applications. Many interesting advances were made in the basic understanding of that system and, in general, of the problem of the competition between transitions, having very different and transient values of gain. As mentioned above, nine publications reproduced in the Appendices describe the results of this work on the charge transfer system and the final effort with XeF is reviewed in the following material.

THE NITROGEN ION LASER PUMPED BY CHARGE TRANSFER

Work performed under this contract showed that there are some great advantages to the charge transfer laser, whether operated in a preionized discharge or with e-beam excitation. Operational advantages are very clear and include the use of innocuous, chemically stable gases to support lasing directly in the blue-green wavelength region. More subtle, but no less important, intrinsic advantages exist at the atomic level.

The particular system studied in this work was pumped by charge transfer from He_2^+,

$$He_2^+ + N_2 \rightarrow N_2^+(B) + 2He \quad , \tag{1a}$$

$$He_2^+ + He + N_2 \rightarrow N_2^+(B) + 3He \quad , \tag{1b}$$

and one of three vibrational components of the $B \rightarrow X$ transition of N_2^+ was subsequently stimulated. The inherent advantages of this system are threefold, the first being that the vibrational excitation remaining in the lower laser level is rapidly quenched by a process unique to molecular ions. This makes possible four-level, quasi-cw operation of the laser.

A second advantage is that the operating wavelength is longer, and hence, less energetic, than the thresholds for photoionization and photodissociation of all of the important kinetic intermediaries. This means that even very high powers circulating in the laser cavity do not disturb the kinetics. Finally, because the laser transition occurs between bound electronic states of the N_2^+ molecule, the bandwidth of the gain is small, and hence, the maximum gain is large. As a consequence, saturation is reached at smaller inversion densities than, for example, in excimer transitions.

The data and detailed analyses of both the e-beam and discharge pumping of the helium-nitrogen laser are found in existing publications reproduced in the Appendices, but the most important characteristics can be summarized as follows:

1. The kinetic scheme is now known. Efficiencies, power outputs, and the times for the onset of threshold obtained with discharge excitation all agreed with the predictions of the kinetic model developed from the e-beam results. The model contains no steps which might be disturbed by high field intensities.
2. As long as the E/p can be maintained in a discharge at a value in excess of 2v/cm/Torr, current densities of the order of $100A/cm^2$ will give a power transfer efficiency of 2% at 427.8 nm in a self-excited laser oscillator.
3. Operation of the discharge laser as an optical amplifier will approximately double output powers through earlier saturation of the laser transition. This is not to be confused with bottlenecking for which no evidence was found. At moderate levels of operation of the discharge laser, i.e., 500KW, small

signal gains of 15%/cm were found with saturation intensities of only 50KW/cm^2. The bottlenecking intensity can be assumed from the e-beam results to lie above 20MW/cm^2 so that a wide range of output powers may be sustained at a constant efficiency of the order of 3 to 4%.

4. The relatively narrow gain bandwidth of 5 cm^{-1}, realized from this laser transition between bound electronic states of N_2^+ compensates the collisional quenching of the upper laser level and thus brings the saturation intensity down to 50KW/cm^2, a value which can be reasonably attained in a master oscillator. Since the quenching channel can be bypassed if laser intensities in the plasma significantly exceed the relatively modest saturation intensity, the collisional quenching becomes an asset by suppressing uncontrolled superfluorescence. In fact operation of the system as an optical amplifier was achieved at megawatt/cm^2 power levels for an overall gain of 18, conditions relatively near the ideal extraction of power at zero gain.
5. The gain-narrowed linewidth of the output from the optical amplifier was measured to be 0.007 nm without any supplementary interferometric narrowing of the oscillator. Thus all of the power output is concentrated in a relatively narrow line, as compared with excimer lasers.

While the instantaneous power conversion efficiency attained in the charge transfer amplifier developed under this contract readily reached values ranging from 2 to 4%, the overall efficiency remained a more

persistent problem. This resulted primarily from the speed with which the electrical avalanche has developed in the discharge tube and was not a problem unique to charge transfer lasers. However, other discharge lasers based on excimer transitions generally contain significant concentrations of attaching gases such as F_2 or HCℓ. Although these tend to remove free electrons and stabilize the discharge by raising the conductivity, in either case the avalanche finally develops and effectively short-circuits the electrical driving circuit.

The power density which can be developed in a laser plasma is generally maximized by increasing the risetime of the current and coincidently increasing the rate of avalanche. Specific output power densities achieved in the charge transfer laser have been high, even in comparison with excimer lasers, being of the order of 30 to 50 MW/liter in discharge devices. At these power levels the avalanche has proceeded very rapidly and effective power transfer has been maintained for times only of the order of 5 nsec.

Traditionally high energy densities have been achieved in discharge lasers through the increase in pulse duration which, as mentioned earlier, depended upon the stabilization of the plasma conductivity through electron attachment. However for those applications such as ranging which necessarily require short output pulses, the power density achieved (as opposed to energy density) is the best figure of merit. Unlike the case with UV excimer lasers, the entire kinetic chain pumping the charge transfer laser is completely transparent to the output radiation. Thus, it can sustain very high specific power densities at the cost of pulse duration, which does not become a disadvantage, at least for some types of applications.

Considering then the particular merits of the charge transfer system to be its high instantaneous efficiency, high power density and short pulse duration, a clear need existed to demonstrate that the overall efficiency could be made to approach the instantaneous efficiency through proper matching of the discharge to the load. Efforts to demonstrate the feasibility of such a matching necessitated a specific optimization of the hardware.

Several devices were developed in the course of this work that represented major landmarks for the advancement of the technology needed for the efficient operation of this type of laser in the domain in which characteristic times for pumping, storage and output all lay in the range from 1 to 10 nsec. These included the following systems.

A. A master oscillator power amplifier (MOPA) configuration switched by a single hydrogen thyratron so that repetitively pulsed operation would be possible with a precision of synchronization of the order of 1-2 nsec. This system was extremely effective in supporting the measurements of gains and saturation intensities in laser media of this type in which the impedances, and hence, the power input changed drastically on a time scale of a few nanoseconds.

B. A traveling wave laser and a traveling wave amplifier. The laser was constructed with no optics whatever, and output windows were antireflection coated to avoid spurious asymmetries in propagation of the output along the two possible directions on the laser axis. The control established over the progression down the axis of the phase of the electrical breakdown was

sufficient to yield a contrast ratio of 1000:1 between co-propagating and counterpropagating waves. In terms of output pulse energies measured from the two ends of the device the ratio was 10^4:1 at megawatt levels of output intensity.

C. A near-resonant preionized discharge tending to optimize the match between ringing half-period of the discharge current and the lifetime of the optical gain. This device contributed significantly toward the approach of the wall-plug efficiency to the power conversion efficiency relative to deposition.

D. A regenerative amplifier scheme. When excited by an e-beam discharge the amplifier section had sufficient gain pathlength product to function efficiently as a regenerative amplifier at 470.9 nm.

Detailed descriptions of the devices and their performances are contained in the published works reproduced in the Appendices. They provided a strong foundation of technology upon which to base the final phase of research under this contract that attempted to switch the UV output from XeF into the blue-green.

THE BLUE-GREEN TRANSITION OF XeF

The general problem limiting the usefulness of the XeF laser at visible wavelengths is the competition from the UV transition. Technically the blue-green and UV transitions originate from different molecular levels. However, because of collisional mixing, the XeF system usually functions as if there were a single upper level for the two transitions. Exceptions occur under extreme experimental conditions, such as very low pressures or very low temperatures. Since the uniquely high efficiencies

of the excimer lasers basically accure from extremely efficient collisional processes, the minimization of collisional effects must necessarily lead to substantial reductions of these efficiencies. This can be clearly seen in the relatively poor results from photolytically pumped, cold thin XeF samples from which laser outputs have been obtained at blue-green wavelengths.

What appears essential is a way of selecting the desired output wavelength by some optical means which does not disturb the kinetics pumping the laser levels under conditions of maximal efficiency. If it is accepted that the problem is actually that of selecting a weak transition in the presence of a strong one having the same upper laser level but a different lower level, the resulting analysis is more fruitful. The technology described in the previous section had already been developed for dealing with that situation and the concern of this phase of the work was to what extent it could be adapted to XeF.

The energetics of the radiating system are shown schematically in Fig. 1. The weak transition is the one desired as it corresponds to a transition wavelength of 480 nm. The assumption that neither lower level can become appreciably populated because of their essentially repulsive characters, implies immediately that whichever transition saturates first will be the one through which the stored energy of the excited state will be extracted. However, the saturation intensities of the two transitions are not more favorably related than are their respective transition probabilities, so the weak transition must have a higher saturation intensity.

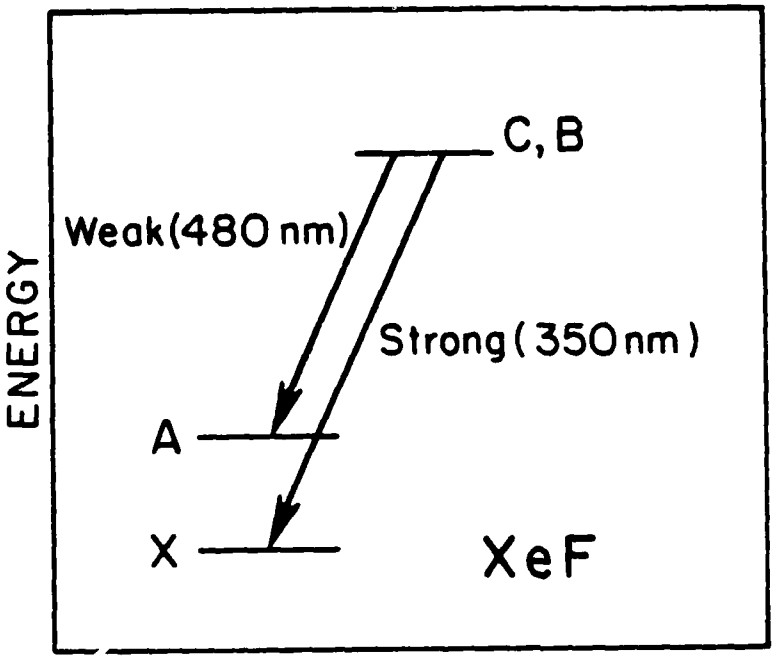

Figure 1

Schematic representation of the energy levels of XeF important in this model.

The most natural approach toward the problem of selecting the weaker of two transitions is to contain the excited medium in an optical cavity arranged to have high losses at the wavelength of the higher gain transition and low losses for the weaker transition. However, because of the practical limitations upon optical coatings it can be shown that it is difficult to succeed when the relative small signal gains differ by even one order of magnitude. Even then it is almost impossible to scale such devices because every ray at the undesirable wavelength which

can propagate in the medium must be selectively attenuated by the mirrors before its more rapid exponential growth leads to the predomination of its intensity. This, in fact, means physically small systems bounded by extremely selective mirrors. Such techniques hold little a priori promise for large scale XeF devices.

At the next level of sophistication an oscillator-amplifier combination could be arranged, at least in principle. The amplifier would be saturated at the wavelength of the weak transition by an input taken from the oscillator at a level comparable to its saturation intensity. Once the weaker line were saturated, the gains of both transitions would be reduced and lasing could not subsequently start on the undesired transition. Such a technique had been demonstrated in this laboratory to be extremely effective in the analogous system, the helium-nitrogen laser, in which a similar relationship of excited states existed. However, there was an immediate difficulty in adapting it to the XeF system, the XeF oscillator.

Presumably, then, the excitation of an XeF amplifier in the blue-green would require some other type of laser, such as a dye laser or an XeF device operating under extremely inefficient conditions. In that case, for the overall system to be efficient the pulse energy from the oscillator would need to be substantially less than the energy extracted from the high efficiency amplifier.

It can be shown that under saturated conditions an intensity, ΔI, can be extracted from an amplifier of

$$\Delta I \cong I_s \gamma L \left(\frac{I_o}{I_o + I_s} \right) \quad , \tag{2}$$

where I_s is the saturation intensity, γL is the logarithmic gain of the

amplifier under small signal conditions, and I_o is the oscillator intensity. Since noise is amplified by a factor, exp(γL), to avoid uncontrolled superfluorescence the amplifier needs to be arranged so that $\gamma L \lesssim 12$ over the longest path through the plasma. This means that for the extraction of at least 3/4 of the available power of the amplifier $I_o \geq 3I_s$ so that $\Delta I \sim 4I_o$. It is clear that since the XeF kinetics are one or two orders of magnitude more efficient than other possibilities which might be used for the oscillator, the power input to the oscillator must exceed that to the amplifier by an order of magnitude.

Apparently the only way in which such a system could work effectively with an inefficient oscillator would be if the oscillator pulse duration were orders of magnitude less than the duration of the amplifier excitation. An external mirror could provide for regeneration of the optical amplifier and the oscillator would need to supply power only for a period long enough to "fill" the length of the amplifier plasma. As described in the previous section, precisely such a system was demonstrated in the analogous helium-nitrogen laser. An inefficient dye laser producing an output pulse of relatively short duration was used to start a regenerative amplifier of higher efficiency for the production of a much longer output pulse.

The requirements for such a system can be obtained by examining the differential equations for the growth of the intensitites of transitions coupled through the same upper state. These can be approximated

$$\frac{dU}{dz} = (1 + U + FV)^{-1} (U + \beta) \qquad (3a)$$

$$\frac{dV}{dz} = (1 + U + FV)^{-1} \; GV \qquad (3b)$$

where now U and V are the ultraviolet and visible intensities, respectively, in units of the saturation intensity of the strong transition, β is the intensity from spontaneous emission reduced by the fractional aperture for superradiancy (somewhat larger than the geometrical output aperture), $(1 + U + FV)^{-1}$ is the saturation parameter, and F and G are the ratios of the saturation intensities and of the gains for the two transitions, respectively. The quantities F and G are related, so that the only uncertain parameter is G, the ratio of the gain of the V to the U transition.

In this development the propagation variable, Z, has been scaled, also, so that it represents the physical distance, x, divided by the probable distance, D, for small signal stimulated emission on the strong transition. Since $D = \gamma^{-1}$, then $Z = x \cdot \gamma$. This is particularly useful because it reduces the number of independent assumptions about the physical size and level of excitation. The magnitude of the amplifier is expressed by the maximum propagation variable Z which is the number of small signal gain lengths for the strong transition spanned by the optical path through the system. For perspective, the overall small signal gain through the system would be exp(Z) for the ultraviolet transition.

Figure 2 shows the solution to the extraction equations in these normalized units for a case in which the relative gain parameter G was assumed to be 0.05 (i.e., 20:1). The input intensity has been assumed to be $V_o = 1$. There are two resulting curves for V. The solid curve is for an unsegmented system and the dashed, for a segmented discharge arranged so that filters between sections reject the U transition from propagating to larger values of Z.

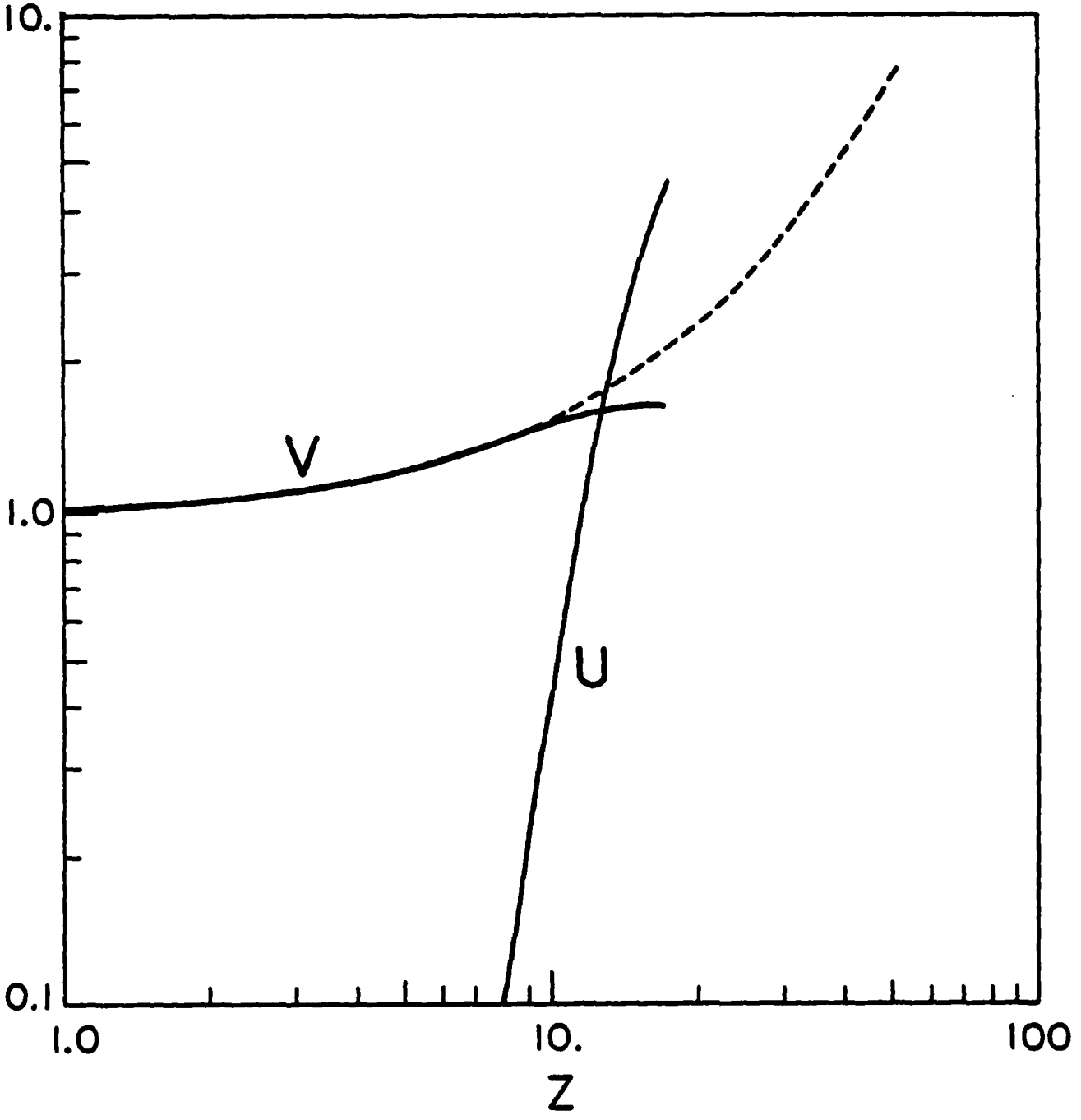

Figure 2

Solid curves plot the solutions to the set of coupled equations (3a) and (3b) describing the growth of the strong transition, U and the weak transition, V in terms of penetration into the amplifying medium. Units are scaled as discussed in the text. The dashed curve shows the effect of segmenting the medium and filtering between sections to remove the growing intensity of the U component.

The significance of Fig. 2 is found in the intersection of the U and V curves near the system size Z = 13. This means that even with the injection of $V_o = 1$, an intensity of the visible transition equal to the saturation intensity of the ultraviolet transition, the system would output the wrong transition if its size were greater than Z = 13. Yet at Z = 13, the V output is only 1.8, representing the extraction of only 6.2% of the available intensity of 13 of these units of power. (In these units the power available from a gain length of Z is Z units.)

At this point several conclusions can be drawn which render the further development more tractable.

1) In order to avoid the use of the exceedingly high levels of expensive oscillator power that would be necessary to avoid larger Z systems degrading spontaneously from the V to the U transition, the system must be partitioned so that after every path length of $Z \sim 8$, an optical element is used to reject the U radiation building up from amplified spontaneous emission.

2) In order to achieve efficient extraction of the available energy high values of Z must be used. For example, it can be seen that a Z of 50 would correspond to a 13.6% extraction efficiency. However, since the maximum physical length is assumed limited to 150 cm this would require a small signal gain for the strong transition of .33/cm which is probably not feasible for a large aperture amplifier. Some compromise appeared warranted and Z = 30 was used in subsequent analyses.

3) At these necessarily high levels of excitation, discharge stability may limit operation to pulse durations of the order of 50-100 nsec.

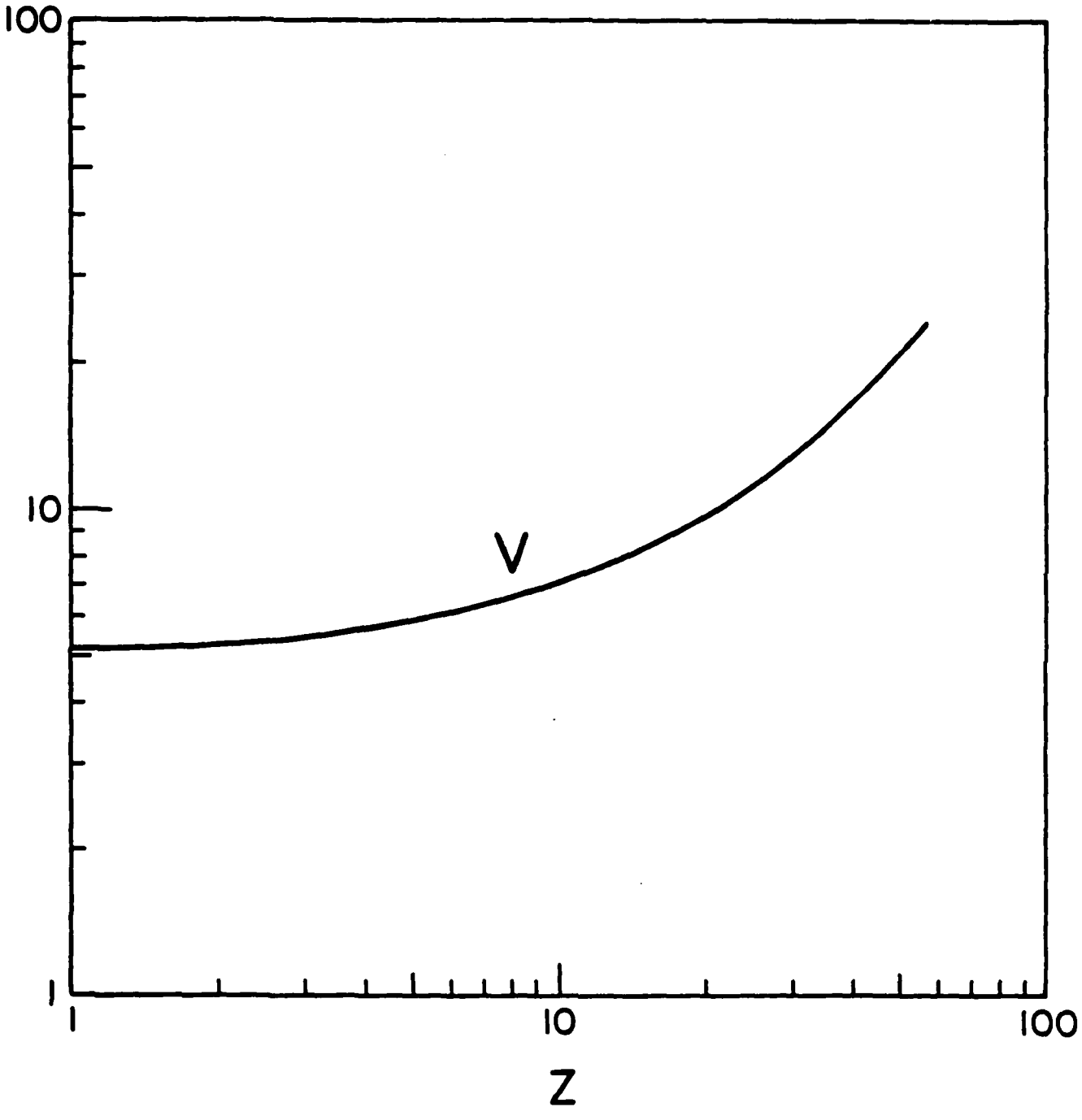

Figure 3

Solution to the set of coupled equations (3a) and (3b) for the growth of the weak transition, V for the case of a plasma segmented by the insertion of filters to remove the growing intensity of the strong, U transition.

Subject to these guiding assumptions the characteristics of a typical blue-green, power amplifier stage can be derived. It should be a medium aperture device, excited by a preionized transverse discharge at a high level of pulsed power deposition. The excitation should be maintained for as long as possible, but probably will be limited to 100 nsec by the onset of discharge instabilities. The performance of the stage will be determined by the V-curve shown in Fig. 3. In that figure the growth of the visible output has been presented for the same conditions as used to obtain Fig. 2, but for a higher level of power input from the oscillator. Only data for the segmented system has been shown as that represents the only practical case.

Because of the system of units, the results shown in Fig. 3 are reasonably universal and can be adjusted for a variety of inputs. Although drawn specifically for an input intensity, $I_o = 5.0$, the performance for a larger input, $I_o = 8$, can be readily obtained. For example, a value of V of 8 in Fig. 3 can be found for a Z of about 14. This gain of Z = 14 can be assumed to have occurred somewhere before the amplifier being modelled. Then if V = 8 at the amplifier input and the gain over the full length of the amplifier is 30, as assumed in 2), above, the intensity at the output will be found at $Z_{out} = 30 + Z_{in}$. Thus, for this illustrative case $Z_{out} = 44$. For that value of Z, a corresponding growth of V to a value of 18 is shown in Fig. 3. In summary, if Z grows by 30 in the amplifier, from 14 to 44, then the intensity will grow from 8 to 18. This means the extraction of 10 I_s from the plasma out of a possible 30 I_s, that stored and potentially available in the U transition. Therefore an extraction efficiency of

33%, relative to storage, is computed for this example of an input of $V_o = 8$.

To place these results in tangable form it can be estimated that the product of the saturation intensity by which U and V were scaled and the aperture of the amplifier will be of the order of 1 MW. There the amplifier characteristics modelled above can be estimated in physical units as follows:

Table 1

Performance levels proposed for the idealized XeF Amplifier Stage configured for operation at blue-green wavelengths.

Wavelength	:	480	nm
Output power	:	10	MW
Pulse duration	:	100	nsec
Pulse energy	:	1	J
Overall efficiency of Amplifier Stage	:	3.3%	
Input energy cost	:	30	J
Small signal gain ratio G^{-1} assumed in this model	:	20	

To achieve these outputs would require an input pulse of 8 MW supplied only for as long as necessary to fill the amplifier volume, provided regeneration of the input were obtained. In such an arrangement an output coupler and associated optics would be introduced in order to reflect a portion of the output back to the amplifier input. This portion of the intensity would need to be large enough so that it would be equal to the original I_o when it reached the input. In this

idealized case, 8 MW would need to be returned to the input, so that of the 18 MW available at the output end of the amplifier, 10 MW could be coupled into the output beam and 8 would be returned to continue the saturating function originally accomplished by the external oscillator pulse. For analysis a simple ring geometry can be assumed in which the amplification occurs in one 5 nsec branch and the beam reflected by the output coupler is returned in the other passive 5 nsec branch. Results are equivalent if a cavity is used instead. Then, in such a geometry the original oscillator pulse needs to have duration of only 10 nsec.

This analysis has tacitly assumed that the oscillator pulse used initially to fill the amplifier cavity will, itself, benefit from the amplification. However to accomplish this requires a further important refinement, the use of traveling wave excitation of the amplifier of the type demonstrated in the previous section. Without the use of the traveling wave configuration, the initial "filling" of the amplifier cavity would require an input larger by the fraction coupled out before the amplifier discharge was excited. In the case described above this would require an input of 18 MW rather than the 8 MW needed with traveling wave excitation.

The determination of the feasibility of this idealized device formed the central objective of this final phase of research. The critical issues to be resolved were: 1) the maximum level of gain pathlength product, Z, that could be developed in an intense preionized discharge and the maximum duration over which it could be maintained and 2) the ratio of gains between the strong and weak transitions. The principal technological problems concerned the adaptation of the helium nitrogen discharge system to the more aggressive gas mixtures. This

latter task was the first completed and led to near record levels of output power density from an XeF discharge laser. We obtained 5.3 MW peak power from 24 cm^3 for an output density of 220 MW/liter. The corresponding pulse energy of 50 mJ represented an efficiency of 0.75% with respect to the energy originally contained in the storage capacitor. This particular system also gave the maximum gain pathlength product, Z. A smaller device yielded 303 MW/liter with a 1.4% efficiency relative to stored energy. However, as in the case of the nitrogen ion laser, the wall plug efficiency was about a factor of 2 less than this efficiency relative to stored energy because of the additional energy that had to be wasted in inverting the switching capacitor. Nevertheless, these seemed to be state-of-the-art devices which should have been adequate for a definite test of the feasibility of extracting the output in the blue-green.

An oscillator/amplifier configuration was constructed at this high level of excitation and the gain and saturation intensity for the 358 nm line were measured using the same techniques proven in the He-N_2 laser studies. Typical data are shown in the figure below together with curves computed from a model containing adjustable values for Z and effective saturation intensity, I_s. This effective intensity is the textbook quantity multiplied by the ratio of $(t_2/2\tau)$ where t_2 is the upper state lifetime and τ is the pulse duration. It is the effective intensity actually determining the growth and saturation of the propagating waves.

From the figure it can be seen that the result of the model agrees reasonably well with the data. This particular case corresponded to $I_s = 0.82$ MW/cm^2 and Z = 6.3. Variations in Z of ±1.0 in the model gave the results plotted by dashes that appear to bound the range over which agreement with experiment could be obtained.

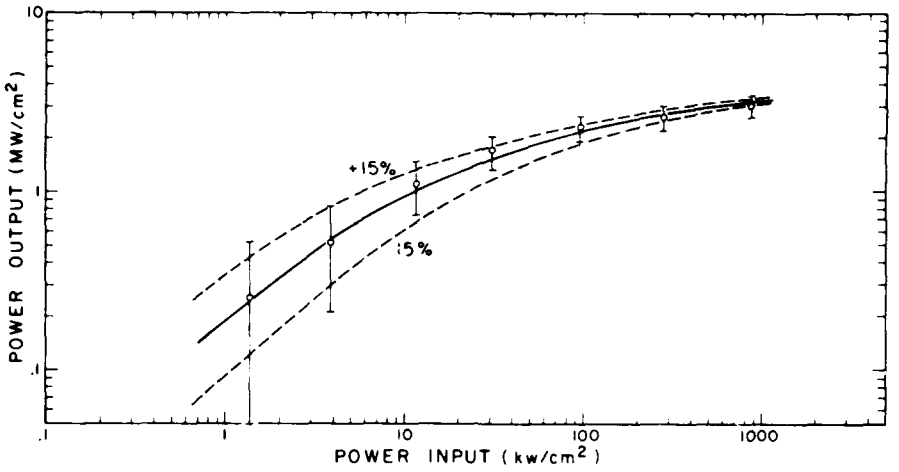

Figure 4

Graph of the data obtained for peak power outputs from the optical amplifier for various values of input pulse amplitudes at 358 nm. The solid curve plots results of a theoretical model and the dashed curves show sensitivies of the model to changes of Z of $\Delta Z = \pm 1.0$

The saturation intensity is only weakly dependent upon experimental variables, so that once it is known, the gain can be reasonably determined under other conditions from knowledge of only the power input to the amplifier stage and the power output. From this it was concluded that the maximum gain x pathlength achieved was 11.23 over a 48 cm path for 10 nsec duration. In fact, this corresponded to the record output of 220 MW/liter.

The implications of the preceding mathematical analysis of gain saturation resulting from competing transitions were that the most accessible figure of merit was the limiting Z which could be achieved with folded paths. It corresponded to the gain, γ times the total distance of propagation that was possible during the life of the plasma.

In this case cited the limiting Z would have been 70 which was clearly adequate for testing the regenerative amplifier concept described in the original proposal.

In the model described above the gain in the visible transition had been assumed to be 0.05 of the gain of the 358 *nm* line. This was thought to be conservative, but extremely critical estimate. Since a gain pathlength product of 70 had been achieved at 358 nm, it became essential to determine whether this must be reduced by 20 or some other factor in order to describe the growth of the visible transition. This was the next phase of the research. It was implemented with a regenerative amplifier arrangement very similar to the one described in the helium nitrogen studies, except this time the medium was pumped with a short section of the preionized discharge and was contained in an optical cavity having mirrors selectively reflecting 95 + 1% of the blue-green and less than 10% of the UV. In effect this segmented the gain so that the growth of the UV could be controlled.

To be certain of starting the oscillations in the blue-green, a small amount of output from a synchronously pumped dye laser was injected into the cavity. Since electrical power input to both the XeF gain medium and the dye laser were switched by the same thyratron, reasonable synchronization could be maintained, unlike the case reported earlier for the helium nitrogen system which employed an amplifier excited by a separate e-beam discharge. Observation of the effect of adjusting the optical delay between the dye laser output and the fluorescence reradiated from the cavity containing the XeF amplifying medium provided a reasonable means of searching for the onset and extent of the amplification of the injected pulse.

Limitations on this method were principally twofold. First, since the system was operating near the absolute limits for survival of the electrical components, stability of the level of excitation was not ideal. Moreover, variations in optical delay caused other minor changes in the precise geometry of the dye laser beam and, hence, in the coupling of the input into the cavity. Nevertheless, the composite effect of all instabilities would certainly not have masked an enhancement of exp (2) and probably not an enhancement of exp (1).

The second limitation on sensitivity resulted from the technological necessity for a certain amount of "dead space" in the laser cavity to protect the mirrors. The maximum Z of 70 which might have been obtained had to be reduced by the ratio of the effective length of the laser plasma to the physical length of the cavity. Further a factor had to be subtracted that was approximately N log R to accommodate the losses at the mirrors, where N was the number of transits of the cavity that was possible in the 10 nsec duration of the gain and R was the reflection coefficient of the mirror. Approximating

$$Z_{eff} = Z\zeta - N \log R \quad , \tag{4}$$

where ζ is the filling factor, the maximum Z_{eff} available for this test could be evaluated.

The value of ζ needed in Eq. (4) was estimated by observing that the UV output was growing rapidly toward the threshold for oscillation at the maximum level of excitation even with the blue-green mirrors. Assuming R(358 nm) ~ 8% and that the subthreshold condition observed corresponded to $Z_{eff} \sim 10$, gave $\zeta = 0.685$, a value not particularly

sensitive to modest changes in Z_{eff} around the value of 10. This seemed a reasonable estimate of ζ as it indicated an effective length of the laser plasma equal to 84% of the physical length of the electrodes. Because of some rounding at the ends of the electrodes to avoid arcing, the plasma was visibly weaker near the ends so this result seemed credible.

Substituting the value of filling factor deduced above into Eq (4), this time evaluated at 480 nm for which R = .95 ± .01 and recognizing that Z is in units of gain at 358 nm times pathlength gives $Z_{eff} \approx 32$. Reference to Fig. 2 shows that even if the intensity level coupled into the cavity had been as great as the order of the saturation intensity, the growth of the injected signal should have reached the value shown at the ordinate corresponding to Z = 32, about a factor of 4. Such an increase would have been clearly visible, but was not detected. Since the intensity of the injected signal was always less than the saturation intensity, the conclusion that the gain ratio is worse than 20:1 is inescapable.

Confirming limits can be obtained by using Eq. (4) directly to estimate the small signal gain. Considering the limits of detectability to be either exp (1) or exp (2) and the mirror reflectivity to have been 95% or 94% the following table summarizes the resulting limits on the gain ratio.

Table 2

Summary of lower limits on the ratio by which the gain of the UV transition exceeds that of the blue-green transition.

Level of insensitivity to detection	Mirror reflectivity (%)	Minimum gain ratio
exp (2)	95	17
exp (2)	95	16
exp (1)	94	27
exp (1)	94	24

IMPLICATIONS

In fact, no evidence of amplification in the blue-green was detected in this phase of the research dealing with XeF. While such negative results are difficult to interpret absolutely, qualitative experiences suggest that enhancements of less than exp (1) would have been detected and in this case it is the considered opinion that this negative result can be interpreted as indicating the gain ratio to be even less favorable than 30:1. The technology was confirmed to be operational through the many cross-verifications described in this technical report, but the gain in the blue-green simply did not materialize. The inescapable conclusion is that the blue-green transition of XeF is too weak with respect to the competing UV transition to support the development of any practical device pumped by a preionized discharge.

Conversely, the implications of the earlier phases of the studies with the helium nitrogen system are quite positive for applications other than those involving blue-green wavelengths. This system was shown to have a comprehensive figure-of-merit in terms of efficiency and scalability that approach one-half that of the best inert gas halide lasers. The narrow bandwidth and particularly high power densities that

can be obtained with this system, together with its immunity to uncontrolled superfluorescence could make it even superior in some applications.

APPENDICES

Publications resulting from work performed under this contract.

I. "The nitrogen ion laser pumped by charge transfer," by C. B. Collins, IEEE-J.QE., (Invited-pending).

II. "Charge transfer pumping of the helium-nitrogen laser at atmospheric pressures in an electrical avalanche discharge," by C. B. Collins, J. M. Carroll, and K. N. Taylor, J. Appl. Phys. 49, 5093 (1978).

III. "Gain and saturation of the nitrogen ion laser," by C. B. Collins, J. M. Carroll, and K. N. Taylor, Appl. Phys. Lett. 33, 175 (1978).

IV. "Dyes pumped by the nitrogen ion laser," by C. B. Collins, K. N. Taylor and F. W. Lee, Opt. Commun. 26, 101 (1978).

V. "A regenerative power amplifier operating on the blue-green line of the nitrogen ion laser," by C. B. Collins, J. M. Carroll, K. N. Taylor, and F. W. Lee, Appl. Phys. Lett. 33, 624 (1978).

VI. "Gain and saturation of the nitrogen ion laser," by C. B. Collins, J. M. Carroll, and K. N. Taylor, in Proceedings of the International Conference on LASERS '78, edited by V. J. Corcoran, (STS Press, McLean, VA, 1979) pp. 363-369.

VII. "Traveling wave excitation of the nitrogen ion laser," by C. B. Collins and J. M. Carroll, in Proceedings of the International Conference on LASERS '79, edited by V. J. Corcoran, (STS Press, McLean, VA, 1980), pp. 646-650.

VIII. "Traveling wave excitation of the nitrogen ion laser," by C. B. Collins and J. M. Carroll, J. Appl. Phys. 51, 3017 (1980).

IX. "An atomic-fluorine laser pumped by charge transfer from He_2^+ at high pressures," by C. B. Collins, F. W. Lee and J. M. Carroll, Appl. Phys. Lett. 37, 857 (1980).

The Nitrogen Ion Laser Pumped by Charge Transfer*

by

C. B. Collins
Center for Quantum Electronics
The University of Texas at Dallas
Box 688, Richardson, Texas 75080

* Research supported by the Defense Advanced Research Projects Agency by the Office of Naval Research and by the National Science Foundation under Grants No. ENG 74-06262, ENG 78-16930, and ECS 8018730.

ABSTRACT

Charge transfer from He_2^+ to N_2 has been used in a variety of devices to pump significant levels of inversion of the $B^2\Sigma_g$ electronic transition of N_2^+. Laser output has been achieved at three wavelengths, 391.4, 427.8 and 470.9 nm. Each has corresponded to a transition from the same upper laser level to lower levels having vibrational quantum numbers equal to 0, 1, and 2, respectively. With proper mirror sets each has been individually excited. Studies of the scaling and efficiency at which the laser output could be obtained have been made with devices pumped by e-beams, preionized avalanche discharges, and preionized resonant and traveling wave discharges. The possible efficiencies for the extraction of the energies stored in the inversions have been examined for various configurations of the coupling of the optical fields to the plasmas. Resulting devices have included self-excited oscillators, regenerative amplifiers, and master oscillator power-amplifiers. The experimental results have supported a kinetic model which generally explains the unique features of the nitrogen ion laser. Of particular interest is the capacity of these systems to support the simultaneous optimization of both scale and efficiency. With e-beam excitation optical power densities of 320 MW ℓ^{-1} have been achieved at a constant power transfer efficiency of 3%. With resonant discharge excitation 44 MW ℓ^{-1} have been demonstrated at power conversion efficiencies of 2% and overall efficiencies ranging from 0.2 to 0.4%. From these results the kinetic model has projected an overall efficiency of 0.9% to be ultimately realized in a discharge device.

INTRODUCTION

The idea for a molecular change transfer laser is traceable to the observations in the early 1960's that intense, selective excitation of spectra could result from the reactive collisions of inert gas ions with neutral molecules [1], [2]. In those experiments it was generally found that such reactions were favored by energy resonances between the reactants that tended to minimize any changes of kinetic energies. Because of this selective nature of the energy transfer process, the general potential of the charge transfer mechanism for the development of population inversions of the product ions was appreciated as early as 1965 by McGowan and Stebbings [3].

It is interesting that at the time the original suggestion was made, Fowles and Jensen [4] had independently demonstrated laser oscillations on transitions between electronically excited states of I^+, the pumping of which they attributed to charge transfer from He^+. Almost immediately, the prospects for the practical implementation of this mechanism improved when the NOAA group reported that the rate coefficients for charge transfer reactions occurring at thermal energies often approached gas kinetic values [5]. At that time it could have been reasonably expected that charge transfer would offer a considerable advantage over other laser pumping mechanisms because the reaction rates were typically an order of magnitude larger than the rates for other excitation transfer sequences involving neutral atomic and molecular species. As a consequence, a charge transfer reaction having the potential for pumping a laser transition could have been readily arranged to be the dominant process for the loss of the primary ionization created in an inert gas plasma containing a small component of some other species. In fact, this

possibility was pursued in only a limited fashion in the development of some of the many variants of metal ion devices buffered with inert gases, such as the helium-cadmium and helium-zinc lasers. Some of the lines from Cd^+ and Zn^+, for example, were apparently pumped by direct charge transfer from He^+, but usually the strongest outputs were the result of Penning ionization of the metal atoms by neutral metastable helium atoms. The distinction between that process and charge transfer is an important one. Because of the variable energy of the free electron emerging with the product atom, the Penning process is always resonant and, hence, the transferred energy is not selectively channeled into a particular state of excitation of the products.

While even commercial significance finally resulted from these lasers based upon excitation transfer between atoms, the detailed consideration of the kinetics that limited their performance lies outside the scope of this work. To some extent the scaling to higher powers was hindered by the difficulty in obtaining larger volumes of the metal vapor reactants and by the relatively low densities of atomic ions of the inert gases which could be obtained in the low pressure discharges in which the systems had to operate. Considering these intrinsic difficulties, it is almost surprising that nearly a decade elapsed between the initial suggestion for a charge transfer laser and the first demonstrations of stimulated emission from such a system [6] involving scalable molecular reactants.

It seems clear, now, that the protracted delay in the actual demonstration of a scalable charge transfer laser was a consequence of the several unique features of this type of pumping that contribute to its advantages but force their realization into areas of technology not

already existing as by-products of the development of the more traditional types of devices. In fact, it appears that the full realization of the potentials of this type of system will be made with another generation of devices for the excitation of laser media which are characterized by time scales for pumping of the order of nanoseconds in contrast to the tens of nanosecond scale currently encountered near the state of the art.

Partly this is traceable to the resonant nature of the transfer which constrains, perhaps overly so, the choice of reactants which might be used in a laser device. In practice such accidental resonances are seldom found and the criterion must be relaxed through the consideration of reactions pumped by the ions of molecules, such as those of the inert gases, whose neutral ground states are unstable. Because of the varying energy of repulsion of the constituent atoms of the neutral molecule remaining after the transfer of charge, the actual energy available from a molecular ion of the inert gases can vary by about 5% depending upon the internuclear separations of the component atoms at the time the electron is captured from the reacting partner. However, even this flexibility does not remove the requirement that the atom or molecule to be excited must have its upper laser level in near resonance with the available energy of the donor so that the ionization potentials of the two reactants must differ by approximately the energy of the anticipated laser photon. If it is desired to operate at near-visible wavelength with reactants having reasonable vapor pressures at room temperature, a survey of tabulated energy levels [7], [8] shows a rather restrictive field of possibilities, seemingly limited to charge transfer from He_2^+ to molecular gases such as N_2, CO, and O_2. Consonant with this deduction

are the essentially negative results of studies seeking charge transfer spectra pumped by argon ions [9] in a manner analogous to the positive results observed in helium [1].

It is the combination of He_2^+ reacting with a molecular gas that introduces the features peculiar to the scalable charge transfer laser that give it unique advantages and difficulties. To form appreciable concentrations of He_2^+, as opposed to He^+, requires either high pressures of helium or long-lived plasmas since the conversion of the ions from atomic to molecular form proceeds most favorably by three-body collisions. Both conditions pose particular problems. The latter is generally precluded by the time scale set by the spontaneous lifetimes of the excited states of the reaction products considered as laser candidates. The former causes significant pressure broadening of the molecular transitions because of the relative frequency of collision with the background helium atoms. The result is that the cross sections for stimulated emission are typically peaked at 0.01 to 0.1 nm^2 [10], values which are three to four order of magnitude below those characteristic of the laser transitions of Ne and Cd^+ when pumped by excitation transfer from the neutral energy storing species of helium. Thus, the inversion densities required for threshold populations to be excited by charge transfer from He_2^+ must be expected to exceed those characteristic of the helium-neon and helium-cadmium lasers by orders of magnitude, a requirement not consonant with the relatively low stopping power of helium for the deposition of energy from the energetic electrons in an e-beam or discharge. These somewhat conflicting requirements have comprised the underlying problems delaying the original realization of the

charge transfer laser and subsequently impeding its development. Nevertheless, they have also offered almost unique benefits that can be realized in scaling such a system to high power.

The threshold for the sustained oscillation of a scalable laser pumped by charge transfer was finally achieved in 1974 [11] with the demonstration of the nitrogen ion laser pumped by charge transfer from He_2^+, through the reactions,

$$He_2^+ + N_2 \rightarrow N_2^+(B) + 2He \quad , \tag{1a}$$

$$He_2^+ + N_2 + He \rightarrow N_2^+(B) + 3He \quad . \tag{1b}$$

The laser output belonged to the $B^2\Sigma_u^+ \rightarrow X^2\Sigma_g^+$ electronic transition of N_2^+. Probably because of the Franck-Condon factors favoring excitation of the vibrationless, v' = 0, state of the upper laser level from the v" = 0 state of the ground electronic state of the neutral, N_2, molecule, the products of the charge transfer step seemed to be predominantly vibrationless. Although in principle a sequence of transitions to final states having different vibrational quantum numbers, v", in the $X^2\Sigma_g^+$ electronic level of N_2^+ have the potential for inversion, the rapid decrease in the Franck-Condon factors with increasing v" provided a practical limit of v" $\leqq$ 2. These relatively favorable transitions correspond to the following wavelengths for the values of (v',v") indicated: (0,0), 391.4 nm; (0,1), 427.8 nm; and (0,2), 470.9 nm. With the proper mirror sets each can be individually excited as will be discussed in the following sections.

Although the explosive development of the inert gas halide lasers during the same period of time has tended to eclipse the accomplishments

realized with other scalable systems operating in the same wavelength range, the performance of the nitrogen ion laser has placed it into the same class of reasonably efficient, scalable, high power devices capable of output at visible wavelengths.

Since its introduction, it has shown even a few advantages over other laser types operating at comparable wavelengths. Linewidth as narrow as .007 nm was demonstrated at high intensity levels for wavelengths which were not energetic enough to disturb the kinetic sequence pumping the transition. When excited by an intense electron beam with currents of the order of 1 KA cm^{-2}, quasi-cw operation of the laser was achieved [12] at 427.8 nm and output power was found to accurately follow input power after the onset of threshold. A time-dependent power conversion efficiency of 3% was reported to persist over 80% of the duration of the discharge pulse [12] and no evidence of bottlenecking was found over a range of circulating intracavity intensities up to 30 MW cm^{-2}. Extracted power densities as great as 320 MW ℓ^{-1} gave no evidence of disrupting the kinetic sequency pumping the laser transitions. [13]

In preionized discharged [14], [15] the overall efficiency had been initially observed to degrade, but more recent time-resolved measurements [16] of the parameters of the helium nitrogen charge transfer laser in such environments have shown characteristics at lower excitation current densities which were similar to the e-beam results. At E/p values of the order of 5 V $cm^{-1}Torr^{-1}$ and at a current density of 100 A cm^{-2} instantaneous power conversion efficiencies of 2% were reported, [16] with peak powers in excess of 1 MW. The most recent scaling studies [17] have brought output powers to 5 MW and the corresponding efficiency

for the utilization of the energy stored on the final discharge capacitor to 0.4%. With the nearly-resonant discharges described here, best efficiencies reached 0.6% without yet reaching a peak. Both in timing and efficiency the performance of the discharge pumped laser is consistent with the results of the e-beam excitation.

In some respects, such as in the ability of the kinetic channels and intermediate species to withstand very high circulating powers without disruption, in the transparency of the laser medium to the output line, and in the relative freedom of the laser transition from runaway superfluorescence, the potentials of the charge transfer laser exceed those of even the rare-gas halide systems. While such results clearly do not disturb the general concensus that the inert gas halide laser represent the best of current technology in the short wavelength region, they are, perhaps, more positive than is usually realized. Comparative data between laser types is difficult to assess in any circumstance, and particularly so in this instance. The detailed results of rather extensive investigation into the helium nitrogen system are generally unavailable [12], with published reports giving only preliminary and fragmentary indications. This is most acutely the case with the results of electron beam excitation which showed the best levels of output and efficiency. It is partly the purpose of this work to report those results, together with new measurements obtained with nearly-resonant discharges, while attempting to synthesize a general perspective on this particularly scalable laser pumped by charge transfer from He_2^+. It will be seen that aspects resulting primarily from the fact that the laser transition connects highly excited states of a molecular ion have caused the realization of the potential benefits of this system to lag considerably behind the development of the excimer devices.

The first of these problems is that the output scales with ionization but the laser medium contains no attaching gases so that efforts to reach higher output energy densities in discharge devices have necessarily resulted in electrical avalanches to successively lower values of load impedance. This growing impedance mismatch with the driving circuit has limited the useful duration of the pumping pulse to a time comparable to that required for the avalanche to develop in the laser medium. Thus a dominant factor controlling the overall efficiency of such a discharge device is the extent to which the stored energy can be completely discharged through the laser medium in a time comparable to the relatively few nanoseconds required for the electrical avalanche. This has transformed the problem of optimizing the charge transfer laser into an effort in technology development. While the excitation of the system with an e-beam avoids this problem, the relatively low stopping power of the laser medium introduces concerns for the maximum power density which can be achieved. It is possible that direct ion-beam or nuclear pumping holds the greatest potential for the excitation of this system to high levels of energy density because the stopping power of helium for both ions and neutrons greatly exceeds that for electrons.

The second difficulty specific to this system has resulted from the relatively small amount of fluorescence emitted from the upper laser level under non-lasing conditions. This low fluorescence efficiency clearly suggests that rates for collisional quenching processes significantly exceed the relatively slow spontaneous transition probability corresponding to a lifetime of 66 nsec. Such a circumstance immediately implies that the threshold would more difficult to attain in a helium nitrogen, charge transfer plasma because of the greatly reduced t_2

lifetime of the upper state. However this is the same effect that makes such lasers less susceptible to uncontrolled superradiancy, as has been observed to be the case with both e-beam and pure discharge excitation.

Lest it be prematurely concluded that such a high rate of quenching precludes effective operation of a charge transfer device, it must be recalled that the probability of extracting one photon per inversion is given by the ratio $I/(I + I_s)$, where I and I_s are the circulating intracavity intensity and the saturation intensity, respectively. The fact that the transition occurs between bound molecular levels has been recently shown [18] to lead to a bandwidth of the gain of only 5 cm^{-1} and thus, to bring the saturation intensity down to a reasonable value of the order of 50 KW cm^{-2}, a value that can be readily attained in a small discharge oscillator. This factor, together with the relatively short time during which the discharge impedance remains matched to the driving circuitry immediately suggests that the nitrogen ion laser would show its best performance when coupled to the fields in an oscillator-amplifier configuration. In fact, used as an amplifier, a charge transfer plasma excited in a preionized transverse discharge, 85 cm in length exhibited [18] an overall gain of 18 at extraction levels of 1 MW cm^{-2}, conditions relatively near the ideal extraction of power at zero gain. The intensity of uncontrolled superfluorescence was found to be less than two orders of magnitude below that value. Measurements of the power extracted from the amplifier for various levels of inputs power were found to agree with a simple model of gain saturation and yielded a value of the order of 58 KW cm^{-2} for the saturation intensity.

All elements of the existing data base, whether obtained with e-beam or direct discharge pumping, can be reconciled with a relatively

straightforward kinetic model incorporating the following principal advantages of the charge transfer scheme of laser pumping:

1) Since the sequence can operate as a four-level system, it should be readily adapted to a variety of excitation devices as the output should continue as long as the population of the energy storage level is replaced.

2) Since the operating wavelength is generally longer than the photoionization and photodissociation thresholds for all of the important species in the kinetic sequence pumping the inversion operation at high power density should be possible with no loss of efficiency.

3) Because the laser transition occurs between bond electronic states of a molecular ion, the bandwidth of the gain is small, and, hence, the maximum gain is large. As a consequence, saturation should be reached at smaller inversion densities than in excimer transitions.

The limiting kinetic efficiency predicted by the kinetic model most appropriate to this system is somewhat in excess of 50%. When multiplied by the quantum efficiency of 6.5% computed with respect to the energy cost of producing a primary ion, a power transfer efficiency of the order of 3% is estimated, in good agreement with results measured for both e-beam and discharge excitation. The overall efficiency with respect to pulse energy is projected to be degraded in a discharge by about an order of magnitude as a result of the impedance mismatch which currently limits the duration of the usable deposition of power to about 10% of the occurrence of power flow into the laser medium. The resulting estimate of 0.3% is the magnitude of the overall efficiency actually

observed in a discharge device. Conversely, the model predicts no such limitation on the overall efficiency for the output energy which might be obtained with e-beam, ion-beam, or nuclear pumping. The full 3% should be attained, thus making possible devices of extremely large scale.

KINETIC BACKGROUND

Past attempts to quantitatively model the kinetic sequence pumping the nitrogen ion laser have suffered from the paucity of rate coefficient data appropriate to atmospheric pressures. Although this can be viewed as a general problem of high-power lasers excited in high pressure plasmas, it is interesting to note that the existence of the type of charge transfer reaction pumping this system was unsuspected prior to the development of the laser. In fact prior to the work of Lee and Collins [19], it was generally assumed that the extensive literature [20] on charge and excitation transfer reactions derived from low pressure experiments could be used to adequately model the high pressure laser environment. Unfortunately, it has been recently shown that many of the bimolecular reactions studied at low pressures have their termolecular analogs which dominate at pressures around one atmosphere because of the importance of multibody collisions [21], [22]. A semi-classical model of such reactive collisions has been reported [21], [22], which now provides guidance in estimating these new reaction channels which may be of importance to a variety of lasers operating in high pressure plasmas.

Recently Petersen [10] has presented the results of an analysis of the fairly extensive data base built from e-beam measurements and has reconciled his model with the independent measurements [19], [21], [22]

of certain of the component steps in the kinetic sequence pumping the nitrogen ion laser. Critical pathways were identified in his work and through fitting procedures values were obtained for the other important reactive steps not independently measured. A revision of the kinetic scheme over those shown in previous works [12-14], [16], has been made and the resulting energy pathways are charted in Fig. 1. The primary steps in the pumping sequence are shown by the heavy arrows and the principal competing processes are indicated by the heavy dashed lines. Other supplementary processes are shown by the light arrows being either solid or dashed to identify their supportive or competitive nature, respectively. The kinetic sequence begins at the upper left with the population of He^+ that is created primarily by the electron impact excitation of ground state He. The laser transition is indicated by the wavy arrow in the upper center of the figure. Constituent species of the laser medium shown in the proximity of the arrows identifying the kinetic pathways denote the reactant partners acting to transform the populations of the states connected by the arrows.

The rate coefficients and branching ratios descriptive of the component reactive steps charted in Fig. 1 are summarized in Table 1. The resulting sequence has served to explain all of the elements in the existing data base comprising the results of measurements on devices pumped by e-beams, as shown by Petersen [10]. Subsequently the results obtained from discharge excitation were found to confirm this model, as well [24].

The value of a comprehensive kinetic model lies in the guidance it provides in the selection of operating parameters that optimize the flow of energy through the desired pathways. Unfortunately, an understanding

of much of the early work was confounded by the properties peculiar to the kinetics of this type of system. In this system the operating parameters that are chosen to facilitate the onset of cavity oscillations do not necessarily optimize the power flow available to the laser transition. This is perhaps typical of a device operating on a heavily quenched transition for which the ratio of available fluorescence to the power flow in the upper state is a strong function of experimental parameters that is not readily determined. It appears, a posteriori, that many of the early measurements were dominated by the resulting difficulty in attaining threshold and in fact, the values of parameters most often used did not even approximate those optimizing efficiency.

From Fig. 1 and Table 1 it can be seen that the rate limiting step in the growth of the inversion leading to cavity oscillation is the charge transfer step which scales with the concentrations of both helium and nitrogen. Howver, at helium pressures compatable with the experimental apparatus generally used, once the laser transition is saturated the probability of extracting one photon per ion initially produced is determined primarily by the competition between the reaction channels of He^+. The branching ratio between those channels should asymptotically approach unity as the partial pressure of nitrogen is reduced, thus posing a requirement inconsistent with those needed to attain threshold. The extent to which the kinetic scheme reviewed in Table 1 prohibits the simultaneous optimization of gain and efficiency can be appreciated in Fig. 2. There the kinetic efficiencies and small signal gain coefficients are shown as functions of the power densities deposited in plasmas of the typical composition indicated. The values actually plotted were calculated assuming steady state pumping conditions and full saturation

of the optical transition in the case of the kinetic efficiencies. The gain coefficients which are presented are those characteristic of zero-field levels. Effectively, what is illustrated is the anticorrelation between the ease of attaining laser threshold and the efficiency with which the deposited power is extracted once it is achieved. As a consequence, this together with the generally small spontaneous fluorescence emitted confirms the indications that the nitrogen ion laser must be expected to operate most efficiently as an optical amplifier in which the growth of the circulating intensity from spontaneous fluorescence is not a factor.

The kinetic efficiencies shown in Fig. 2 did not represent the maxima attainable over all possible variations of experimental parameters. In the limit of increasing helium pressure with a decreasing fractional concentration of nitrogen and a decreasing pumping rate, the kinetic efficiency for the production of the upper laser level should approach the branching ratio of 75% characteristic of the direct charge transfer step producing that level as a product. However, the concurrent reduction in gain would make even a viable amplifier unlikely. A somewhat cursory survey over a more practical domain of parameter space showed that a value of 60% represented the best kinetic efficiency which might be reasonably expected. For example, values ranging from 50 to 60% were calculated for plasmas of 10 atm helium containing 0.075% nitrogen sustained by power depositions ranging from 1 to 100 KW cm^{-3}. It is interesting to note, that as shown in Fig. 2, the lower pumping intensities that would be characteristic of nuclear induced plasmas were generally found to give the highest efficiencies of operation, assuming a fully saturated amplifier.

One of the more arbitrary features of the kinetic model summarized in Table 1 is the recombination loss of He_2^+ competing with the charge transfer step. Some previous models [25] of charge transfer lasers have used room temperature rate coefficients, values which lead to effective recombination rates in excess of 2×10^{-6} $cm^3 sec^{-1}$, even under the conditions of relatively weak pumping levels of the order of 1-10 KW cm^{-3}. This would imply a 5 to 10% loss of He_2^+ to recombination in competition to charge transfer. However in measurements of recombination rates in e-beam plasmas [26], reheating of the free electrons by superelastic collisions with the Rydberg molecules resulting from recombination was found to limit the recombination rate of He_2^+ to a few x 10^{-8} $cm^3 sec^{-1}$. Extrapolations [26] of low pressure measurements have indicated that the recombination rate should display a strong and complicated dependence upon electron temperature and neutral gas pressure, generally increasing with inverse temperature. Reasonable agreement with that approximation has indicated that over the range of parameters considered in these experiments the electron temperature could be expected to be in the range of 1500 to 2500°K. In the example discussed above the electron temperature was assumed to be 1500°K and for Fig. 2, 2500°K. Such values are most nearly consistent with the recombination lifetimes measured at high pressures and give predicted kinetics efficiencies and gains in good agreement with experiments.

The conditions shown in Fig. 2 more nearly approximate those describing electric discharge excitation, while those that led to 50% kinetic efficiency discussed above are appropriate to weak e-beam excitation. In the former case the depositions typically achieved were of the order of 300 KW cm^{-3} which would imply a kinetic efficiency of about 30% and a

gain of 0.2 cm^{-1}. Considering the energy cost of producing an He^+ ion to be 42.3 eV, the quantum efficiencies for the excitation of the 428 and 471 nm lines are 6.8 and 6.2%, respectively, so that a power transfer efficiency of 2.0% would be expected at 428 nm. Experimental results presented in the following sections show power transfer efficiencies measured in discharges to be in excellent agreement with this value of 2% while gains were found to be more typically around 0.17 cm^{-1}. The data obtained with e-beam excitation showed power conversion efficiencies which remained constant at 3% for the duration of the e-beam pulse in good agreement with the 50% value of kinetic efficiency expected for those conditions. Both cases tended to confirm the assumptions of an electron temperature elevated to 1500-2500°K.

As mentioned above, the relatively small gains computed under conditions supporting such favorable kinetic efficiencies occur principally because of the collisional quenching of the upper laser level by N_2, leading probably to the formation of N_4^+. This process dominates the losses determining the peak inversion density prior to lasing. Table 1 shows this quenching rate to be

$$Q = 4 \times 10^{-10}[N_2] + 6 \times 10^{-8}\ [e]\ (sec)^{-1} \quad , \qquad (2)$$

where brackets denote concentrations and where the latter term is negligable in lower density plasmas. [24] This quenching together with the rate for spontaneous emission gives values typically of the order of 10 nsec for the lifetime of the inversion obtained with discharge pumping.

Again, lest it be immediately concluded that such a high rate of quenching precludes the effective operation of a device pumped by charge transfer from He_2^+, it must be emphasized that the probability of

extracting one photon per inversion is given by the ratio $I/(I + I_s)$, where I and I_s are the circulating intracavity intensity and the saturation intensity, respectively. The fact that the bandwidth of the gain is only 5 cm^{-1} brings the saturation intensity down to a reasonable value of 50 KW cm^{-2}. This value can be readily attained in a small discharge oscillator and immediately suggests that the nitrogen-ion laser would show its best performance when coupled to the fields in an oscillator-amplifier configuration.

ELECTRON BEAM EXCITATION

Because of the high values of gain resulting from the larger energies that could be deposited, the first studies of the nitrogen ion laser were made with a laser medium pumped by an e-beam discharge. The resulting plasma was coupled to the fields in the geometry of a self-excited oscillator. At first outputs were small, 9 KW, but efficiencies were around 1.8% [11]. However, excited volumes were quite small, 0.63 cm^3, and an early concern was to determine the scalability of this result to larger volumes more nearly corresponding to the use of the entire transverse cross section of the e-beam.

The subsequent series of experiments reported [27] served to raise outputs and lower efficiencies, slightly to 1.6%. As discussed above, the complicated effects that resulted from the anticorrelation of gain and efficiency tended to confuse the early phenomenology. In a final series of experiments the performance data was found to be characterized by relatively few free parameters. With the optimization of those variables efficiencies of 3% were achieved [12].

Apparatus

The excitations of the charge transfer plasmas used throughout this research were produced by the APEX-1 electron beam device constructed by Systems, Science & Software of Hayward, California. It is a fast pulse, sheet beam gun emitting 100 KA pulses of 1 MeV with a 1 x 10 cm transverse cross section. Burn patterns showed the current distribution to be uniform to visual inspection at the plane of entry into the laser cavity. As used in most studies, pulse shapes were nearly triangular with 20 nanosecond FWHM and, optionally, with the fall time controlled by a shorting electrode. The anodecathode spacing in the output diode was usually increased to give a larger diode impedance and consequently peak currents between 10 and 30 KA were obtained. Larger currents were not attempted in general as the operation under those conditions was rendered difficult by problems of foil survivability.

The experimental chamber used in these experiments consisted of an optical cavity mounted to a foil support assembly and contained in a cylindrical high pressure vessel with its axis of symmetry along the axis of beam propogation. The assembly was constructed of UHV-grade stainless steel with windows and gas handling connections made with Varian-type copper shear seals. The laser cavity consisted of a pair of dielectric mirrors which were mounted to allow angular alignment, spaced with 14 cm invar rods, and contained in the pressure vessel with the optical axis parallel with the longer 10 cm transverse dimension of the e-beam.

In operation the system was pressurized with 1 to 35 atmospheres of a mixture of helium and nitrogen. Useful partial pressures of nitrogen ranged from 2 to 120 Torr. Excitation was provided by the electron beam

from APEX entering through a supported, 0.002-in (0.05 mm.) thick titanium foil window and propagating in a direction perpendicular to the optical axis.

Effects of Mirror Geometries and Coatings

With this system, three laser lines were excited in mixtures of helium and nitrogen pumped by charge transfer from He_2^+. As expected, each corresponded to transitions from the same upper vibrational state, v' = 0, of the $B^2\Sigma_u^+$ electronic state to different lower vibrational states of the $X^2\Sigma_g^+$ electronic state of the N_2^+ molecular ion. The three lines and their respective vibrational transitions were: the 391.4 nm (0,0), the 427.8 nm (0,1), and the 470.9 nm (0,2). With the proper mirror set, each was excited individually. The most work was done on the (0,1) transition at 427.8 nm but since each had the same upper state, those same results should be roughly characteristic of all with the exception of the (0,0) transition which self-terminated at very early times.

Figure 3 provides a comparison typical of the time dependence of the power emitted in each of the three laser lines. Each was excited individually to obtain the data shown. As would be expected, a priori from the 25:4.4:1 ratio for the Franck-Condon factors from the upper v' = 0 state to the lower v" = 0,1, and 2 levels, respectively, the onset of threshold was proportionally delayed for the transitions to the states with greater v". As can be seen, the 391 nm component self-terminated in about 2 nsec and gave a measure of the time required for the lower laser state to "fill." Since the lower state of the 428 nm line differed only in vibrational quantum number, it had the same

degeneracy and should have "filled" to terminate the 428 nm transition in a comparable time. That it did not, as seen in the figure, is strong evidence for the existence of the unblocking process tending to quench the vibrational excitation of the lower, v" = 1, state of the 428 nm transition.

As initial examination of the raw data relating pulse energy to e-beam deposition did not reveal a trend suggesting the nature of the dependence of output on the various diverse experimental parameters. In fact, a highly degenerate system was found for which the same output was achieved, often with highly variable pulse shapes, from quite different experimental arrangements. Figure 4 illustrates this point, presenting results obtained at a relatively low beam current for a variety of gas compositions and mirror reflectivities. Each datum has three common features, a standard excitation pulse depositing 78 mJ atm^{-1} into the volume coupled to the detected fields, a plane-parallel optical cavity, and the emission of the single laser line at 427.8 nm. Both efficiencies and output are relatively far from optimal and the data is only interesting for its strong dependence on "spurious variables."

Although the plane-parallel optical cavity generally appears the most attractive in terms of analysis, a priori, in fact this is only the case for cw oscillation after stable cavity modes have developed. The transient response of such cavities to self-excitation is quite complex. This problem was considered in detail in contract reports [28] and an analytical procedure was developed to describe the time-dependent growth of the plasma volume interacting with the cavity fields. The results described the relative fractions of the energy extracted from the inversion that were coupled into the output at each particular instant and were

used to deconvolute the time-dependent laser intensity observed for a given measured average beam divergence. In this way the average field-plasma interaction volume and the fraction of the energy extracted from the plasma that was emitted into the output beam in comparison with that "walking off" the mirrors was determined for each measurement. Figure 5 shows the application of the resulting unfolding processes to data typical of that plotted in Fig. 4. The type of cavity, plane or hemispheric is denoted by P or H, respectively, followed by the output coupling fraction. Quite a variation of functional forms had been measured for the time-dependent intensity but all led to average volumes between 12 and 22 cm^3. That this unfolding process was meaningful is based on pragmatism. As will be shown below, it reduced the multivariate dependence of all the data obtained to a form dependent upon a single parameter, the pressure.

For the data at the lower end of Fig. 4, to exceed threshold, highly reflective mirrors had to be used which greatly raised the ratio of circulating power to emitted power on any particular pass. As a result, walk-off losses were very large. Figure 6 illustrates the effect of correcting this data with the ray-tracing program to obtain the total energy extracted from the plasma. The data for the first two cases of coupling shown in Fig. 5 are presented. Since average volumes were the same in both cases, the effect of walk-off was isolated. As can be seen, the pronounced differences in emitted energy are not found in a comparison of extracted energies.

The same agreement was found in all data taken with plane mirror sets, except those oscillating very near threshold at pressure of 3 to 4 atm. This analysis served to show that all of the available energy was

being extracted from the plasma by the fields even at relatively low intracavity powers and that the only effect of the varying mirror coefficients was to determine the rate at which that energy was extracted and whether it was routed into the transmitted beam or walked off the mirrors. This was a very important conclusion because it greatly facilitated the parameterization of the data.

To confirm the concept that the total energy extracted was independent of mirror parameters, over the range spanned by these experiments an effort was made to obtain a cavity geometry with low walk-off losses. It could be reasonably assumed that for hemispheric cavities with large angular aperture compared to the output beam divergence, ray stability existed for an appreciable region around the cavity axis. For such cavities the walk-off fraction could be expected to be negligible in comparison with plane-parallel cavities. For the same plasma conditions, then it could be expected that the energy emitted from a hemispheric cavity would roughly equal the total extracted with either mirror geometry and this was found to be the case experimentally. Thus, the overall procedure of data reduction of the laser pulses at 428 nm was found to simplify the multivariate dependence of all the measurements obtained from plane cavities into a form dependent upon a single parameter, the pressure, and to yield a value in agreement with the output measured from hemispheric cavities, assumed to be lossless.

Electron Beam Propagation and Energy Deposition

To determine the efficiency of the extraction of output energy the deposition of electron beam into the laser cavity must be accurately calculated. An essential factor in the understanding of the energy deposition from the beam lies in the fact that scattering and stopping

power do not have the same dependence [29] on atomic number, Z. As a consequence, it is possible to have a situation in which a considerable fraction of beam energy is stopped without appreciable scattering or, conversely, that the scattering is so great that the simple approximation of the product of the stopping power and penetration depth seriously underestimates the energy deposition, even for small fractional losses of beam energy.

The almost singular case of the light inert gases excited at beam currents below 20 KA falls into the first category, and simplifying assumptions exist which render the problem tractable without resort to the complex deposition code necessary for the computer modeling of inert gas halide laser. Subject to limitations on the product of gas density and beam penetration depth, discussed in previous work, [28], [30] the problem can be resolved into that of the differential energy loss in the gas of the electrons in the beam, the morphology of which is completely determined by the foil window through which the beam has entered. For a titanium foil, 0.05 mm thick, the following bounds on the domain of gas transparency were obtained.

$$PX(He) \leqq 273 \text{ atm cm} \tag{3a}$$

$$PX(Ne) \leqq 13 \text{ atm cm} \tag{3b}$$

$$PX(Ar) \leqq 4.3 \text{ atm cm} \tag{3c}$$

where P is the gas pressure in atmospheres and X is the penetration depth of the beam into the gas.

It can be seen from these results that, whereas the simplifying assumptions break down for argon (Z=18) at an inch of penetration at two

atmospheres, they remain valid in helium (Z=2) over the entire span of parameters required for practical operation of a small test laser device. For example, at 30 atmospheres pressure, the simplified model is valid to at least 9.1 cm depth of penetration which is sufficient to describe about a half liter volume excited by a 1 x 10 cm electron beam of divergence characteristic of transmission through a 0.05 mm titanium foil window at 1 MeV for currents less than 20 KA. At higher currents, the "drag e.m.f."[31] resulting from the return currents should be considered.

A complete analysis for helium including the dependence of stopping power and foil scattering on time-dependent beam energy has been calculated [28], [30]. It led to an average power deposition constant of 17.3 Megawatts/ℓ/atm/KA on the plateau and slightly different values on the leading and trailing edges of the pulse. However, in view of the uncertain detail of the time-dependence of the beam such analysis was deemed to be excessively tedious. A re-examination of the beam scattering as evidenced by burn patterns on plastic targets led to an expression for the average power deposition of

$$17.2 \text{ Megawatts}/\ell/\text{atm}/\text{KA} \quad , \qquad (4)$$

on the beam axis at the depth of penetration of the cavity center. This value was used for the calculation of efficiencies throughout the work reported here.

The actual values of current density in the electron beam were measured with a calibrated Faraday cup which replaced the pressure vessel and laser cavity. Particular attention was paid to relative timing and cable lengths so that the temporal relation between beam current and laser output could be determined subsequently. Output from the Faraday cup was directly recorded with a 519 oscilloscope. Laser

performance data were collected over a broad span of experimental parameters. Total pressures ranged from 1 to 35 atmospheres with partial pressures of nitrogen varying from 2 to 120 Torr. As discussed immediately above, the variation of cavity constants affected the rate of energy extraction from the e-beam plasma, but had little effect on its total. To within rather unrestrictive limits the deconvolution program was able to reduce the parameterization of the laser performance to dependence upon a single variable, the total pressure. The limits bounding this parameterization were primarily a consequence of three effects.

1) If the ratio of nitrogen to helium was so excessive that the conversion reactions changing He^+ to He_2^+ could not go to completion, the laser output was drastically reduced or prevented altogether.

2) If the combination of mirror loss and gas composition was such as to delay the onset of lasing until beam current was beginning to decrease at the end of the e-beam pulse, the outputs were again reduced or terminated. Evidently, in this case, the excited state chemistry was altered by the termination of the beam and competing processes such as recombination with the cooling electrons became important.

3) If the output coupling was so excessive that threshold was delayed for a time comparable to the quenching lifetime of the upper laser level, output energies were proportionally reduced.

Except for data obtained under those conditions, most of the data could be reconciled with a very simple parameterization of the total energy extracted from a standard plasma volume.

Laser Output

The largest laser outputs found at 427.8 nm in the raw data were from the hemispheric cavity having 27% output coupling and the average

volume appropriate to that data was 16.2 cm^3. This was chosen as the "standard volume." Since walk-off was assumed zero for the hemispheric cavities, the largest laser outputs, those from the 20-35 atm data, simply corresponded to unscaled measurements of the total energy emitted into the output beam. For the purposes of parameterization, other measurements was scaled to obtain the total energy extracted from a 16.2 cm^3 volume of the plasma, so that $E_x = (1 + \bar{W}) \times (16.2/\bar{V}) \times E_e$, where E_e was the energy emitted by the cavity into the laser beam, E_x was the total energy extracted from the plasma by the field, $\bar{V}$ was the average volume from which it was extracted, and $\bar{W}$, the average ratio of energy walking-off the mirrors to that emitted into the beam. As mentioned above, for hemispheric cavities, $\bar{W}$ was assumed to be zero.

Of the other laser lines, the problem of determining the absolute energy deposition from the electron beam in the radiating volume was particularly acute in the case of the 391.4 nm emission. Since the laser output in this case occurred so early in the course of the e-beam pulse, it would have been misleading to correlate the laser pulse energy with the entire e-beam input energy. Clearly it was only the e-beam energy which was deposited before the termination of the laser pulse that contributed to the laser excitation. In contrast to the case of the 428 nm line for which the energy deposited during the entire duration of the e-beam was assumed to contribute to the input "cost" of excitation, in the case of the 391 nm output the procedure was adopted of considering only that fraction of the e-beam energy input prior to the termination of the laser output pulse.

Because of the drastic difference in the pulse shape of the 391 nm transition the growth of the interaction volume in the laser cavity was

quite different as evidenced by the considerably increased divergence of the output beam. This, consequently, offered the best test of the deconvolution procedure because the variance of divergences and interaction volumes had been relatively small in the case of the (0,1) transition at 428 nm. For the self-terminating (0,0) transition at 391 nm the average interaction volumes were found to vary from 3.4 to 14 cm^3, a range which was more than sufficient to mask other systematic variation of laser output with experimental parameters such as pressure and current. Figure 7 shows the almost random appearance of the performance data for the 391 nm output energy plotted in the lower half of the graph. The marked improvement obtained in the upper half was the result of the deconvolution analysis, particularly the removal of the dependence on interaction volume. All data are represented in the upper half and the shading of the points to indicate the beam current has been removed to reduce confusion. Whereas the organization of the data into a compact group is the result of scaling the interaction volume, the large displacement of the points upward is the result of correcting for absorption and walk-off.

Because of the drastic difference in the pulse shape of the 391 nm output two expressions for the energy extracted were necessarily considered. First was the net energy extracted from the plasma, which was the measured output emitted into the beam corrected for walk-off losses according to the previous expression. For this case these losses were comparable to those observed for the 428 nm data at comparably low pressures. Second, however, was the gross energy extracted. This was the net energy plus the energy extracted by the fields in the cavity and subsequently re-absorbed at the end of the laser pulse. This re-absorption loss was also calculated by the unfolding program and in the case of the data of

Fig. 7 it was quite significant. Again, this is in contrast to the 428 nm data for which re-absorption was always less than 7% of the output and, hence, was neglected. This correction for re-absorption is the largest contribution to the upward displacement of the data seen in Fig. 7 and required that the data of the upper half of the graph be considered the gross energy extracted from the plasma by the fields in the cavity.

The resulting summary of measurements at both 428 and 391 nm is presented in Fig. 8. The total energy extracted from the 16.2 cm^3 of the charge transfer plasma is plotted as a function of total gas pressure. Data have all been scaled to correspond to excitation at the level of 76 mJ/atm by a standard discharge pulse containing 275 μ coul of integrated current. As mentioned earlier this choice sets all scale factors to unity for the higher pressure conditions run with hemispheric cavities so that the larger pulse energies shown in Fig. 8 are simply equal to the values measured in the output beam. When plotted in this manner the gross extraction of power by the circulating fields from the population inversion pumped by the kinetics can be shown to comprise the "master curve" of laser performance depending upon a single parameter, the total pressure. The particular form of the master performance curve shown in Fig. 8 is in good agreement with the kinetic model described in the previous section [10].

It can be seen from Fig. 8 that even though the 391 and 428 nm outputs start at substantially different times in the life of the plasma, the same integrated extraction efficiency is achieved. That this energy is not extracted in the (0,2) transition at 470.9 nm is a consequence of the relatively small cross section for stimulated emission, as well as the small transition probability and, hence, slow accumulation

of spontaneous emission at this wavelength necessary to initially excite the cavity oscillations. Evidentally the cooling of the plasma at the end of the e-beam discharge destroys the stored energy of the inversion by recombination of the ions. Either a longer duration e-beam pulse or an external source of cavity excitation would be necessary to extract the stored energy at 471 nm.

Operation of a Regenerative Power Amplifier at 470.9 nm

As shown in Table 1, the cross section for stimulated emission on the (0,2) vibrational component at 470.9 nm should be smaller than the corresponding cross section at 427.8 nm by a factor of about 3.6. However, the resulting difficulty in starting cavity oscillations is not the only factor impeding the effective operation on this line. The problem of the efficient extraction of the energy from the inversion is further compounded by the correspondingly increased saturation intensity. Elementary considerations show that the saturation intensity at 471 nm reaches 190 KW cm^{-2} when the value at 428 nm is the measured 58 KW cm^{-2}. If oscillations could be started despite the smaller gain, it would be necessary to maintain a higher level of circulating power in order to achieve comparable efficiencies. Both effects contribute to the relative weakness of the outputs from self-excited oscillators operating on this blue-green line, even with high levels of excitation as shown in Fig. 3.

Not only must the growth rate of the intensity at 471 nm be adequate to attain the saturation intensity in a time comparable to the lifetime of a photon in the cavity but another criterion must be met to attain successful operation in the self-excited oscillator geometry. The desired growth of the blue component must exceed that of other components

resulting from transitions from the same upper laser level. This requirement can be conveniently expressed,

$$R_B \ell^{\gamma_B L} > R_V \ell^{\gamma_V L} \quad , \tag{5}$$

where the subscripted B and V denote the blue and violet transitions at 471 and 428 nm, respectively, the γ represents the small signal gain per unit length of the plasma, the R represents the mirror reflectivity for the indicated component, and L represents the length of the amplifying medium. If Eq. (5) is satisfied, then upon each transit of the plasma followed by reflection at the mirrors, the intensity of the blue transition will grow more than that of the violet. Saturation of the gain will, of course, render the equivalent inequality for higher intensities more complex but since both transitions have the same upper level, both will be reduced by the saturation and thus, the transition "starting first" will extract most of the energy stored in the upper state population.

Over the useful range of operating parameters, the inequality of Eq. (5) can be reduced to a more tangible form by recognizing that in practice the "lasing" of a self-excited oscillator means having achieved a total small signal growth of the initial spontaneous intensity of a factor of the order of 10^6 to 10^7 after N transits of the medium so that

$$\ell^{N\gamma_B L} \sim 10^6 \quad , \tag{6}$$

represents an approximate quantification of the condition for successfully exciting the blue line. Solving Eq. (6) for

$$\ell^{\gamma_B L}$$

and substituting from Table 1 the relation $\gamma_V = 3.6\ \gamma_B$ gives an approximation for the number of cavity transits required for the oscillation of the system individually on the blue line and not on the violet,

$$N \gtrsim 35\ [\log(R_B/R_V)]^{-1} \quad . \tag{7}$$

The critical parameter for the isolation of the less probable blue line is the ratio R_B/R_V which is a measure of the wavelength separation factor of the mirrors for the two transitions. For the data of Fig. 3 the value of R_B/R_V was about 3 so that $N > 33$ transits of the cavity should have been necessary for the initiation of laser output at 471 nm. The time for a transit was of the order of 0.5 nsec so that "threshold" should have occurred around 18 nsec, an expectation in reasonable agreement with the results observed.

About the best separation factor which can be obtained for the mirrors appears to be around 25 if a bandwidth comparable to that of the gain is to be maintained. This offers only modest improvement, to $N \geq 11$, and suggests that the operation on the blue line is best achieved with some variety of amplifier geometry. In agreement with these expectations the best outputs actually achieved with such mirrors were of the order of a few hundred KW and occurred too late to approach a level of energy extraction comparable to that achieved at 428 nm. Moreover, these considerations seem to preclude the individual excitation of the (0,3) transition at 522.8 nm, at least with the existing e-beam machine. For that transition in the yellow, $\gamma_Y = 14.0\ \gamma_V$, and the numerical factor in Eq. (7) would become 180 instead of 36. With a comparable

separation ratio for the 523 nm line as was used to obtain the data of Fig. 3, even comparably low output would be obtained only after about 90 nsec of excitation.

The value of saturation intensity required at 471 nm is not large in comparison with that of excimer transitions. In fact it is reasonable to expect that 200 KW cm^{-2} peak power might be readily achieved in a small oscillator and then injected into the e-beam cavity in order to achieve an early saturation of the charge transfer plasma.

Such an experiment has been recently reported [32] in which an optical regenerative amplifier was operated successfully on a component of this blue-green (0,2) band of N_2^+. The optical cavity used in those experiments consisted of one plane and one concave mirror separated by 12.5 cm and arranged on an axis perpendicular to the direction of e-beam propagation. Dielectric coatings were obtained to give a mean photon lifetime in the cavity of 20 nsec at 470.9 nm and only 0.8 nsec at the 427.8 nm wavelength corresponding to the (0,1) component, thus corresponding to a wavelength separation ratio, as shown in Eq. (7) of 25.

A master oscillator was constructed from a pulsed dye laser using coumarin 1 dye pumped by a conventional nitrogen laser with a peak power of several hundred kilowatts. An intracavity telescope together with an 1800 line/mm grating in the dye laser cavity gave an oscillator bandwidth corresponding to about 0.07 nm at 470.9 nm. Peak power of the order of one kilowatt were obtained within this bandwidth.

Output from the master oscillator was coupled into the cavity of the regenerative amplifier through the partial transparency of the plane mirror. Unfortunately the relatively long photon lifetime in the cavity together with the rather short duration of the oscillator pulse combined

to render the coupling of the oscillator to the amplifier comparatively weak. Most of the illumination incident upon the amplifer cavity was rejected and the intracavity fields could not in single pulses build to values much in excess of the external fields. As a result, it was estimated that the peak oscillator power actually coupled into the amplifier was of the order of a few hundred watts at best.

Synchronization of the dye laser oscillator with the e-beam was accomplished by delaying a timing pulse from the e-beam command circuit with a variable delay generator and then using it to trigger the thyratron switching the nitrogen laser pumping the dye. Overall system jitter was of the order of 50 nsec and was observed to be quite random. This required an undesirably large number of e-beam discharges be made in order to obtain a few in which synchronization occurred to an accuracy comparable to the mean lifetime of an oscillator photon in the amplifier cavity.

Figure 9 shows typical data obtained when favorable timing was achieved. The intensity of the amplifier output at 470.9 nm is shown as a function of time following the onset of the e-beam current. Under these conditions the amplifier plasma was being pumped by an e-beam sheet reaching a peak current of the order of 22 KA with transverse dimensions of 1 × 10 cm. The dotted lines in Fig. 9 bound the variance in the times at which the e-beam current had decayed to 1/e of the peak value. This variance itself was contributed by an auxiliary crowbar electrode in the e-beam diode envelope which served to chip the low energy tail of the pulse in order to improve the foil lifetime.

Data from two separate discharges are shown in Fig. 9 together with the individual oscillator pulses injected into the amplifer cavity. In

order to render both signals visible on the same scale the pulse from the oscillator was obtained from the dye laser beam rejected by the amplifier cavity. Being of low divergence it passed completely through the apertures providing geometric attenuation of the more divergent beam subsequently emitted from the cavity. Thus, although the sensitivity scales were the same between the successive discharges shown in Fig. 9, the oscillator pulses were not on the same scale having bypassed a total of several order of magnitude of attenuation.

The upper trace in Fig. 9 can be seen to correspond to nearly optimal occurrence of the oscillator timing. The lower occurred too early by about two mean photon lifetimes in the cavity implying that the oscillator intensities circulating within the amplifier cavity were down by more than a factor of 7 at the start of the e-beam discharge. Nevertheless, even this reduced level of injected energy resulted in some output as the power emitted from self-excited oscillations in the amplifier was generally inadequate to record on the oscilloscope and could only be dimly seen as a very diffuse pattern on a screen in a darkened room. In contrast the output corresponding to the upper trace was visibly both intense and compact as expected from the appearance of the pattern of the oscillator power re-emitted from the amplifier cavity in the absence of e-beam excitation.

Figure 10 shows the dependence of the amplifier output on the time delay between the onset of e-beam current pumping the amplifier and the arrival of the optical pulse from the oscillator. This delay could not be controlled on the time scale shown and the points plotted represent the random delays resulting from the system jitter. The data from the lower trace in Fig. 9 is not shown as it would have plotted below the

coordinates chosen. The decrease in output with the increasingly early arrival of the oscillator pulse is roughly consistent with the inferred lifetime of those photons in the amplifer cavity.

Somewhat surprising is the apparent occurrence of the peak in Fig. 10 at small negative times. This may have resulted from non-optimal coupling of the oscillator fields into the cavity. The mean photon lifetime in the cavity quoted earlier as 20 nsec corresponded to purely axial propagation. Since this represented fewer than 50 cavity transits, the excitation of stable cavity modes could not have been necessarily expected. If the amplifier cavity is considered to have been an optical waveguide folded upon itself, the stably propagating modes must have consisted of bundles of rays periodically converging and diverging upon reflection at the cavity mirrors. For non-ideal bundles of rays initially incident upon such a structure the divergence is great after several reflections and the fraction of propagating photons walking-off the mirror on the next reflection is large. However, once the maximum divergence has been past the subsequent pattern of focusing and defocusing is simply periodic and the remaining photons stay in the cavity until they are transmitted through the mirrors. It can be reasonably expected that the energy finally emitted into the output beam would be greater if the maximum divergence of the circulating intensity, with its high loss of photons, had passed before amplification ensued. This would require an early arrival of the incident pulse from the oscillator and could explain the peak performance seen in Fig. 10 at small negative times.

Interferometric measurement of the amplifier output showed the laser line to be considerably narrowed. An FWHM of 0.007 nm was found in contrast to either the 0.07 nm bandwidth of the oscillator pulse

originally injected into the cavity or to the 0.11 nm pressure-broadened bandwidth of the gain of the medium. Thus it appears the system described here was not working as a conventional injection-locked oscillator in which a narrow band input serves to frequency-lock a broadband amplifier. This was confirmed by the inability of the amplifier to track the oscillator as it was tuned to either side of the output line by a measurable amount. Rather the system seemed to operate as an optical regenerative amplifier in which the useful portion of the input bandwidth excited growing oscillations in the amplifier cavity. In any case it appears that the injection of broadband illumination near 470.9 nm into an amplifier cavity offers a means not only of switching the nitrogen ion laser output into the blue-green but also provides the radiation needed to reach an early saturation of this low-gain transition so that optimal efficiency may be achieved.

Temperature Dependence

With the e-beam excitation the most recent advances in laser performance have resulted from cooling the gas. Recognizing that the effectiveness of the multibody reaction channels appearing in Fig. 1 should be inversely correlated with the gas temperature, it was expected that the overall laser output would be somewhat temperature dependent. Unfortunately the existing laser device was not designed for thermal cycling and this together with the relatively high thermal conductivity of helium made the accurate control of gas temperature very difficult. Best control was obtained by mounting the device on a 30 cm drift tube which was then connected to the electron beam gun with an additional foil assembly. When the drift tube was filled to a rather critically defined pressure of nitrogen of around 0.5 Torr about half the electron

beam current could be conducted to the laser device. Under those conditions the more limited thermal conductivity reduced the thermal flow from the gun and afforded some control over temperature in the laser.

Cooling in that arrangement was accomplished by circulating cold liquid nitrogen vapor through a heat exchanger attached to the pressure vessel containing the laser device and the average gas temperature in the cell was determined by measuring the pressure as the system cooled. Since the laser cavity was positioned closest to the source of the thermal flow into the heat exchanger, the actual temperature in the laser cavity was necessarily higher than the average gas temperature. Hence, the following data presented underestimate the effect on laser output of reduced gas temperatures by underestimating those temperatures. However, the variation of laser output with changes in average gas temperature in the pressure vessel could be obtained. Figure 11 shows the effect of continuously cooling the gas prior to the electron beam discharge at a nominal current down the drift tube of 11 KA. As can be seen factors of improvement of as large as 10 were achieved for a 42°C decrease in average gas temperature. As might be expected, the limiting temperature appears not to have been reached at -20°C.

In an attempt to verify that the thermal enhancement observed was not limited to excitation at the low current available from the drift tube, the laser device and liquid N_2 heat exchanger were connected directly to the electron beam gun. Though not as remarkable as the effects on the outputs from the drift tube configuration shown in the previous figure, the effects of a similar decrease in average temperature on discharges at higher currents and pressures were substantial. "Best" outputs at each pressure were increased by a factor of approximately 2

for a 40 to 50°C decrease in the average gas temperature which in this configuration even more seriously underestimated the actual gas temperature in the laser cavity. It was found that the low temperature data had the same dependence upon the total gas pressure shown in Fig. 8, but was raised by a scale factor of approximately 2. In fact the data was closely approximated over the range of pressure examined to 30 atm by the parameterization of the efficiency

$$\varepsilon(-20°C) = 6.8\% \ (P/56)^{1.2} \quad , \tag{8}$$

where P is the equivalent gas pressure at room temperature, and 6.8% is the limiting quantum efficiency.

The actual dependence of laser output on gas temperature is, in fact, more complex than might be inferred from Eq. (8). In part, this results from the effect of cooling on the quasi-cw operation of the laser. Probably, through an enhancement of the three-body reactions in the kinetic sequence and through some narrowing of the pressure-broadened gain bandwidth, cooling of the gas tends to initiate quasi-cw operation at a lower operating pressure than would otherwise be possible. This is best seen in Figs. 12a and 12b which show the time dependence of the power emitted at a relatively low pressure for nominal discharge currents of 15 and 20 KA, respectively. To facilitate the estimation of the time dependence of the efficiency for the emission of the output power relative to the input power to the cavity, a constant fraction of the input power has been shown by the dashed curves.

It can be immediately seen that in neither case is quasi-cw operation in evidence at room temperatures. In both figures the output is seen to terminate before the input. However, as the temperature was decreased,

two effects were noticed. First, quasi-cw operation was maintained for later times and the constancy of the power conversion efficiency improved with decreasing temperature. Secondly, at sufficiently low temperature, around -20°C, the onset of threshold occurred earlier with operation at constant efficiency being more rapidly attained. From the standpoint of efficiency with respect to input power, the constant level of 1.9% seen in Fig. 12a achieved after onset of threshold at 7.7 atm pressure and 15 KA excitation current is considerably in excess of the value of 0.6% consistent with the parameterization given by Eq. (8).

The same general behavior was found at higher pressures as shown in Fig. 13 for the excitation of 11 atm of gas mixture at a nominal 20 KA of beam current. These results suggest that the efficiency most characteristic of the laser performance is the steady state value of the power transfer efficiency reached at later times when the transition is fully saturated. At least over the range of times available to these experiments it appears that at low temperatures the laser output can be expected at that level of efficiency for as long as it is pumped by the electron beam. Such operation is of extreme importance as it points the way toward much longer output pulses to be obtained from longer discharge pulses. The processes which must ultimately limit completely continuous operation could not be determined from this data as no degradation of output could be detected over the range of times for which excitation could be sustained.

Finally this quasi-cw operation characteristic of a 4-level laser was observed at the highest pressures which could be accommodated by the existing pressure vessel. As seen in Fig. 14 operation at a steady-state power efficiency of 3% was achieved at -20°C for an average gas density

corresponding to a pressure of 35 atmospheres at room temperature. The corresponding pulse energy was 80 mJ and represented a peak power density of 320 MW ℓ^{-1}, and an energy density of 5 J ℓ^{-1} at an efficiency of 3%. Intracavity circulating powers reached a peak of over 1.2 GW ℓ^{-1} at an intensity greater than 20 MW cm^{-2} with no evidence of either bottlenecking or photoionization of any of the species important to the kinetic chain.

DIRECT DISCHARGE EXCITATION

Early reports [14], [15] of the discharge excitation of the laser transition at lower current densities than used in the e-beam studies presented output efficiencies of only about 0.05% of the total stored energy. No instantaneous efficiencies were reported and whether the lower overall values resulted from a decoupling of the plasma load from the driving circuit or whether it resulted from some failure of the kinetic mechanisms in the discharge environment was not determined. Other discrepencies were found in the timing of the development of the laser pulse that intensified concern over the similarity of the pumping mechanisms under the different conditions of excitation. While the results for e-beam pumping had indicated a delay of 5-10 nsec between the onset of the excitation current and the initiation of the laser output, a more immediate development of the laser output was observed from the discharge plasmas having greater gain pathlengths. Less than 1 nsec delay was observed with an output pulse risetime of the order of 2 nsec. Using the accepted values of the binary rate coefficients available at that time, the lifetime against charge transfer from helium to nitrogen should have been in excess of 10 nsec at 3 atm pressure of the gas compositions generally used. This apparent inability of charge transfer

to pump the laser transition fast enough together with the lower efficiencies led Ischenko et al. [6] to misidentify the principal kinetic step as being direct collisional excitation of neutral nitrogen by hot electrons in the tail of the energy distribution present in their wall-stabilized discharge.

The multibody charge transfer collisions reported subsequently [19], resolved this problem by providing the necessarily high rates of reaction. For example, at 5 atm pressure the reaction time for the charge transfer step shown in Fig. 1 was reduced by nearly 60% to a value of 1.8 nsec for the gas mixture containing 0.15% N_2 usually used. It thus became consistent with the timing of the laser outputs to attribute the operation of the helium-nitrogen laser under either e-beam, or direct discharge pumping to the common excitation scheme charted in Fig. 1 for the rate coefficients summarized in Table 1. In fact the studies of the instantaneous power transfer efficiencies reported in part in recent notes [16]-[18], showed that the lowered output efficiencies generally occurred as the result of a loss of coupling between the electrical load and driving circuits caused by the time-varying impedance of the laser tube. At the E/p values of the order of 5 V cm^{-1} $Torr^{-1}$ and the current densities of 100 A cm^{-2} employed in that work power transfer efficiencies of 2% were reported, with peak powers of 5 MW.

Preionized Atmospheric Electrical Avalanche (AEA) Lasers

A schematic representation of the main discharge system together with the principal diagnostic circuitry used in the studies mentioned above is shown in Fig. 15. The laser tubes consisted of machined delrin or acrylic pressure vessels containing electrodes which could be varied

in length from 10 to 137 cm. The thickness and separation of the electrodes could be varied to give apertures ranging from 0.1 to 1.4 cm^2, though not necessarily for each possible length.

The data most suitable for analysis in terms of power transfer efficiencies were obtained with a configuration employing 87 cm long electrodes of 0.3 cm thickness separated by either 1.3 cm or 1.7 cm [16]. The current flow in the tube was transverse to the optical axis giving computed inductances for the laser tube of 0.23 and 0.3 nH, respectively, for the two possible electrode spacings. Measured values agreed with the computed values to within experimental error. As shown in Fig. 15 the laser tube was connected in a lumped Blumlein circuit switched by an EG&G 3202 hydrogen thyratron. For the studies of power transfer efficiency the capacitors marked C in the figure were constructed from 0.08 cm thick G-30 printed circuit board, copper clad on one side and contacted to two sheets of 0.039 cm thick mylar on the other. A foil electrode contacted to the outer surface of the mylar completed the capacitors giving a value of C=12 nF for each. Other configurations were utilized in scaling studies.

In operation the electrical performance of the main discharge circuit resembled that of the neutral N_2 laser described and analyzed in detail by Fitzsimmons [33]. Because of the relatively high inductance of the thyratron, the switching circuit functioned as a lumped LCR circuit which, upon commutation of the thyratron, tended to invert the voltage across the left capacitor in Fig. 15. The ringing period of the switching circuit was of the order of 100 nsec in this arrangement.

As the voltage across that capacitor proceeded toward a full inversion, the voltage across the laser tube tended toward twice the original

charging voltage. At some point, depending upon the pressure and gas composition in the laser tube, the E/p would reach a value sufficient to support the avalanche growth of the ion concentration in the gas mixture, thus initiating the kinetic chain pumping the laser transition. As the laser medium became more heavily ionized, the conductivity increased permitting the energy storage capacitor to the right of the first laser tube in Fig. 15 to discharge through the laser plasma on a time scale short compared to the original ringing period of the switching circuit. In the atmospheric electrical avalanche (AEA) device finally realized in those experiments, discharge currents up to 30 KA could be attained with risetimes of a few nanoseconds. Switched voltages approaching 50 KV could be developed across the laser tube prior to breakdown.

As the avalanche proceeded to completion in the laser medium, the conductivity of the plasma continued to increase until the discharge impedance dropped below the impedance of the stripline comprising the energy storage capacitor. At that point the laser tube effectively short circuited the line allowing it to discharge at high current with little voltage drop across the laser plasma. The resulting decrease of E/p in the plasma then permitted the electrons to "cool", effectively terminating the laser pumping kinetics by stopping the production of new ionization. In fact it was found that useful power was coupled into the plasma load only for relatively short times and the majority of the energy originally stored in the capacitors persisted in ringing through the electrically shorted plasma remaining at the end of the avalanche. This suggested the use of several identical laser tubes coupled to the driving circuit in a transverse series connection, as shown schematically by the dotted portion of Fig. 15 so that one tube could act as the

switching device for the next. In this way a relatively fixed synchronization could be maintained between the plasmas and the laser output from one could be threaded back through the next after an appropriate optical delay had been introduced so the entire system could function in a master oscillator power amplifier MOPA configuration. Moreover, the overall efficiency would be improved, since the energy stored on the first capacitor and lost in the commutation would be needed only once in the system. In operation each laser tube would be driven by the energy stored in the capacitor, C, of the stripline immediately to its right as shown in Fig. 15. The operation of such a discharge sequence is discussed in the following section.

It was found that regardless of the number of component tubes excited adequate preionization was necessary before the main discharges could develop uniform and stable plasmas. In the AEA laser finally realized in this work spatial uniformity was achieved up to 9.3 atm pressure in discharges with transverse aspect ratios varying from 1 x 1 to 6 x 1 through the use of displacement current preionization, a technique superior to UV-preionization in relatively "transparent" gases such as helium. For each tube a potential of the order of 40 to 50 KV was applied to an electrode outside its pressure vessel in a manner to create an intense electric field perpendicular to the axis of discharge current flow and perpendicular to the optical axis. The high voltage pulse was developed by a cable transformer driven by a grounded grid thyratron switching a low-inductance capacitor. A delay of the order of 0.5 to 1.0 microsecond between the preionization and the main discharge was found to be necessary. Since both the preionization and the main discharge were switched by hydrogen thyratrons the AEA laser could be

readily operated at repetition rates from 1 to 30 Hz. Because of the longitudinal gas flow, excessive heating prevented the operation of the device at high repetition rates. However, it appeared that a transverse gas flow would allow operation at much higher repetition rates.

As shown in Fig. 15, the electrical performance was monitored by voltage and current probes connected to the first laser tube. A tapped water resistor was placed across the tube and inductively decoupled from the ground of a Tetronix 519 oscilloscope to provide the means for measuring the voltage difference applied across the laser tube. The current flowing in the discharge loop was monitored with a $\dot{B}$ loop which could be rotated through 180°. In fact, this rotation proved necessary because of the capacitive coupling between the loop and the extended capacitors. Each measurement of current was determined from the difference of two measurements of $\dot{B}$ made with the plane of the loop being rotated through 180°.

Typical diagnostic data were presented in Ref. [16] together with performance data which will be reproduced here for convenience. Optimal performance of the laser, when operating with a single tube coupled to the fields in the geometry of a self excited oscillator, was found to correspond to conditions for which the duration of the avalanche spanned the time of occurrence of the maximum in the open circuit voltage developed across the tube under calibrating conditions for which the avalanche was inhibited. As was expected, increases in pressure in the laser tube caused progressive increases in the delay of the onset of the avalanche with corresponding increases in the voltage developed until the desired maximum was reached. For example, at a charging voltage of 24 KV, the optimal performance was found to occur for pressures of the order of

3.7 atm in agreement with the maximum actually observed in the laser output. Conversely, at a high pressure of 5.1 atm the developing avalanche was found to be competing for stored charge with the "ringing down" of the voltage in the switching circuit. A correspondingly lower laser output was observed in that case.

The time dependent current was obtained by numerically integrating the dI/dt curve obtained with the $\dot{B}$ probe. The absolute scale factor was obtained by setting the second integral of dI/dt equal to the charge stored in the series capacitance formed from the two capacitors at the time of breakdown. The instantaneous power dissipation in the load was then obtained by forming the product of the two curves of current and voltage measured across the load, suitably corrected for stray inductive effects [16].

A comparison of the time-dependence of the input power and the laser output power showed that the smaller electrode spacing resulted in a better power conversion efficiency, probably because of a more thorough saturation of the optical transition. Results for the 1.3 cm spacing of the electrodes are shown in Fig. 16 for the four values of gas pressure indicated, each containing 0.15% N_2. The charge voltage was 24 KV and the repetition rate was 10 Hz. Dashed lines show the discharge currents and the voltages which appeared across the resistive part of the load. The powers dissipated in the load are shown by the dotted curves and the solid curves record the laser output power measured in the $(0 \rightarrow 1)$ vibrational component of the $B \rightarrow X$ electronic transition of N_2 at 427.8 nm.

The pressure-dependent delays seen in Fig. 16 between the input powers applied to the plasma and the laser outputs are consistent with the magnitudes of the reaction times for the charge transfer step as

computed from the coefficients shown in Table 1. The scales for the power have been chosen as indicated, so that the close correlations between input and output powers on the leading edges of the curves for the high pressure plasmas correspond to an instantaneous conversion efficiency of 2%. Integrals under the power curves shown in Fig. 16 give values for the energies of the laser pulses of 1.3, 2, 3, and 4 mJ, respectively, for the pressures varying from 3 to 5.1 atm. These results in comparison with the integrals under the input power curves yield efficiencies of 1.3, 1.0, 1.0, and 0.8% respectively, for the conversions of the energies dissipated in the loads for the cases shown in Fig. 16.

The field strength in the plasma corresponding to the maximum observed transfer of power also can be determined from Fig. 16. At the higher pressures where the delays in the kinetic chain were minimal, the highest instantaneous power conversion efficiencies can be seen to have occurred on the leading edges of the pulses where the values of E/p were the greatest. For the times at which the 2% efficiency was sustained the E/p can be computed from Fig. 16 to have been decreasing from 3.5 to 2 V cm^{-1} $Torr^{-1}$. The corresponding current density was increasing from zero to 160 A cm^{-2}. The best efficiency for the energy extracted was found for pulses developed from avalanches initially driven by a peak E/p of the order of 5 to 6 V cm^{-1} $Torr^{-1}$.

It can be seen that the loss of efficiency for the conversion of the pulse energy at the higher pressures resulted from the prolonged flow of discharge current at relatively low E/p. In fact the current pulse was generally observed to ring back and forth through the laser tube until finally damped by resistive losses in the gas. For clarity this subsequent behaviour of the discharge was not shown in Fig. 16.

Although the corresponding value of E/p in the gas following termination of the avalanche was too low to resolve in the figure, its much greater duration provided for a greatly protracted "tail" of low amplitude on the latter part of each of the power input curves. The integral of this dissipation corresponded to the final loss of a significant part of the energy initially stored on the discharge capacitors.

Preionized Avalanche Amplifiers

Attempts to study the scaling of the AEA laser described above were rendered difficult, in part, by the limitations on the range of operating parameters imposed by the dependence on the experimental variables of the level of gain necessary to develop saturation intensity during the relatively brief period of effective power transfer to the load. As described in the discussion of the kinetics pumping the inversion in this type of system, the optimization of the gain generally insured a degradation of the kinetic efficiency. Computations showed that losses of 30 to 50% of the potential efficiency of the kinetic chain could result from optimization of the gain under typical conditions. In fact a recent review of performance data within the extant data base has indicated that the actual outputs achieved from the nitrogen ion laser, whether excited with an e-beam or with a preionized discharge, had been generally dominated by the photon extraction parameters. However since the saturation intensity of the laser transition was shown to be low enough to be readily reached with a small discharge pumped oscillator [18], it became clear that the more efficient mode of operation for these charge transfer devices was not the self-excited oscillator configuration generally employed, but rather an oscillator-amplifier combination

from which the majority of the energy could be extracted at near-zero gain.

The first operation of an optical amplifier for the 428 nm line of N_2^+ pumped by charge transfer from He_2^+ was reported in 1978 [18] and served to provide experimental values of the saturation intensity of the transition. In that work two laser tubes were discharged in the transverse series arrangement mentioned in the previous section. The second laser plasma was used as an amplifier and was connected electrically to the first as shown by the dotted portions of Fig. 15.

In operation the discharge circuitry associated with the first laser tube performed in a manner unaffected by its connection to the second tube. Operation of the second tube was consistent with the same equivalent circuit describing the first except that the first tube played the role of the switching element in place of the thyratron. Because of the lower inductance of the first tube in comparison to the thyratron the ringing time for the inversion of the middle capacitor was shortened by about a factor of two, giving a relative delay of about 25 nsec between the two laser plasmas. Both tubes were synchronously preionized and were switched by hydrogen thyratrons as described above.

When run as independent, self-excited oscillators the two tubes gave essentially the same laser output at 427.8 nm provided operating conditions were not excessively close to threshold. For example, at 3.7 atm of helium containing 0.15% nitrogen and at a charge voltage of 22 KV the first tube produced output pulses with peak power of 225 KW while the second tube gave 270 KW. This was somewhat below the 420 KW produced by a single tube connected between two of the capacitors. Considering the relatively wide range of operating parameters over which an instantaneous

power conversion efficiency of 2% was achieved in such a single tube, it is more likely that the lowered outputs from each of the two tubes in series resulted from less input electrical power being successfully coupled into the plasmas rather than from a loss of instantansous conversion efficiency within the plasmas. Unfortunately, because of grounding problems the instantaneous electrical characteristics could not be directly measured as had been done when a single tube was used.

When the mirrors were removed from the second tube under the same operating conditions the output dropped over two orders of magnitude indicating that uncontrolled superfluorescence had been of negligible importance. Then about 10% of the output from the first tube, running as a self-excited oscillator, was suitably delayed and threaded back through the second tube. Under those conditions the output from the second tube was measured to be 560 KW and the beam divergence was reduced by a factor of better than two below that which had been obtained from the same tube running as a self-excited oscillator. The insertion of calibrated neutral density filters into the beam from the oscillator input to the amplifier permitted the quantitative measurement of the amplification factor of the second laser plasma over a dynamic range of five orders of magnitude. Typical data are shown in Fig. 17 for one of the different operating conditions for which the discharges could be synchronized with the same optical delay line. The data shown correspond to an operating pressure of 3.7 atm and to a charge voltage of 22 KV. The growth of an optical pulse in an amplifying medium has been shown theoretically [34] and confirmed experimentally in the helium nitrogen system [18] to be described by the expression,

$$I_{out} = I_s \ln[1 + \ell^{I_{in}/I_s} - 1) \ell\gamma L] \quad , \qquad (9)$$

where γ is the gain, L is the length of the plasma, and I_{in} and I_s are the input and saturation intensities, respectively. In the limit of an input intensity from an external oscillator which is large compared to the saturation intensity, the expression takes a particularly simple form

$$I_{out} = I_{in} + \gamma L I_s \quad . \tag{10}$$

This is the ideal limiting case of the extraction of power at zero gain and corresponds to the removal of an optical power of γI_s from the plasma per unit length. The intensity, I_s, is an intrinsic parameter depending little upon experimental conditions and γ is an extrinsic variable directly related to the strength of the pumping. While the simple expression for kinetic branching $I/(I + I_s)$ predicts 50% extraction when $I_{in} = I_s$, the growth of the intensity increases this amount.

The solid curve in Fig. 17 plots the output powers computed from Eq. (9) where the two parameters have been adjusted to obtain the agreement shown. The value of saturation intensity, I_s, used was 58 KW cm^{-2}. The sensitivity of the model to this adjustable parameter was greatest at the higher input powers where Eq. (9) reduces approximately to the asymptotic form, Eq. (10), the expression for the extraction of power from the inversion under the fully saturated conditions of zero-gain. Thus, at the limits of high input power the uncertainty in the product $I_s \gamma L$ was linearly dependent upon the uncertainty in the measurement of the output intensity. As seen in Fig. 17, this was about ±15%. The sensitivity of the model to the gain, γL, was greatest under small signal conditions as shown in the figure where the effect of varying the gain by ±10% is illustrated. Even the poorly resolved data obtained from the amplification of 10 mW input pulses were sufficient to determine

the overall gain parameter, γL, to within 10%. The particular value corresponding to the solid curve approximating the data was 14.5.

It is interesting to notice that in these particular cases the overall gain which depends upon the inversion density, was reported [18] to have scaled in a manner directly proportional to the pressure. The saturation intensities, while not resolved significantly, appeared to have scaled more slowly with pressure and a dependence on $\sqrt{P}$ was suggested. As discussed above, since I_s is essentially an intrinsic parameter only a very slow variation with operating conditions would be expected through changes in the bandwidth of the gain. The two values of I_s reported previously [18] corresponded to linewidths centered around 4.9 cm^{-1}, a reasonable value for pressure broadening at 3 to 4 atmospheres.

Under the highest gain conditions reported, those of Fig. 17, a small signal gain along the 85 cm path of 1.5×10^6 was observed with little uncontrolled superfluorescence and the corresponding zero-signal gain was $\exp(14.5) \sim 2 \times 10^6$. Under the same operating conditions a gain of about 18 was found at output intensities of 1 MW cm^{-2}, conditions relatively near the ideal extraction of power at zero gain. At input intensity levels of the order of I_s, 50 to 60 KW cm^{-2}, the power extracted from the amplifier was over twice that obtained from the same plasma coupled to the fields in a self-excited oscillator.

More recently it was desired to confirm those measurements of saturation intensities and gains in several different amplifier geometries, but without the direct electrical connection between the oscillator and the amplifier. Two completely independent devices were constructed and synchronized to discharge with a reasonably constant phase delay. The smaller of the two was coupled to the fields in the geometry of an

oscillator and its output was threaded through the 137 cm length of the larger device after undergoing a suitable optical delay. The cross sectional area of the plasma in the amplifier was 1.4 cm^2 in contrast to the 0.6 cm^2 used to obtain the data reported previously [18].

When operated at a charge voltage of only 22 KV, discharges into 4.3 atmospheres of helium containing 0.15% N_2 resulted in the extraction of 2.8 MW in a 14 mJ pulse with an input from the oscillator of only 16 KW. However for consistency with previous work, the measurements of the gain and saturation were performed at 3.7 atm pressure. A charge voltage of 20 KV provided a reasonable level of excitation.

Calibrated neutral density filters were again used to attenuate the oscillator power input to the amplifier permitting the quantitative measurement of the amplification factor of the second laser plasma over a dynamic range of six orders of magnitude. The resulting data are shown in Fig. 18 for the two different operating geometries, each being identified by the cross sectional area of the amplifying plasma. The corresponding lengths to the 0.6 and 1.4 cm^2 cross sections were 85 cm and 137 cm, respectively and the charge voltages were 22 and 20 KV, respectively. Common parameters were maintained in the operating media which were 3.7 atm of helium containing 0.15% N_2.

Also shown in Fig. 18 are solid curves plotting the output powers computed from the same model summarized by Eq. (9). The adjustment of the two parameters needed to obtain the agreement shown in Fig. 18 between the model given in Eq. (9) and the experimental data was made while maintaining the value reported previously for I_s of 58 KW cm^{-2}. The sensitivity of the model to γL is greatest under small signal conditions and even the poorly resolved data obtained from the amplification

of 10 mW input pulses were again sufficient to determine this overall gain parameter to within 10%. The values used to obtain the solid curves approximating the data from the larger and smaller devices were 16.2 and 14.5, respectively.

Since γ is simply proportional to the inversion density reached, it is significant that products of γL and cross sectional area from the two systems corresponded to within 10% to the inverse ratio of the source impedances driving them. This is quite consistent with the approximation that the useful power density delivered to the discharge load at constant charge voltage and discharge pressure is simply proportional to the peak current density which in turn is correlated with the inverse source impedance. Thus it appears that not only do the values of saturation intensity agree, but that the differences measured in the logarithmic gains are entirely consistent with the changes in discharge geometry made in the amplifiers.

The extent to which a unit extraction efficiency was achieved in the larger system is shown in Fig. 19. Plotted there are calculations of the derivative of Eq. (9) evaluated for the different conditions indicated using the values of γL and I_s determined experimentally. As mentioned in the previous section, a unit extraction efficiency, and hence, unity in Fig. 19, corresponds to the removal of an intensity of γI_s per unit length from the amplifying medium. It can be seen that an input from the oscillator of 15.6 KW served to saturate the power extraction from the final 87 cm of the amplifier. The overall loss of efficiency resulting from the failure to saturate the first 50 cm of the length of the amplifier can be readily seen from the areas under the curves shown in Fig. 19 which give the actual powers that appeared in the output

beams in units of $\gamma I_s LA$, where A is the cross sectional area. Then the maximum intensity which might have been extracted under ideal conditions corresponds to the rectangular area of unit height and having the width of L = 137 cm. It can be seen that the area under the curve resulting from 15.6 KW input represents most of the area of the ideal rectangle and computation shows that the extraction efficiency under those conditions was 90%. It is interesting to compare that value with the extraction efficiencies computed for the other two cases shown in Fig. 19. The relatively small extraction achieved by superfluorescence amounted to only 5% of the ideal value and the effect of a rear mirror added to form a self-excited oscillator raised this only to 18%. In fact, because of the finite duration of the avalanche the effect of the mirror was only to make the plasma appear to be a longer superfluorescent device. For that case the virtual source of the superfluorescence is indicated on the abscissa of Fig. 19 by the triangle and the direction of propagation and growth was first toward mirror located at zero and then back to L centimeters.

It can be clearly seen that the power input from the 15.6 KW oscillator is much more effective at these levels of pumping than superfluorescence or mirrors in extracting most of the energy stored in the inversion. Evidently, it was this problem with extraction efficiency rather than kinetics that led to the requirement for a high level of pumping in order to achieve the efficient operation shown in Fig. 16. At those levels of pumping γ apparently became great enough that the onset of efficient extraction occurred earlier during the transit of a photon through the plasma and a reasonable fraction of the stored energy was extracted with the use of a single rear mirror.

The difference in the parameterization of the output from an amplifier from that of an oscillator can be seen in Fig. 20. The data shown were obtained from a system driven with stripline capacitors of lower impedance so that the efficiency for the extraction of energy with a rear mirror was considerably greater than the 18% found in the previous case. Nevertheless, the improvement in the extraction achieved from the plasma used as an amplifier was of the order of 3. The parameterization of the output upon voltage and pressure appears more consistent with a simple dependence upon stored energy, thus illustrating the previous concerns that the device performance was almost completely dominated by extraction considerations when run as a self-excited oscillator.

The importance of the results inferred from this work with optical amplifiers lies in the decoupling of the effects of variations in the kinetics pumping the inversion from those caused by changes in the efficiency of extracting the photons. Since the two requirements are not optimized by the same adjustments of experimental parameters it may not be possible to extract the energy efficiently in a single, self-excited oscillator configuration when operating under conditions optimizing the power flow in the kinetics. This work has shown that N_2^+ plasmas pumped by charge transfer from He_2^+ can be more effectively used as optical amplifiers at 427.8 nm at intensities nearing full saturation of the transition over most of the volume of the devices. Under the highest gain conditions examined a small signal gain along the 137 cm path of 10^7 was observed with little uncontrolled superfluorescence. Under the same operating conditions a gain of about 75 was found at output intensities of 0.85 MW cm^{-2}, conditions again relatively near the ideal extraction of power at zero gain. At input intensity levels of 15 KW the power

extracted from the amplifier was five times that obtained from the same plasma coupled to the fields in a self-excited oscillator.

Evidently the relatively narrow bandwidth realized from this laser transition between bound electronics states of N_2^+ compensates the high rate of collisional quenching of the upper laser level and thus brings the saturation intensity down to values which can be reasonably attained in master oscillators. Since the quenching channel can be bypassed if laser intensities in the plasma signficantly exceed the relatively modest saturation intensity, the strong collisional quenching becomes an advantage because it suppresses uncontrolled superfluorescence. Thus, it appears that as an optical amplifier, the helium nitrogen laser holds the potential for efficient, high power operation at several visible wavelengths.

RESONANT AND TRAVELING WAVE DISCHARGES

As mentioned above, the principal difficulty with the discharge excitation of the nitrogen ion laser is that the duration of the intial half-period of the oscillation of the discharge current through the plasma load considerably exceeds the duration of the laser output pulse. It would appear that if the ringing period of discharge circuit could be matched to the composite duration of the development of the avalance plus the reaction times in the kinetic sequence charted in Fig. 1, an overall efficiency with respect to the energy stored on the discharge capacitor to the right of the laser tube in Fig. 15 comparable to the power transfer efficiency of 2% could be approached.

Since the switching capacitor to the left of the tube does not invert to any significant degree before the avalanche develops [35], the

energy stored on it is unavailable to the load on the time scale of the avalanche. Thus, in a device containing a single load the total efficiency can only reach half the overall efficiency computed with respect to the stored energy available to the discharge. In a system employing several loads connected in series, the overall efficiency should approach the efficiency with respect to stored energy, since the energy of the switching capacitor is needed only once to develop the proper initial conditions for the first avalanche.

An examination of components of the extant data base corresponding to the extraction of optical power from fully saturated amplifiers showed there to be only one free experimental parameter of importance in determining the overall efficiency of the device, the ringing frequency of the current loop containing the discharge. The measurements shown in Fig. 21 are typical of data from which such a conclusion can be drawn. Output energies obtained with reasonable saturation of the amplifier are shown as functions of the electrical energy initially stored on the capacitor driving the discharges. The ratio of ordinate to abscissa gives the overall efficiency with respect to storage and is correlated with the thickness of the stripline comprising the capacitor but is not determined entirely by it. Changes of that parameter created groups of data of nearly constant efficiency scaled by the stored energy. However, as seen in Fig. 21, the same stripline thickness could lead to different efficiencies when its length was varied as was done to obtain the two families of data plotted by the square symbols.

It can be readily appreciated that the energy stored on portions of the stripline excessively far from the laser tube in terms of transit time can contribute nothing to the optical output. If the avalanche has

reached the short circuited condition by the time charge from the distant parts of the line pass through the plasma no power dissipated in the load by those elements of charge can lead to the production of ionization and hence to the kinetic source terms ultimately pumping the inversion. Thus, the data of Fig. 21 appear to support the concept discussed above of attempting to correlate the overall efficiency with the degree to which one half of the ringing period of the current discharged through the load matches the natural duration of the avalanche plus the time constants of the reaction steps necessary to pump the stimulated transition. Ideally, a resonant discharge system in which the discharge time matched the ringing half-period of the current should show an overall operating efficiency comparable to the instantaneous power transfer efficiency.

Recent attempts to confirm the concept of a resonant discharge for the excitation of the nitrogen ion laser have succeeded in showing the strong correlation expected between the overall efficiency of the device and the ringing half-period of the discharge circuit. For a discharge system for the excitation of a single plasma load as shown in Fig. 15, the ringing period was determined by the series resonance composed of the capacitances of the striplines in series with the sum of the inductances of the lines and the laser tube. At the time of the avalanche the current loop through the thyratron contained too much inductance to add a parallel resonance of importance.

Performance data were taken on saturated amplifiers operating with a variety of electrode lengths and separations and driven by several striplines of differing impedances and lengths. The resulting overall efficiencies with respect to the stored energies are shown in Fig. 22 as functions of the ratios of the optical pulse widths from the amplifier

to the ringing half-periods of the discharge circuits. The type of symbol plotted denotes the stripline thickness, while the distinction between filled and unfilled symbols identifies the electrode spacing as being either 0.76 or 1.3 cm, respectively. Data showing slightly different efficiencies for the same abscissa and the same device parameters were obtained by varying the discharge voltages and pressures.

A further variant was obtained by configuring a traveling wave discharge in which the active medium consisted of an assembly of short segments arranged end to end and individually excited by preionized transverse discharges. Each segment was electrically phased so that its discharge would start at a time which would become successively later for segments farther down the sequence. Then, when the relative electrical phases were properly adjusted to match the speed of light propagating down the length of the assembly, the leading edge of the output wave traveling through it could be arranged to be always passing through successive plasma segments at the moment of electrical breakdown. Finally, since the length of an individual segment was too short to allow for the growth of the intensity of a counterpropagating wave to reach appreciable proportions after traversing a single section, any possibility that counterpropagating output could start from spontaneous emission was minimized.

Excitation of the conventional N_2 laser in a traveling wave geometry has been previously arranged [36] [37] through the use of commutation switches characterized by very fast rise times. In the usual configuration either individual single-shot switches [36] or shaped transmission lines driven by spark gaps [37] have been used to initiate breakdown waves that had rise times which were short in comparison to the longitudinal

AD-A112 104 TEXAS UNIV AT DALLAS RICHARDSON CENTER FOR QUANTUM E--ETC F/G 20/5
BLUE-GREEN LASER OUTPUT FROM N(+2) AND XEF.(U)
DEC 81 C B COLLINS N00014-77-C-0168
UNCLASSIFIED UTDCQE-ML-07 NL

2 OF 2
AD A
112 104

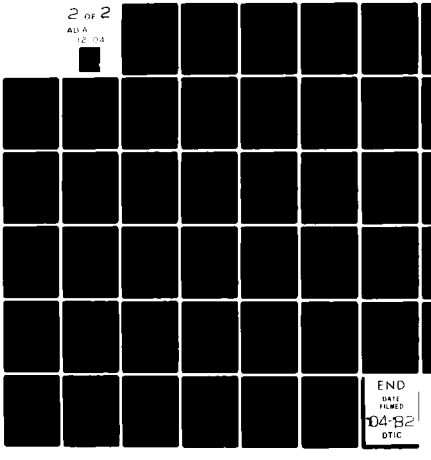

END
DATE FILMED
04-82
DTIC

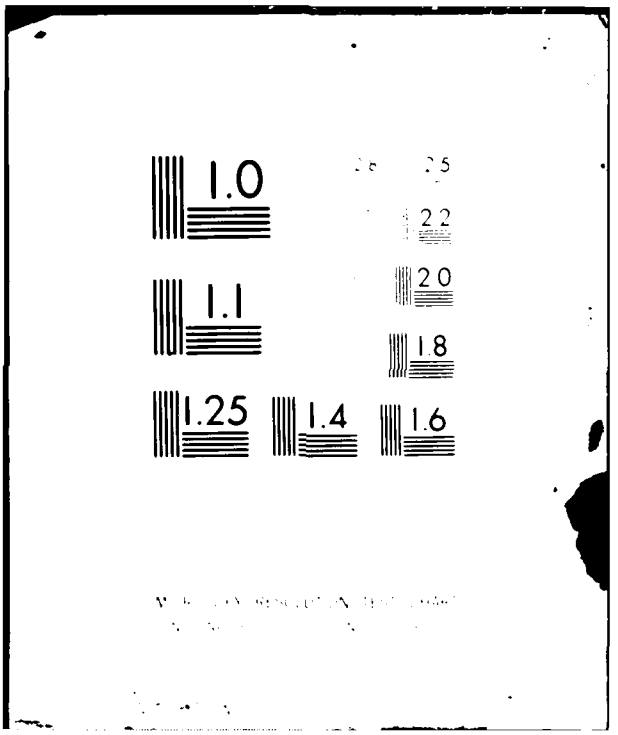
1.0
1.1
1.25
1.4
1.6
2.2
2.0
1.8

transit times of the media. However, this seemed to preclude the operation of these devices at any significant repetition rate. Nevertheless, directionalities as great as 10 to 1 were achieved.

Recently an improvement of these devices has been described [17], [38] in which commutation is effected by a conventional hydrogen thyratron connected to a stripline in a grounded-grid configuration. When used with the helium nitrogen mixture normally employed, the relatively rapid development of the avalanche breakdown in each individual segment tended to sharpen the rise time of the switching wavefront as perceived down the longitudinal axis and provided better definition of the relative phase of each segment than would have been obtained from the slower rise time characteristic of the thyratron alone. It was found by experimentation that an electrode length of 17 cm proved to be short enough to suppress bidirectional output from a single segment, while being long enough to correspond to a nearly discernable change of phase. In actual practice the phase was constant over an individual segment and successive segments were set to phases differing by time of 17/c.

Both a nominal 1.5-m device containing 7 discharge segments and a 5-m device containing 21 segments were constructed in the course of this work. Although some variations of phasing were observed in both devices when operating pressures and voltages were changed, the degree of this variability was acceptable over the working pressure range of 2-4 atm of helium containing 0.15% N_2. These variations were detected in the growth of the duration of the output pulses, as the propagating fields tended to "outrun" the breakdown wave, or in the inverse effect. The latter type of dephasing tended to be the most serious, as the plasma was found to become absorptive at the laser wavelength during the later

afterglow period in agreement with previous measurements. To avoid this possibility for the reabsorption of a "slow" output pulse, the phasing of the discharge segments was adjusted so that in normal operation the leading edge of the output gradually outran the breakdown wave. If not done excessively, the trailing edge of the output contained enough intensity to saturate the transition in the farther segments and in this way the output pulse was gradually stretched by an amount proportional to the number of segments traversed. This technique led to output pulses from the 1.5-m device which were 6 nsec in duration between half-power points, and which were 7-8 nsec for the 5-m system. However, as a test of the extent to which the duration of the output pulse could be controlled in this manner, the 5-m laser was phased to give 15-nsec pulses with no loss of integrated pulse energy by adjusting only the spacings of the electrodes in successive segments.

The directionality achieved with this arrangement was extreme. No optics of any kind were present in the system and the output windows were antireflection coated to avoid any spurious directionality which might have been introduced by possibly fortuitous reflections. Nevertheless front-to-back ratios of intensities at megawatt levels of output power exceeded 1000:1. In terms of pulse energies the directionalities were greater than 10,000:1, because the pulses in the reverse direction were of the order of 1 nsec or less in duration in comparison to the forwardly propagating outputs of 7-8 nsec duration.

Not reported in previous descriptions of this work [17] were the ringing periods. Both the 1.5 m and the 5 m traveling wave amplifiers were composite assemblies of individual discharge segments each having ringing periods of 20 nsec. The overall efficiencies with respect to

the energy of the storage capacitors for both traveling wave configuration are represented by the T symbol plotted in Fig. 22. Variations between the two were smaller than the extent of the symbol.

It appears that the data of Fig. 22 group closely around a line that would extrapolate to an efficiency between 0.7 and 1.0% at the unit value of abscissa characteristic of a resonant discharge. The scale of the output for such a resonant device would be determined by the total stored energy and the principal technological difficulty to be encountered in realizing such a system would be the problem of storing enough electrical energy in sufficient proximity to the laser tube to permit a ringing period of the discharge to be as little as 10 nsec. As mentioned in the introductory material, it appears that the full realization of the potentials of this system will be achieved with the next generation of devices characterized by discharge times faster than those typically achieved in current lasers.

CONCLUSIONS

The greatest power output achieved to date has been 5 MW in a 6 nsec pulse that was achieved with the traveling wave system. The coordinates of that operation in terms of ringing frequency and efficiency are plotted by the symbol, T, in Fig. 22 and show that both scale and efficiency can be simultaneously optimized, something nearly attained in other types of high power lasers, such as the inert-gas excimer lasers, operating at short wavelengths.

A comparison of the results of this work to those from studies of KrF excimer lasers begins to show the peculiar advantages of the charge transfer scheme enumerated in the introductory material. Those features

insure that whereas gain and efficiency cannot be simultaneously maximized, scale and efficiency can. The consequence has been that with e-beam excitation the nitrogen ion laser has achieved a higher specific power output, optical power per unit volume of laser medium, than has been reported from KrF. When normalized to the number of photons extracted per unit volume the differences approach an order of magnitude. Under those conditions the relatively constant efficiency of the nitrogen ion laser is exceeded by the efficiency of the KrF by about a factor of 3 [39].

With discharge excitation the comparison is even more extreme. At large scale the specific output power from KrF is about 5 MW ℓ^{-1} with an energy efficiency relative to deposition of 3% [39]. The nitrogen ion laser has achieved 44 MW ℓ^{-1} at a comparable efficiency of 1%. At the other extreme in an avalanche discharge a high specific intensity of 220 MW ℓ^{-1} has been reported from KrF but at an overall efficiency of only 0.06% [40]. The comparable efficiency from the nitrogen ion laser at 44 MW ℓ^{-1} is shown from Fig. 22 to be around 0.4% relative to stored energy. Table 2 summarized these comparisons. The larger outputs are reported for KrF lasers directly excited by e-beams can clearly be seen to result from a combination of higher energy per photon and longer excitation pulses available on e-beam machines used in the KrF studies. Both lasers operate as 4-level systems and hence, emit until the end of the excitation pulse.

In terms of spectral density the outputs from the nitrogen ion laser greatly exceed those from free-running excimer lasers because of the relatively narrow linewidths resulting from the bound-bound transition in N_2^+. As mentioned previously, the laser linewidth at 471 nm is

.007 nm without any supplimentary etalons in the laser cavity and without injection locking of the frequency to a narrow bandwidth.

The combination of visible wavelengths, simultaneously high output power densities and efficiencies, narrow linewidth, and relative freedom from run-away superfluorescence appears to give to the nitrogen ion laser considerable promise as a practical device. Both theory and the experimental results reported here indicate that the performance of the nitrogen ion laser can approach that of the KrF excimer laser to within a factor of 2 or 3. It appears that all of the advantages of this type of device expected theoretically have been confirmed experimentally and the construction and operation of a device of arbitrary scale for operation of either 428 or 471 nm can now be modelled by the results of this work.

Table 1

Dominant Reaction Channels
in Helium Nitrogen Plasmas Supporting
Stimulated Emission from the B → X
Transition of N_2^+

Reaction rate coefficients are shown in parentheses in units of 10^{-10} cm^3 sec^{-1} and 10^{-30} cm^6 sec^{-1} for those component bimolecular and termolecular reactions, respectively, which dominate the evolution of the reactive species of importance. Branching information is shown as a multiplicative factor preceeding the rate coefficient.

Pumping Channels		Competing Losses	
Ionization			
$He^+ + 2He \rightarrow He_2^+ + He$	(.065)[a]	$He^+ + N_2 \rightarrow$ Products	(12)[b]
		$He^+ + N_2 + He \rightarrow$ Products	(22)[c]
Charge Transfer			
$He_2^+ + N_2 \rightarrow N_2^+(B) + 2He$	.75(11)[d]	$He_2^+ + N_2 \rightarrow$ Other Products	.25(11)[d]
$He_2^+ + N_2 + He \rightarrow N_2^+(B) + 3He$	.75(16)[d]	$He_2^+ + N_2 + He \rightarrow$ Other Products	.25(16)[d]
		$He_2^+ + e + X \rightarrow$ Recombination	( )[e]
Stimulated Emission			
$N_2^+(B) + h\nu \rightarrow N_2^+(X, v=1) + 2h\nu$	( )[f]	$N_2^+(B) + e \rightarrow$ Neutrals	(600)[c]
		$N_2^+(B) + N_2 \rightarrow N_4^+$	(4)[g]
Lower State Quenching			
$N_2^+(X, v=1) + e \rightarrow N_2^{**}(v=1)$	(10,000)[h]		
$N_2^{**}(v=1) \rightarrow N_2^+(X, v=0) + e$			
$N_2^+(X, v=1) + N_2 \rightarrow N_2(v=1) + N_2^+(X, v=0)$	( )[i]		

a. Ref. [23].
b. Ref. [20].
c. Ref. 10.
d. Rate Coefficients from Ref. [19] branching ratios from Ref. 10.
e. This depends strongly on electron temperature and is difficult to estimate meaningfully.
f. $\sigma(428\ nm) = 14\ P^{-0.6}\ A^{o2}$
$\sigma(471\ nm) = 3.9\ P^{-0.6}\ A^{o2}$
where P is the pressure in atmospheres, Ref. 10.
g. Apparently this is 3-body process which effectively occurs as a bimolecular reaction because of saturation, Ref. 10.
h. Estimated, Ref. 12 and Ref. 10.
i. Private communication, F.C. Fehsenfeld, NOAA. A value comparable to Langevin, 8×10^{-10}, is expected.

Table 2

Comparison of the Performances Achieved with the Nitrogen Ion Laser and with the KrF Laser

	Charge Transfer (428 nm)	KrF, Large Scale[a] (249 nm)	KrF, High Specific Power[b]
E-beam Excitation			
Pulse duration (nsec)	17	600	
Volume (ℓ)	.016	60	
Efficiency relative to deposition	3%	10%	
Specific output power (MW/ℓ)	320	9.7	
Specific output intensity ($\times 10^{26}$ photons/ℓ/sec)	6.9	0.12	
Discharge Excitation			
Pulse duration (nsec)	6	300	15
Volume (ℓ)	0.11	30-40	0.18
Efficiency relative to energy deposition	1%	3%	-
Efficiency relative to stored energy	0.4%	-	0.06%
Specific output power (MW/ℓ)	44	5	220
Specific output intensity ($\times 10^{26}$ photons/ℓ/sec)	0.95	0.06	2.8

a. Ref. [39].
b. Ref. [40].

REFERENCES

[1] C. B. Collins and W. W. Robertson, "A flow-system and burner for observing selective excitation of spectra by metastable species in the afterglow of a helium discharge," Spectrochim. Acta, vol. 19, pp. 747-761, 1963.

[2] C. B. Collins and W. W. Robertson, "Spectra excited in a helium afterglow," J. Chem. Phys., vol, 40, pp. 701-712, 1964.

[3] J. W. McGowan and R. F. Stebbings, "Charge transfer as a possible laser pumping mechanism," Appl. Opt. Suppl., vol. 2, pp. 68-72, 1965.

[4] G. R. Fowles and R. C. Jensen, "Visible laser transition in the spectrum of singly ionized iodine," Proc. IEEE, vol. 52, pp. 851-852, 1964; and "Visible laser transition in ionized iodine," Appl. Opt., vol. 3, pp. 1191-1192, 1964.

[5] F. C. Fehsenfeld, A. L. Schmeltekopf, P. D. Goldan, H. I. Schiff, and E. E. Ferguson, "Thermal energy ion-neutral reaction rates. I. Some reactions of helium ions," J. Chem. Phys., vol. 44, pp. 4087-4094, 1966.

[6] It is even more surprising that after such a prolonged latency the discovery should arrive with such simultaneity. Both original references carry the same receipt date:
C. B. Collins, A. J. Cunningham, S. M. Curry, B. W. Johnson, and M. Stockton, "Stimulated emission from charge-transfer reactions in the afterglow of an e-beam discharge into high-pressure helium-nitrogen mixtures," Appl. Phys. Lett., vol. 24, pp. 477-478, 1974.

V. N. Ishchenko, V. N. Lisitsyn, A. M. Razhev, and V. N. Starinskii, "Super-radiance on the 2+ and 1- bands of nitrogen in a discharge at pressures above 10 atm," JETP Lett., vol. 19, pp. 233-234, 1974.

[7] S. N. Suchard , Spectroscopic Data, Volume 1, IFI/Plenum, New York, 1975.

[8] S. N. Suchard and J. E. Melzer, Spectroscopic Data, Volume 2, IFI/Plenum, New York, 1976.

[9] J. F. Prince, C. B. Collins, and W. W. Robertson, "Spectra excited in an argon afterglow," J. Chem. Phys., vol. 40, pp. 2619-2626, 1964.

[10] J. V. Petersen, Theoretical Modelling of Charge Transfer Laser, Unpublished Ph.D. Dissertation, The University of Texas at Dallas, 1977.

[11] C. B. Collins, A. J. Cunningham, and M. Stockton, "A nitrogen ion laser pumped by charge transfer," Appl. Phys. Lett., vol. 25, pp. 344-345, 1974.

[12] C. B. Collins, "The Nitrogen Ion Laser," Unpublished Final Report, UTDP ML-06, The University of Texas at Dallas, pp. 1-48, 1977.

[13] C. B. Collins, J. M. Carroll, F. W. Lee, and A. J. Cunningham, "Thermal modification of the kinetic sequence pumping the helium-nitrogen charge-transfer laser," Appl. Phys. Lett., vol. 28, pp. 535-537, 1976.

[14] J. B. Laudenslager and T. L. Pacala, "Electric discharge-pumped nitrogen ion laser," Appl. Phys. Lett., vol. 29, pp. 580-582, 1976.

[15] D. E. Rothe and K. O. Tan, "High-power N_2^+ laser pumped by charge transfer in a high-pressure pulsed glow discharge," Appl. Phys. Lett., vol. 30, pp. 152-154, 1977.

[16] C. B. Collins, J. M. Carroll, and K. N. Taylor, "Charge transfer pumping of the helium-nitrogen laser at atmospheric pressures in an electrical avalanche discharge," J. Appl. Phys., vol. 49, pp. 5093-5097, 1978.

[17] C. B. Collins and J. M. Carroll, "Traveling wave excitation of the nitrogen ion laser," J. Appl. Phys., vol. 51, pp 3017-3019, 1980.

[18] C. B. Collins, J. M. Carroll, and K. N. Taylor, "Gain and saturation of the nitrogen ion laser," Appl. Phys. Lett., vol. 33, pp. 175-177, 1978.

[19] F. W. Lee, C. B. Collins, and R. A. Waller, "Measurement of the rate coefficients for the bimolecular and termolecular charge transfer reactions of He_2^+ with Ne, Ar, N_2, CO, CO_2 and CH_4," J. Chem. Phys., vol. 65, pp. 1605-1615, 1976.

[20] D. L. Albritton, "Ion-neutral reaction-rate constants measured in flow reactors through 1977," At. Data and Nuclear Tables, vol. 22, pp. 1-101, 1978.

[21] C. B. Collins and F. W. Lee, "Measurement of the rate coefficients for the bimolecular and termolecular ion-molecule reactions of the He_2^+ with selected atomic and molecular species," J. Chem. Phys., vol. 68, pp. 1391-1401, 1978.

[22] C. B. Collins and F. W. Lee, "Measurement of the rate coefficients for the bimolecular and termolecular de-excitation reactions of $He(2^3S)$ with selected atomic and molecular species," J. Chem. Phys., vol. 70, pp. 1275-1285, 1979.

[23] R. Deloche, P. Monchicourt, M. Cheret, and F. Lambert, "High-pressure helium afterglow at room temperature," Phys. Rev. A, vol. 13, pp. 1140-1176, 1976.

[24] At the time of submission of this manuscript it was learned that independent study of the kinetics leading to the production of atomic nitrogen in helium nitrogen plasmas at atmospheric pressures had been studied with a more extensive variety of techniques. The time dependent behavior of the visible fluorescence from the various kinetic intermediaries, including $N_2^+(B)$; of the VUV fluorescence from various population; and of the ion and electron densities were all modeled successfully with a set of rate coefficients that differed from those reported in Table 1 by less than the ±30% margin of uncertainty reported in the original measurements of Refs. 19, 21, 22 and 23. The details of this comprehensive study further tending to confirm the kinetic model reported here are found in J. M. Pouvesle, A. Bouchoule, and J. Stevefelt, "Modelling of the charge transfer afterglow excited by intense electrical discharges in high pressure helium nitrogen mixtures," J. Chem. Phys. (accepted for publication).

[25] W. L. Harries and J. W. Wilson, "Simplified Model of a Volumetric Direct Nuclear Pumped ^{3}He-Ar Laser," NASA-Langley Research Center, Paper presented at the First International Symposium on Nuclear Induced Plasmas and Nuclear Pumped Lasers, 1978.

[26] C. B. Collins and A. J. Cunningham, Recombination Laser, Fourth Semi-Annual Technical Report, The University of Texas at Dallas, No. UTDP A002-4, pp. 1-112, 1974.

[27] C. B. Collins and A. J. Cunningham, "Scaling of the helium-nitrogen charge transfer laser," Appl. Phys. Lett., vol. 27, pp. 127-128, 1975.

[28] C. B. Collins and A. J. Cunningham, The Nitrogen Ion Laser, Sixth Semi-Annual Technical Report, The University of Texas at Dallas, No. UTDP ML-03, pp. 1-54, 1975.

[29] G. Knop and W. Paul in: Alpha, Beta, and Gamma-Ray Spectroscopy, (ed. Kai Siegbahn, North-Holland Co., Amsterdam, 1965) pp. 1-25.

[30] C. B. Collins and A. J. Cunningham, The Nitrogen Ion Laser, Fifth Semi-Annual Technical Report, The University of Texas at Dallas, No. UTDP ML-02, pp. 1-85, 1974.

[31] R. V. Lovelace and R. M. Sudan, "Plasma heating by high-current relativistic electron beams," Phys. Rev. Lett., vol. 27, pp. 1256-1259, 1971.

[32] C. B. Collins, J. M. Carroll, K. N. Taylor and F. W. Lee, "A regenerative power amplifier operating on the blue-green line of the nitrogen ion laser," Appl. Phys. Lett., vol. 33, pp. 624-626, 1978.

[33] W. A. Fitzsimmons, L. W. Anderson, C. E. Riedhauser, and J. M. Vrtilek, "Experimental and theoretical investigation of the nitrogen laser," IEEE J. Quantum Electron., vol. QE-12, pp. 624-633, 1976.

[34] Expression (9) has been taken from an equivalent expression used to describe the integrated pulse energy extracted from an optical amplifier operating on a transition showing homogeneous broadening. See F. Hopf, in: High Energy Lasers and Their Applications (ed. S. Jacobs, M. Sargent III, and M. O. Scully, Addison-Wesley

Publishing Co., Reading, Mass, 1974), p. 96. The conversion from pulse energy in the atomic units of the above reference to intensities results in Eq. (9) where I_s is a factor of $t_2/2\tau$ larger than the textbook saturation intensity, as described in A. Yariv, Introduction to Optical Electronics (2nd Ed., Holt, Rinehart, and Winston, New York, N.Y., 1976), p. 108. The characteristic times t_2 and τ denote the lifetime of the upper laser level and the temporal FWHM of the output pulse, respectively.

[35] According to Ref. [16] the avalanche generally develops when the voltage across the load reaches a value comparable to the original charge voltage on the capacitors.

[36] J. D. Shipman, "Traveling wave excitation of high power gas lasers," Appl. Phys. Lett., vol. 10, pp. 3-4, 1967.

[37] B. Godard, "A simple high-power large-efficiency N_2 ultraviolet laser," IEEE J. Quantum Electron., vol. QE-10, pp. 147-153, 1974.

[38] C. B. Collins, "Repetitively pulsable traveling wave laser," U.S. Patent No. 4,053,853 (1977).

[39] R. Hunter, "Rare Gas Halide Laser Studies," Talk presented at the 7th Winter Colloquium on High Power Visible Lasers, Park City, Utah, February 16-18, 1977.

[40] W. J. Sarjeant, A. L. Alcock and K. E. Leopold, "Parametric study of a constant E/N pumped high-power KrF laser," IEEE J. Quantum Electron., vol. 14, pp. 177-184, 1978.

CAPTIONS

Figure 1: Flow chart of the kinetic processes relevant to the nitrogen ion laser. Heavy arrows denote the dominant kinetic channels. The distinction between solid and dashed lines reflects the difference between reaction paths contributing to the pumping sequence and those competing with it, respectively.

Figure 2: Plot of the kinetic efficiencies for the population of the upper laser level and of the small signal gain of the N_2^+ B → X laser transition at 427.8 nm as functions of the input energy deposition.

Figure 3: Time-resolved power measurements of the nitrogen ion laser outputs for three different mirror sets individually optimizing the (0,0), (0,1), and (0,2) transitions at 391.4, 427.8, and 470.9 nm, respectively. Corresponding total pressures are, from top to bottom, 10.8, 14.9, and 16.3 atm. The time scale is as indicated and has been shifted so that the zero corresponds to the beginning of the e-beam current output.

Figure 4: Summary plot of total pulse energy emitted from a 16 cm^3 volume as a function of relative deposition of energy from the electron beam. Variation of the deposition is obtained by changing the total gas pressure; hence the stopping power. The peak e-beam current is 13 KA in each case. Lines of constant efficiency appear as diagonals. The partial pressure

of nitrogen in Torr used in each series is shown and the difference between open and filled symbols is made by a difference in mirror characteristics.

Figure 5: Summary of various time-dependent functions representing the development of the laser output intensity. To the right of each example are shown the characteristic experimental parameters in the order: nitrogen partial pressure in Torr, cavity type (P, plane; H, hemispheric), mirror loss per round trip, and on the subsequent line the corresponding average laser volume calculated by the unfolding program.

Figure 6: Plots of laser pulse energy as a function of total gas pressure for the data of the first two mirror geometries shown in Fig. 5. Energy extracted from the plasma is assumed to be emitted energy plus energy walking-off the mirrors. Cavity nomenclature is P.(T) where T is the mirror transparency per round trip.

O Emitted energy, P.08 cavity

Δ Emitted energy, P.16 cavity

× Extracted energy, P.08 cavity

\+ Extracted energy, P.16 cavity

Figure 7: Summary plot of laser pulse energy at 391.4 nm as a function of pressure. Data in the upper portion of the graph show the gross energy extracted from the plasmas by the circulating power in the cavity, normalized to a volume of 16.2 cm^3 and a

beam discharge of 275 μ coul. Much of the energy is reabsorbed with only the net energy plotted in the lower half of the graph being detected in the output beam of the laser. In each case the shape of the data point gives the nominal beam current and for the net energy data the partial pressure of nitrogen is given by the shading of the symbol.

Figure 8: Summary plot of total laser pulse energy emitted from a 16 cm^3 volume as a function of total gas pressure. The integrated e-beam current corresponds to 275 μ coul.for each case. Data points represent outputs at 428 nm for the four higher N_2 pressures and at 391 nm otherwise. Different partial pressures of N_2 are indicated by the shape of the data point.

Figure 9: Plot of the output intensities at 470.9 nm from the regenerative amplifier excited by the oscillator pulses seen on the leading edges of the waveforms. Intensities are plotted as functions of time following the onset of the e-beam current. Dotted lines bound variation in the times at which the e-beam current had fallen to e^{-1} of the peak value. Data from two separate discharges with different delays in the arrival of the oscillator pulses are shown with the zeros of intensity offset for clarity.

Figure 10: Peak intensities of the 470.9 nm output from the regenerative amplifier plotted as a function of the delay following the onset of the e-beam current, in the time of arrival at the amplifier of the pulses from the oscillator.

Figure 11: Thermal scaling of the helium-nitrogen charge transfer laser. Plotted parametrically as a function of gas temperature are time resolved power measurements of the violet line at 427.8 nm. Data are shown for the discharge of 190 μ coul. into 21 atm pressure of helium containing 60 Torr of nitrogen. The time scale has been normalized so that the zero corresponds to the beginning of the e-beam current output.

Figure 12: Plot of the time-resolved laser power emitted at 427.8 nm from an electron beam discharge into 7.7 atm pressure of helium containing 15 Torr of N_2 at the gas temperatures shown. The dashed curves show the time dependence of a constant fraction of the corresponding input power deposited in the laser cavity.

(a) Upper curves: Data for nominal 15 KA e-beam current.

(b) Lower curves: Data for nominal 20 KA e-beam current.

Figure 13: Plot of the time-resolved laser power emitted at 427.8 nm from an electron beam discharge into 11 atm pressure of helium containing 30 Torr of N_2 at the gas temperatures shown. The dashed curves show the time dependence of a constant fraction of the corresponding input power deposited in the laser cavity for a nominal e-beam current of 20 KA.

Figure 14: Plot of data showing quasi-cw operation of the helium-nitrogen laser. The solid curve shows output power at 427.8 nm emitted from an electron beam discharge into 35 atmospheres pressure

of helium containing 120 Torr of nitrogen. The dashed curve shows 3% of the corresponding power deposited in the laser cavity.

Figure 15: Schematic diagram of the circuit of the Atmospheric Electrical Avalanche (AEA) Laser used in studies of the instantaneous power transfer efficiency.

Figure 16: Graphs comparing the electrical and optical performance of the laser tube obtained for a 1.3 cm electrode spacing and for the indicated pressures of helium containing 0.15% N_2. Dashed curves plot the voltage and current applied to the laser tube as marked and scaled to the leftmost ordinate. The dotted curve records the instantaneous power dissipation in the laser tube and is scaled to the middle ordinate. The solid curve plots the output power of the laser measured at 427.8 nm and is scaled to the rightmost ordinate.

Figure 17: Graph of the data obtained at a pressure of 3.7 atm for peak power outputs from the optical amplifier for various values of input pulse amplitudes obtained from the synchronized master oscillator. The solid curve plots values computed from Eq. (9) using a saturation intensity of 58 KW cm^{-2} and an overall logarithmic gain of 14.5. Dashed curves show the sensitivity of the model to the changes of overall logarithmic gain indicated on the graph.

Figure 18: Graph of the data showing peak powers output from the optical amplifier at 427.8 nm for various values of input pulse amplitudes obtained from the synchronized master oscillator. Solid curves plot output powers computed from the simple model of Eq. (9) containing the two parameters, the saturation intensity of 58 KW cm^{-2} and the overall logarithmic gain which was adjusted to fit the data. The particular values used to obtain the displayed curves were 16.2 and 14.5 for the amplifiers with the 1.4 and 0.6 cm^2 apertures, respectively.

Figure 19: Plot of the derivatives of the power extracted from the 1.4 cm^2 amplifier plotted as functions of the length of the optical path travelled by a photon from the oscillator as calculated from Eq. (9) using the extraction parameters determined from Fig. 18. Units are γI_s so that unity implies full saturation of the transition at the corresponding point in the plasma. The three different means of coupling the plasma to the fields are identified by the label adjacent to the corresponding curve. In the case of the single rear mirror the position of the virtual photon source is indicated by the filled triangle on the abscissa and propagation is assumed to proceed from the source to the mirror located at the origin and then reflect back to give the values of extraction plotted by the corresponding curve.

Figure 20: Graph showing the parameterization of the charge transfer AEA device operating with 1.3 cm electrode spacing. Peak output

power is shown as a function of helium pressure and parametrically as functions of the charge voltages shown. The geometries for the coupling of the radiation fields to the inversion are identified by the designation of the output device as an oscillator or an amplifier as indicated.

Figure 21: Graph of data showing the correlation between the energies of output pulses at 428 nm from reasonably saturated amplifiers and the electrical energy initially stored on the capacitor driving the avalanche. The type of symbol indicates the thickness of the stripline comprising the capacitor as follows: Δ - 0.38 mm, □ - 0.66 mm, o - 1.22 mm.

Figure 22: Graph of the overall output efficiency with respect to stored electrical energy measured as functions of the ratio of the output pulse durations from saturated amplifiers to the half periods for the ringing of the discharge circuit. The type of symbol denotes the stripline thickness as follows: Δ - 0.38 mm, □ - 0.66 mm, O - 1.22 mm. Filled and unfilled symbols identify data obtained with electrode spacings of 0.76 and 1.3 cm, respectively. The T - symbol locates the coordinates of the maximum output obtained with the available devices.

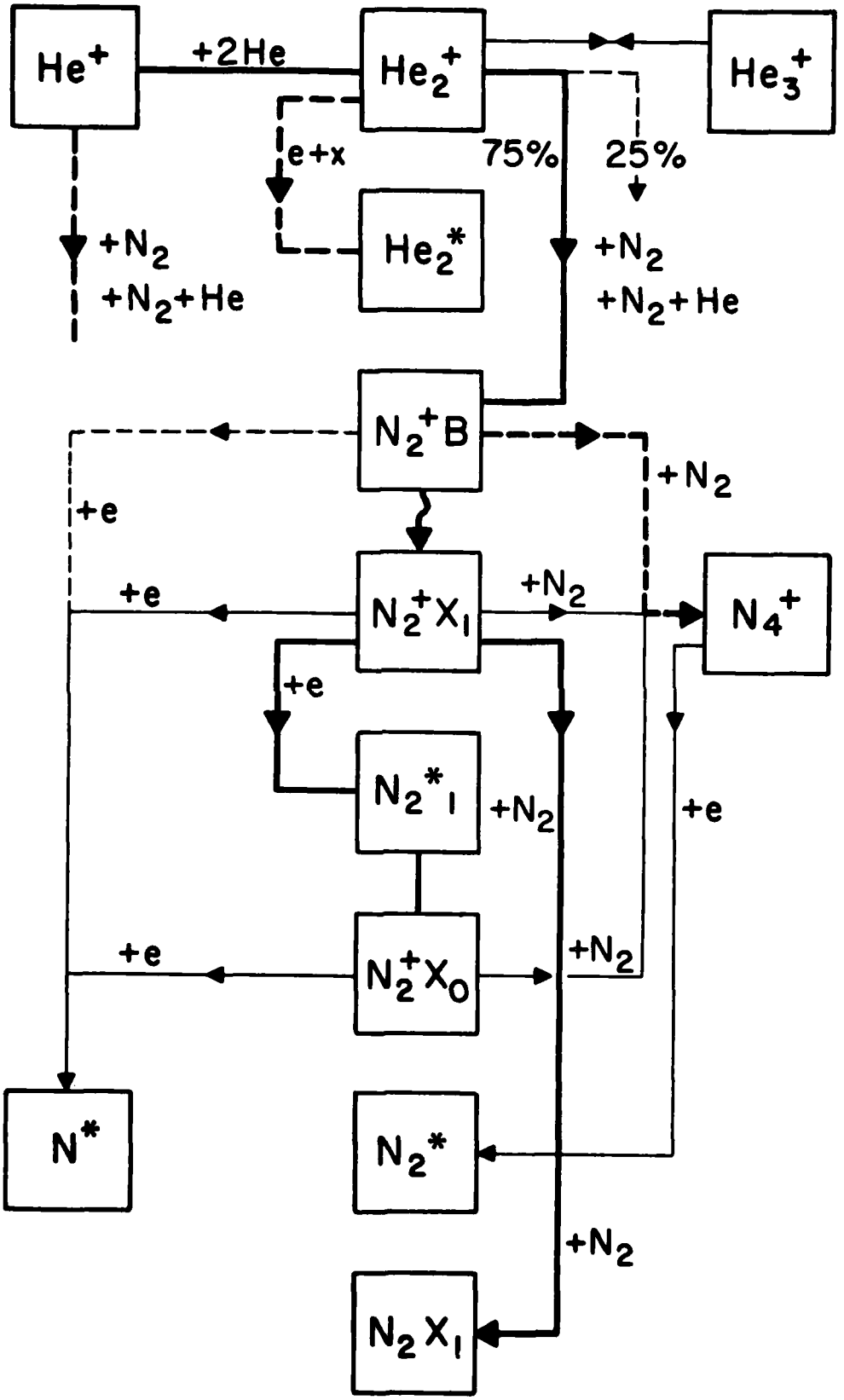
He^+
+2He
He_2^+
He_3^+
e+x
75%
25%
He_2^*
$+N_2$
$+N_2+He$
$+N_2$
$+N_2+He$
N_2^+B
$+N_2$
+e
+e
$N_2^+X_1$
$+N_2$
N_4^+
+e
$N_2^*{}_1$
$+N_2$
+e
+e
$N_2^+X_0$
$+N_2$
N^*
N_2^*
$+N_2$
N_2X_1

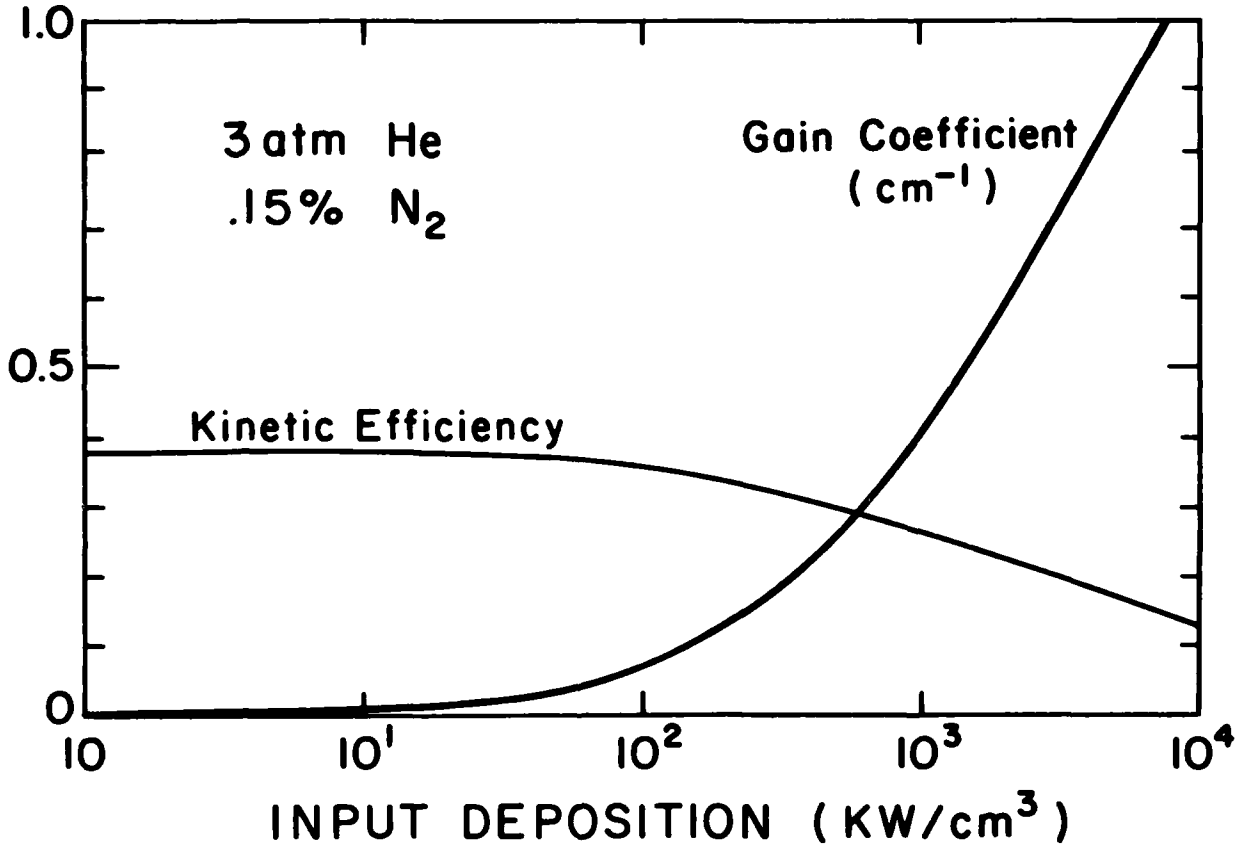
1.0
0.5
0
3 atm He
.15% N_2
Gain Coefficient
(cm^{-1})
Kinetic Efficiency
10
10^1
10^2
10^3
10^4
INPUT DEPOSITION (KW/cm^3)

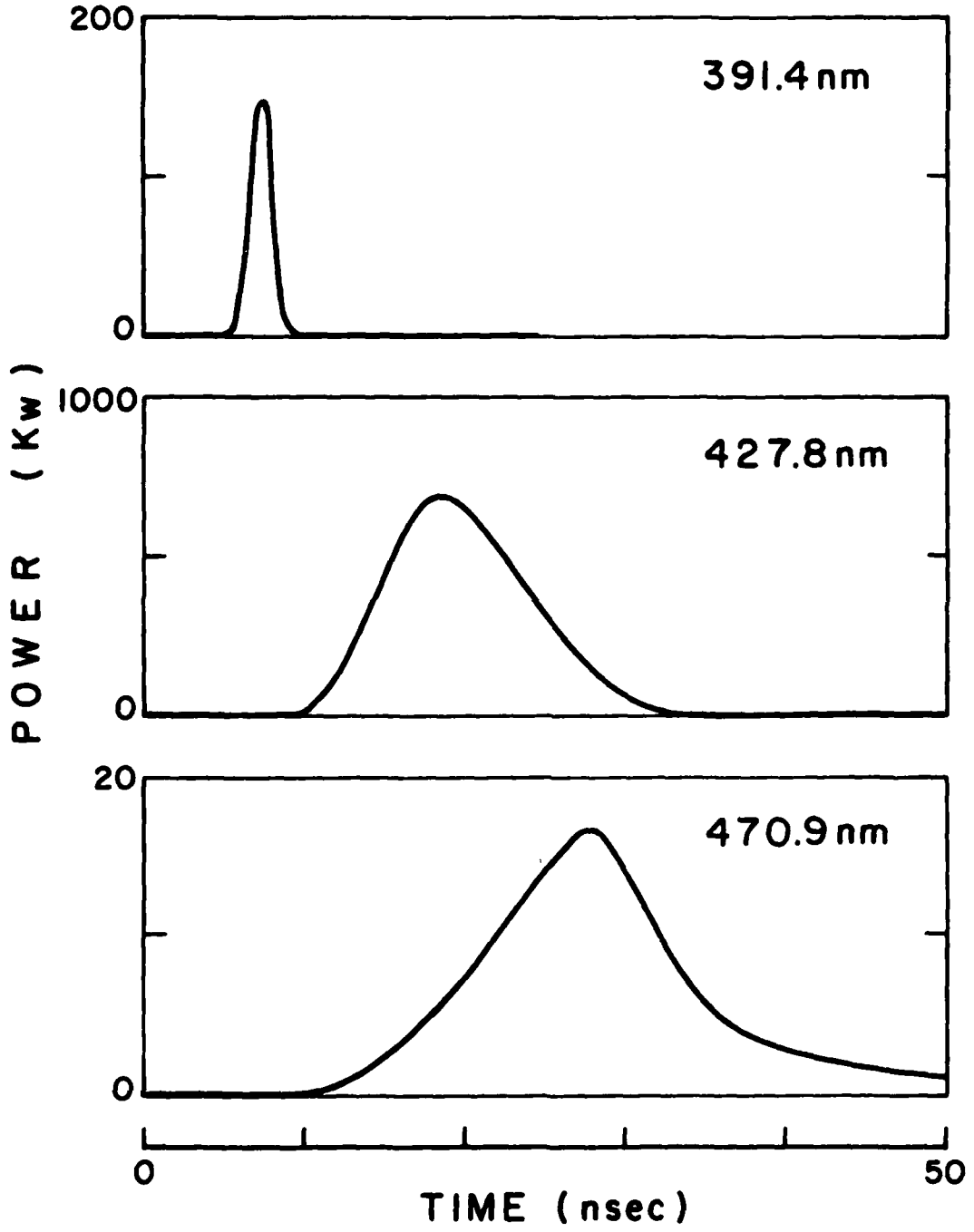
200
391.4nm
0
1000
427.8nm
0
20
470.9nm
0
0
50
POWER (Kw)
TIME (nsec)

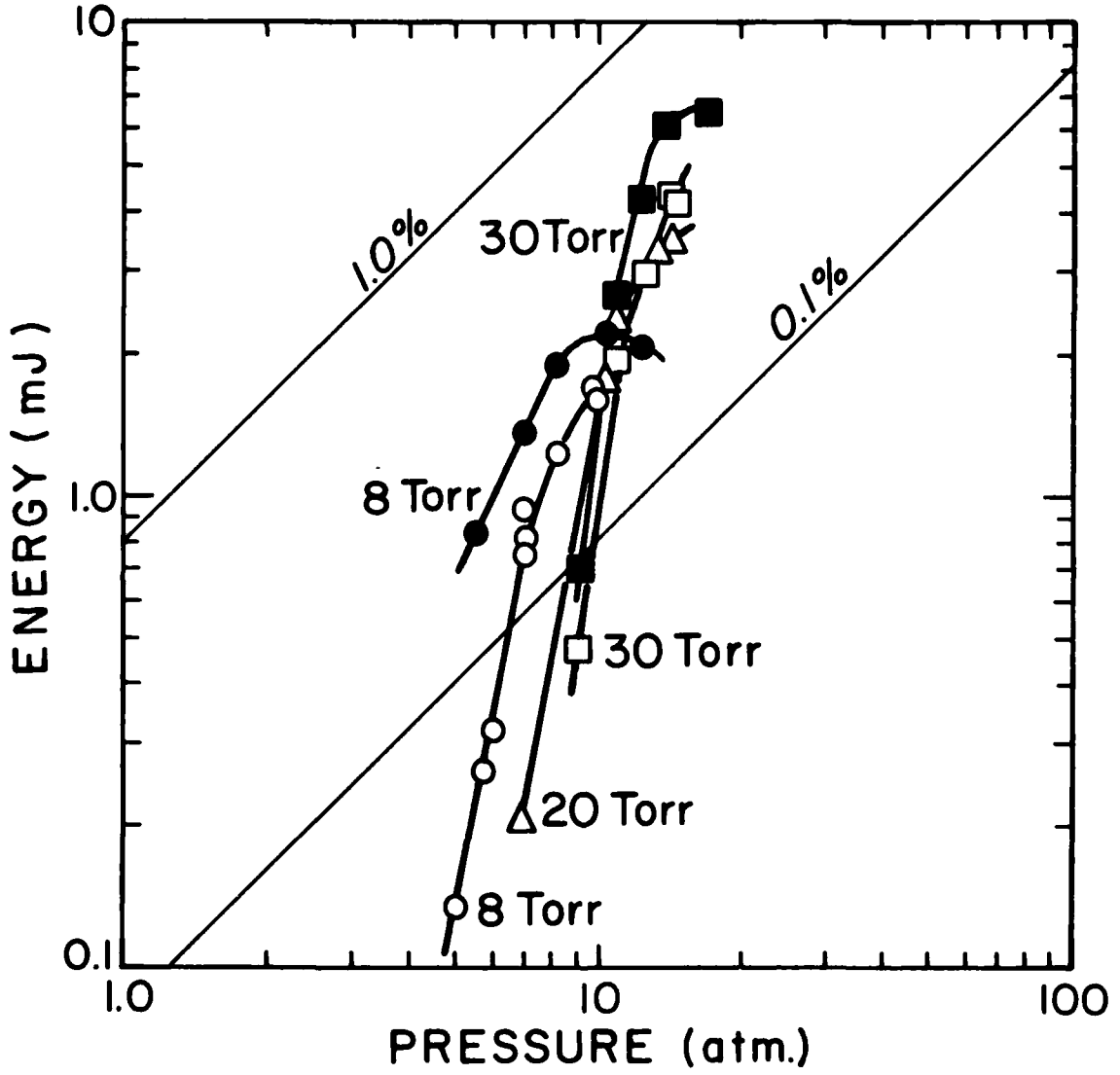
10
1.0
0.1
ENERGY (mJ)
1.0%
0.1%
30Torr
8 Torr
30 Torr
20 Torr
8 Torr
1.0
10
100
PRESSURE (atm.)

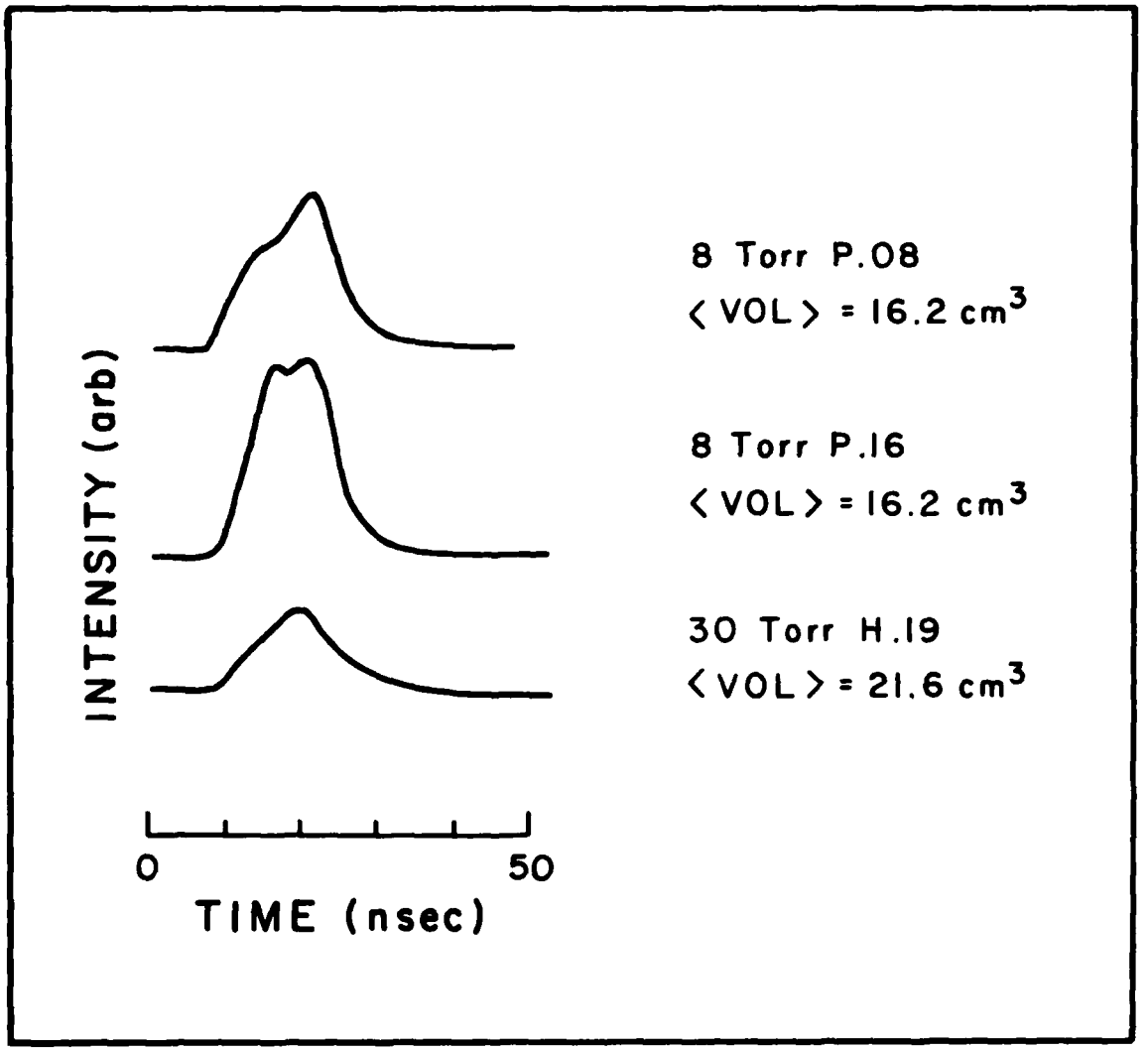
INTENSITY (arb)
8 Torr P.08
⟨VOL⟩ = 16.2 cm³
8 Torr P.16
⟨VOL⟩ = 16.2 cm³
30 Torr H.19
⟨VOL⟩ = 21.6 cm³
0
50
TIME (nsec)

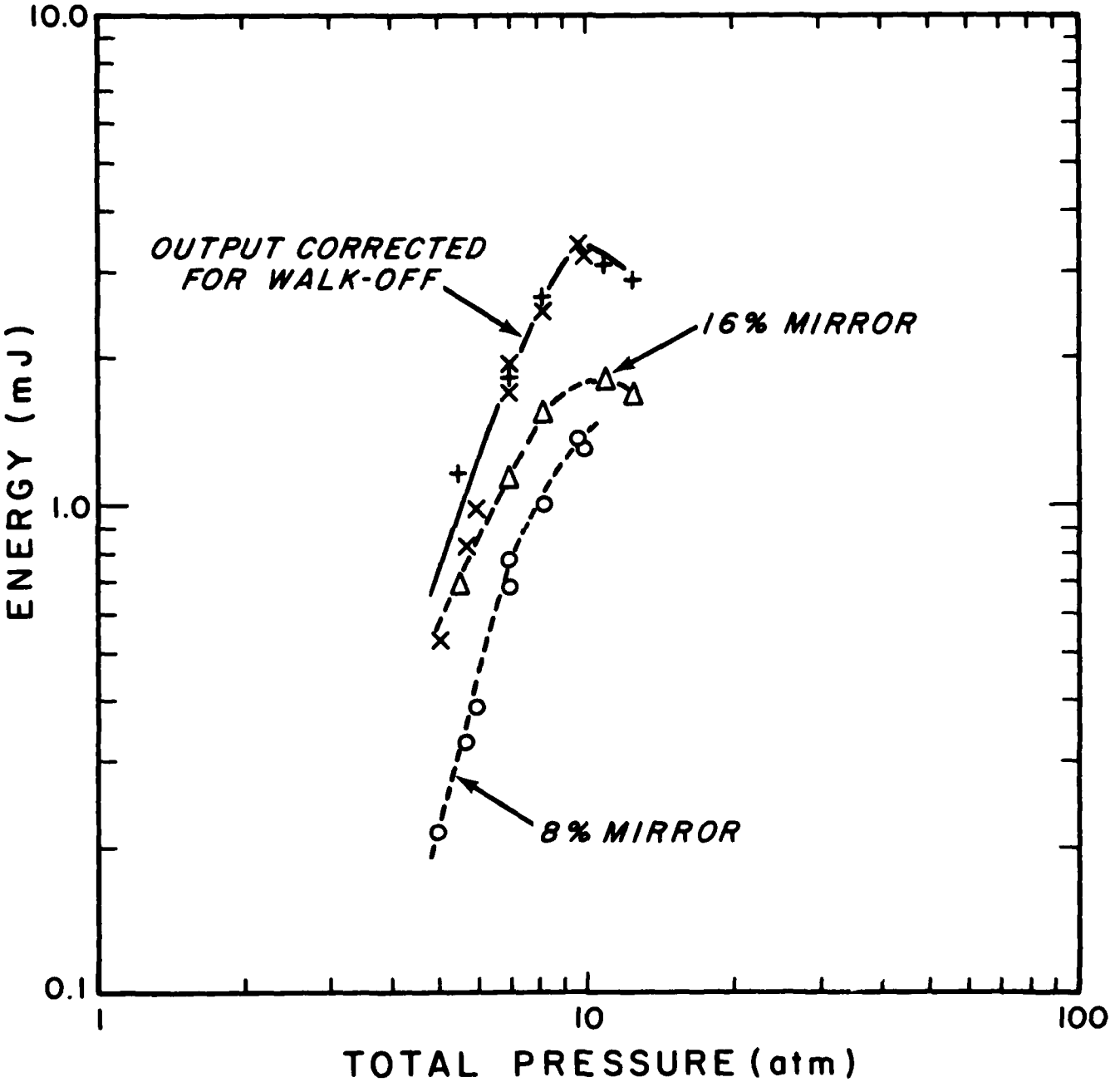
10.0
1.0
0.1
ENERGY (mJ)
OUTPUT CORRECTED FOR WALK-OFF
16% MIRROR
8% MIRROR
1
10
100
TOTAL PRESSURE (atm)

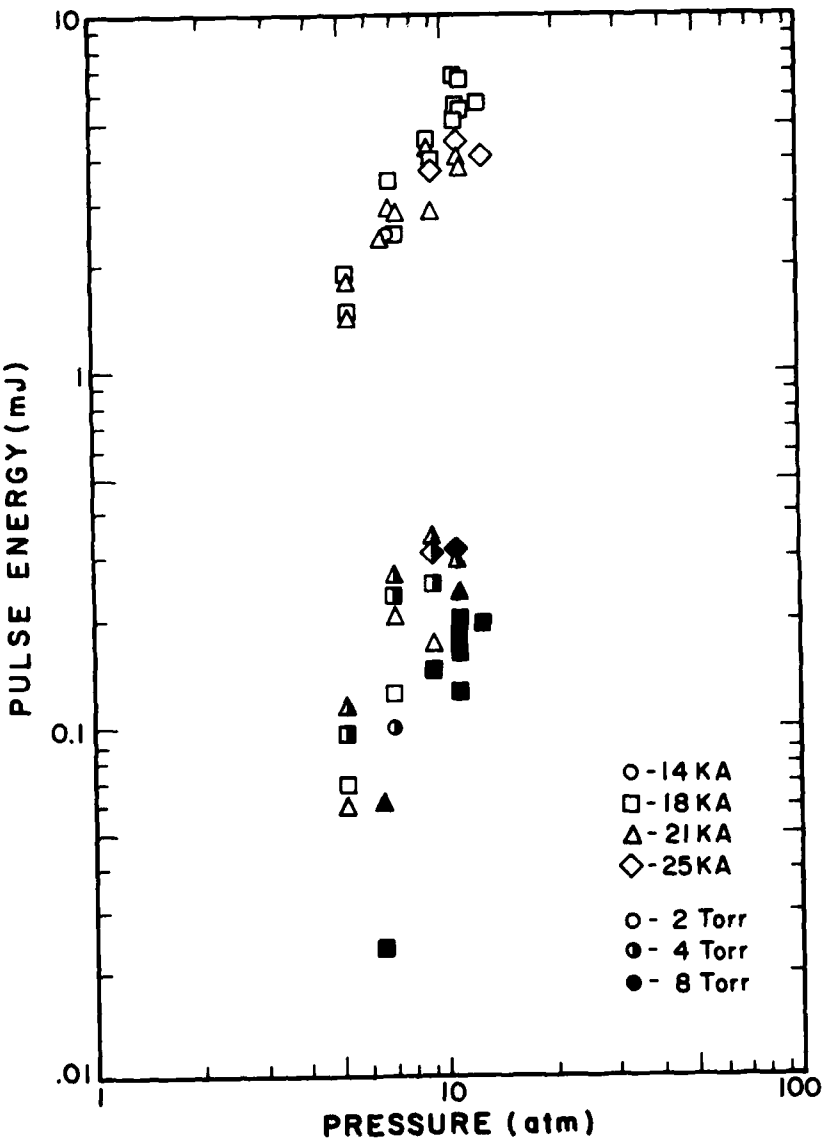
10
1
0.1
.01
PULSE ENERGY (mJ)
1
10
100
PRESSURE (atm)
○ - 14 KA
□ - 18 KA
△ - 21 KA
◇ - 25 KA
○ - 2 Torr
◐ - 4 Torr
● - 8 Torr

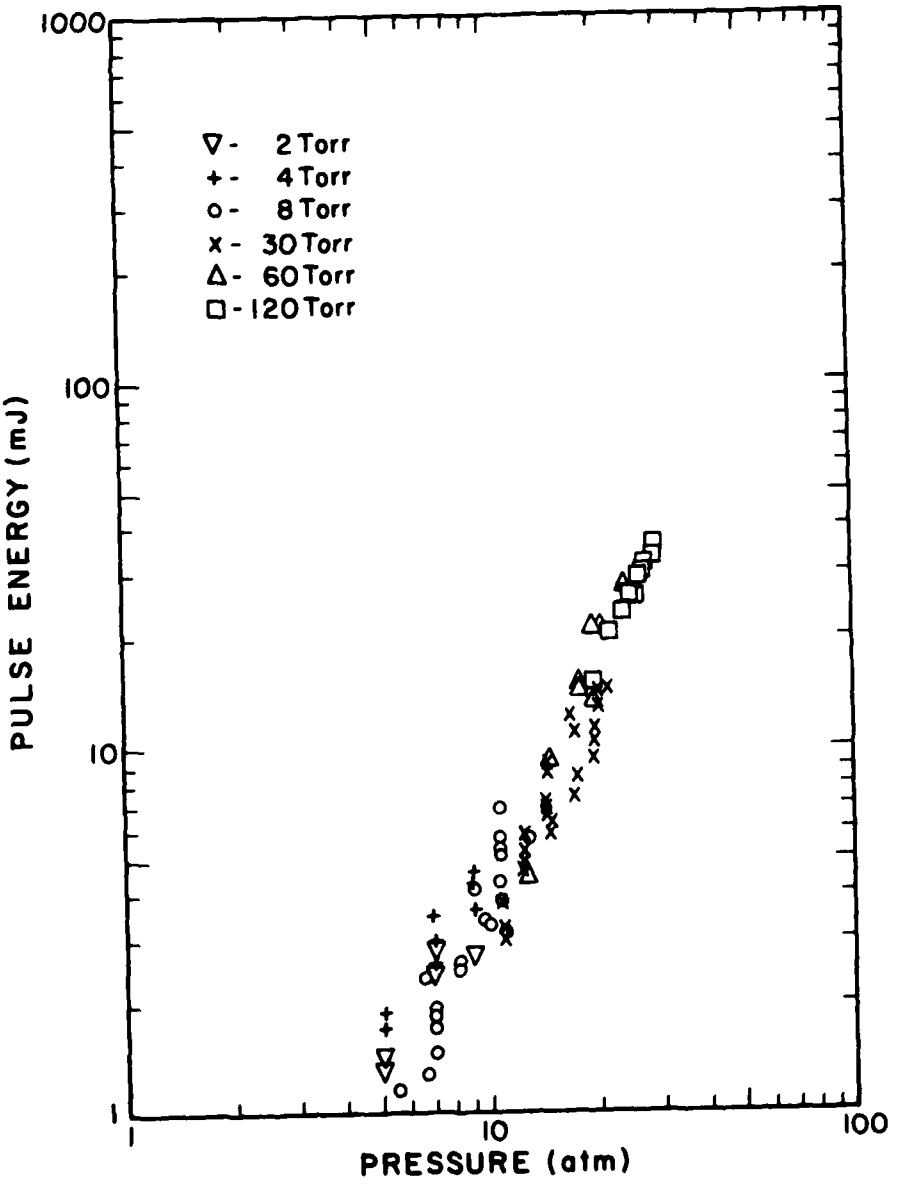
1000
100
10
1
1
10
100
PULSE ENERGY (mJ)
PRESSURE (atm)
▽ - 2 Torr
+ - 4 Torr
o - 8 Torr
x - 30 Torr
△ - 60 Torr
□ - 120 Torr

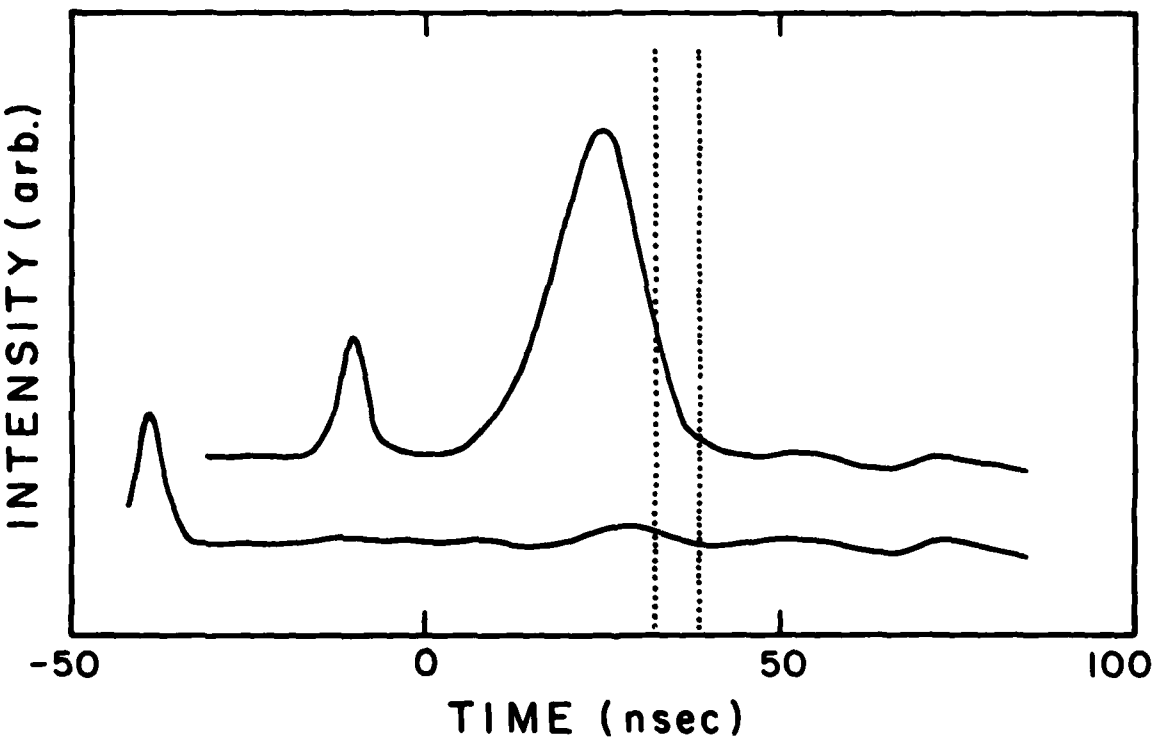
INTENSITY (arb.)
-50
0
50
100
TIME (nsec)

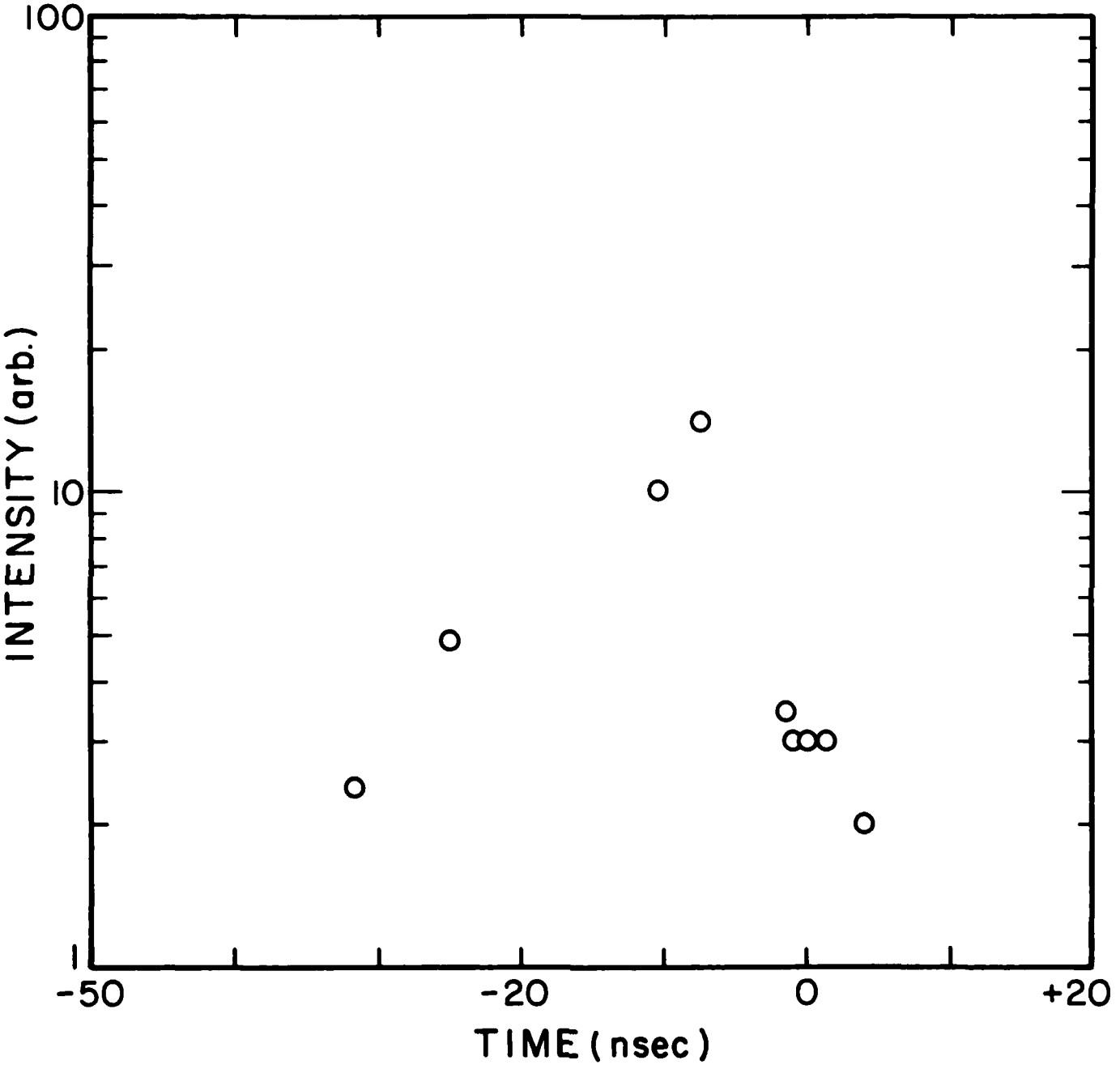
100
10
1
INTENSITY (arb.)
-50
-20
0
+20
TIME (nsec)

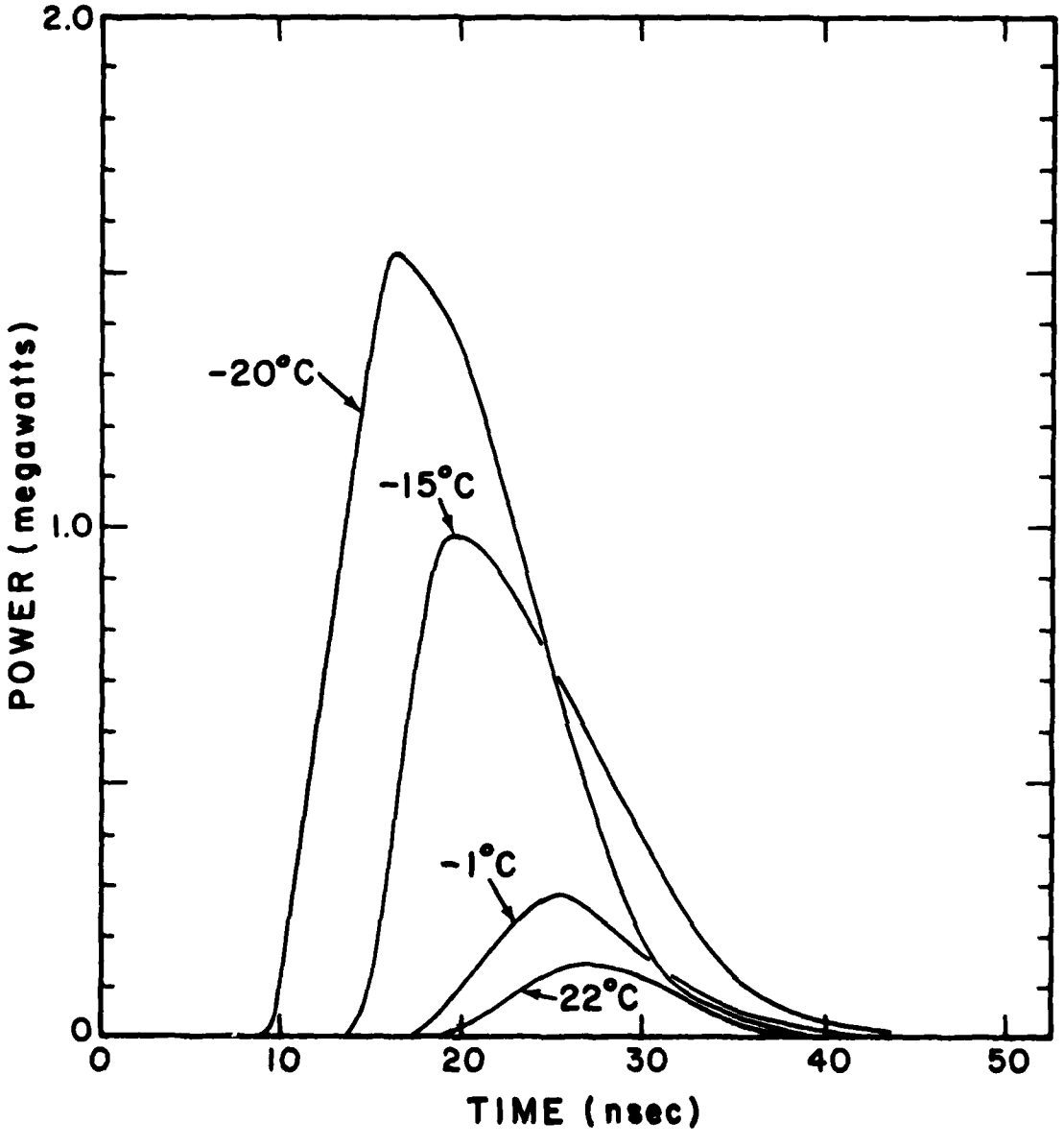
2.0
1.0
0
POWER (megawatts)
-20°C
-15°C
-1°C
22°C
0
10
20
30
40
50
TIME (nsec)

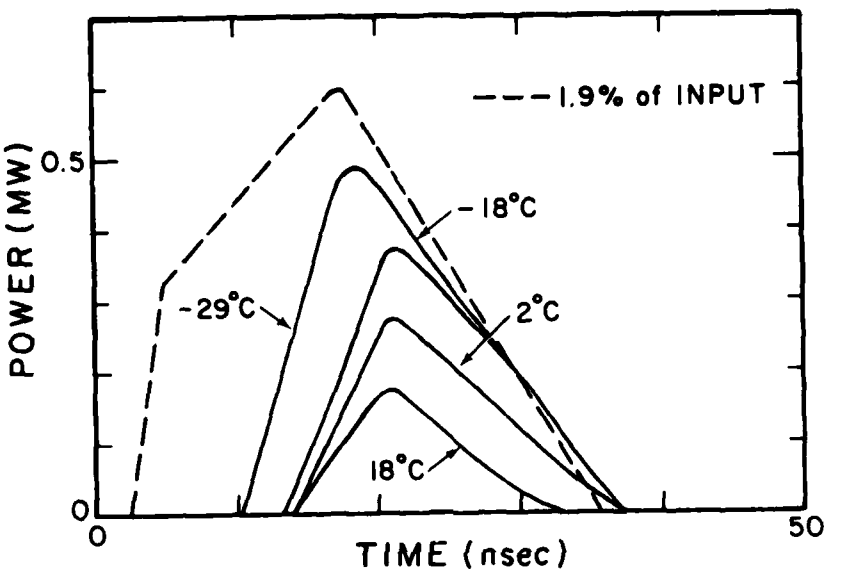
1.9% of INPUT
0.5
POWER (MW)
-18°C
-29°C
2°C
18°C
0
0
50
TIME (nsec)

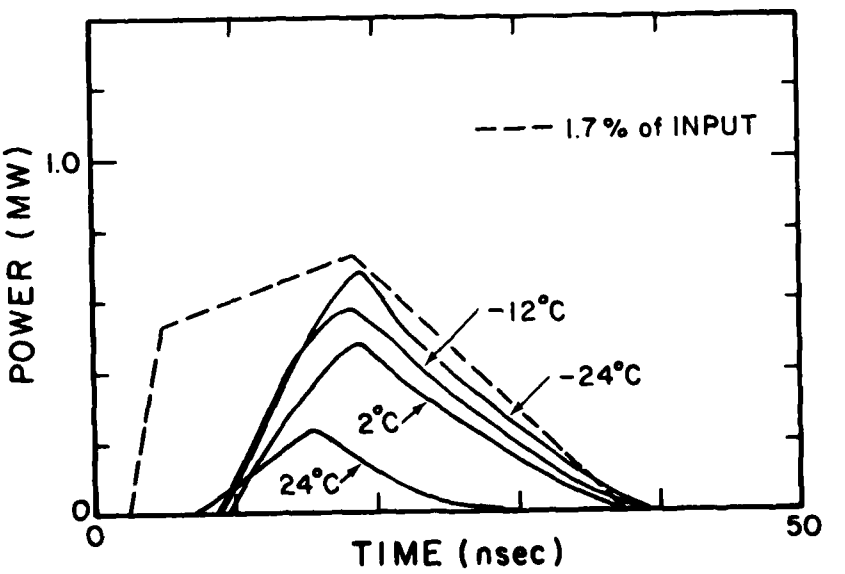
1.7% of INPUT
1.0
POWER (MW)
-12°C
-24°C
2°C
24°C
0
0
50
TIME (nsec)

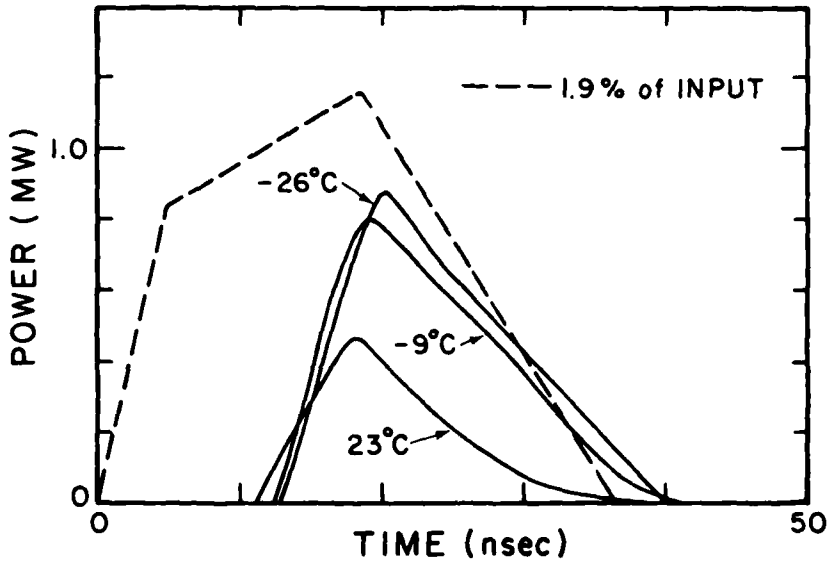
1.9% of INPUT
-26°C
-9°C
23°C
POWER (MW)
1.0
0
0
50
TIME (nsec)

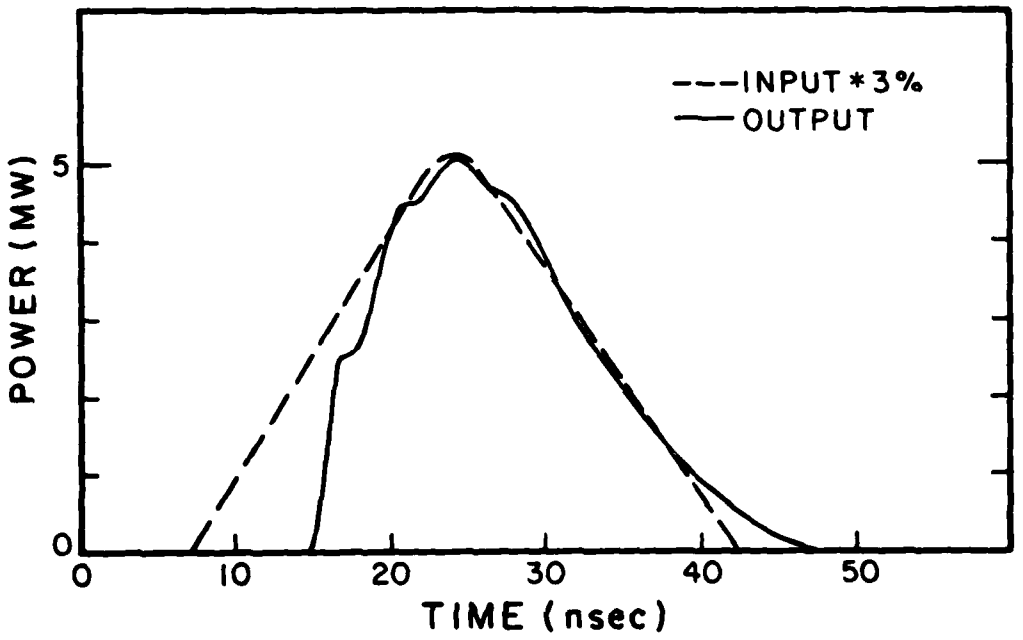
---INPUT*3%
—OUTPUT
POWER (MW)
5
0
0
10
20
30
40
50
TIME (nsec)

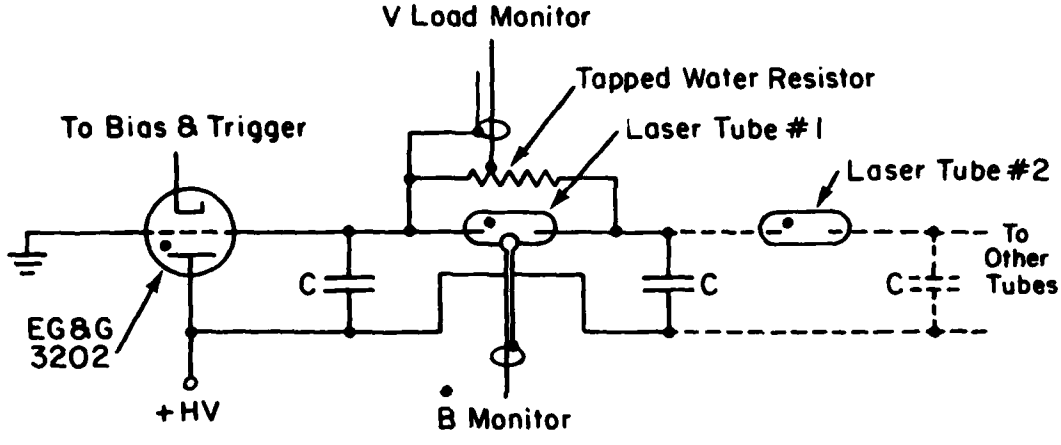
V Load Monitor
Tapped Water Resistor
To Bias & Trigger
Laser Tube #1
Laser Tube #2
To
Other
Tubes
C
C
C
EG&G
3202
+HV
B Monitor

SCHEMATIC

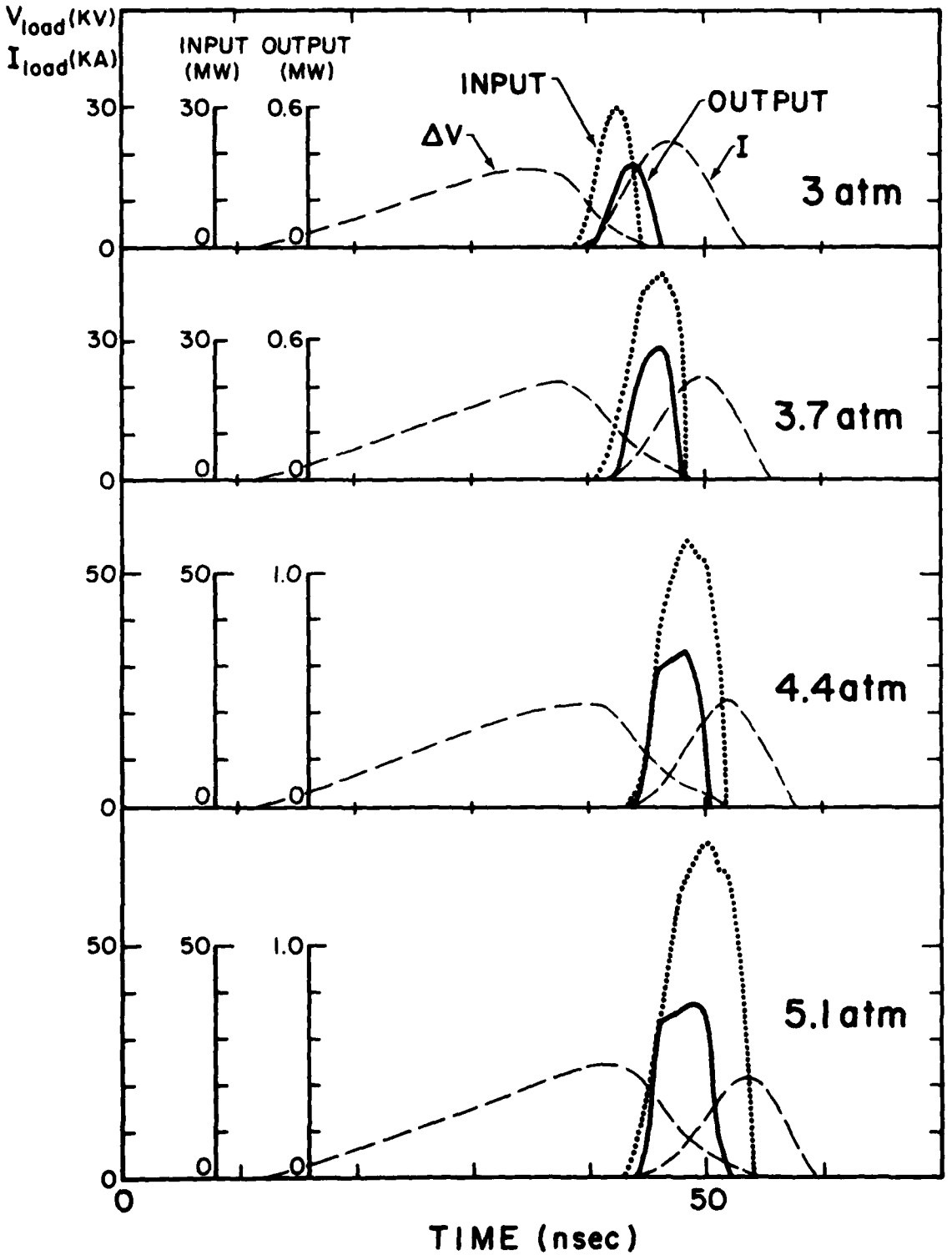
V_{load}(KV)
I_{load}(KA)
INPUT (MW)
OUTPUT (MW)
INPUT
OUTPUT
ΔV
I
3 atm
3.7 atm
4.4atm
5.1atm
30
0
0.6
50
1.0
TIME (nsec)

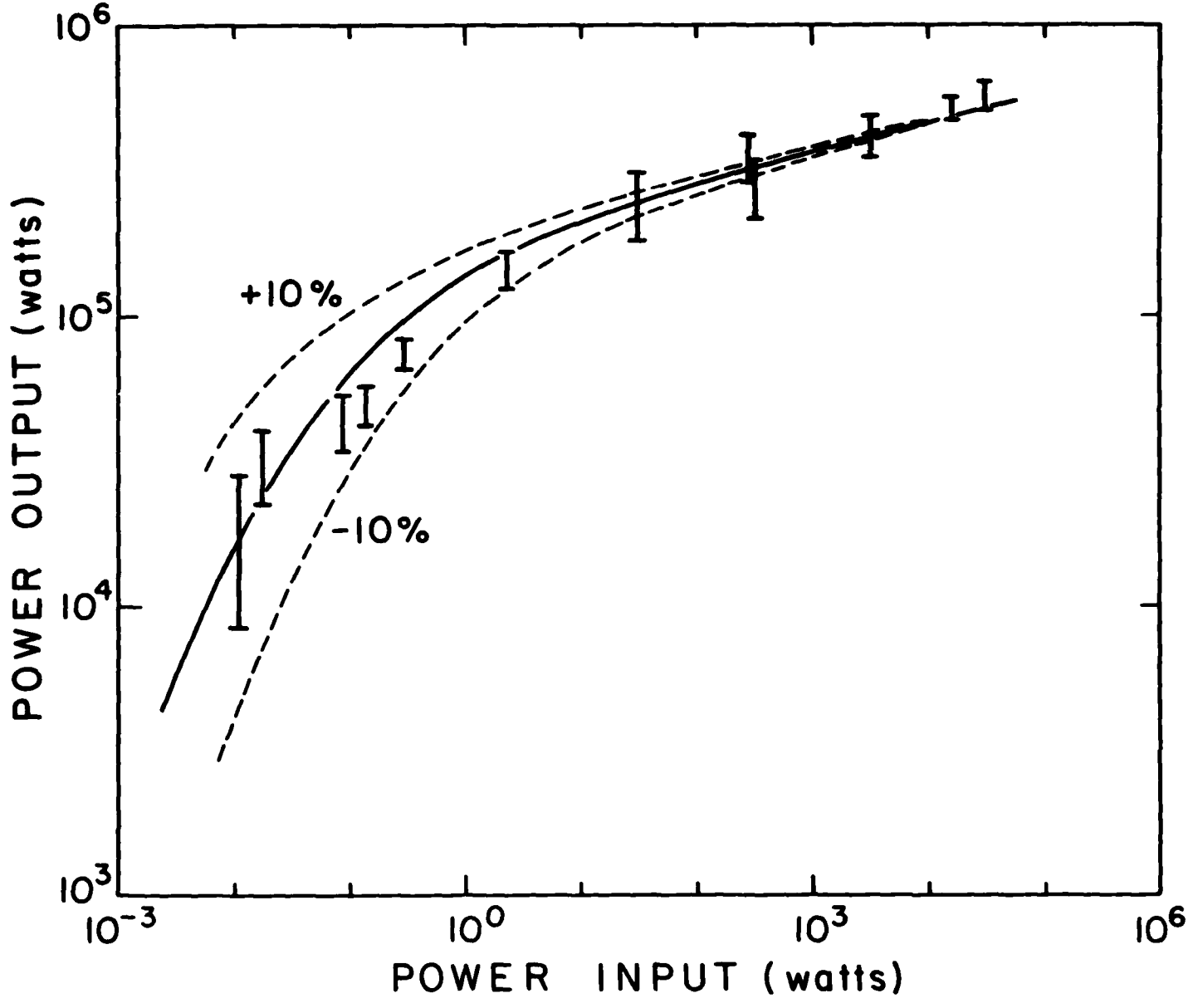
10^6
10^5
10^4
10^3
POWER OUTPUT (watts)
+10%
-10%
10^{-3}
10^0
10^3
10^6
POWER INPUT (watts)

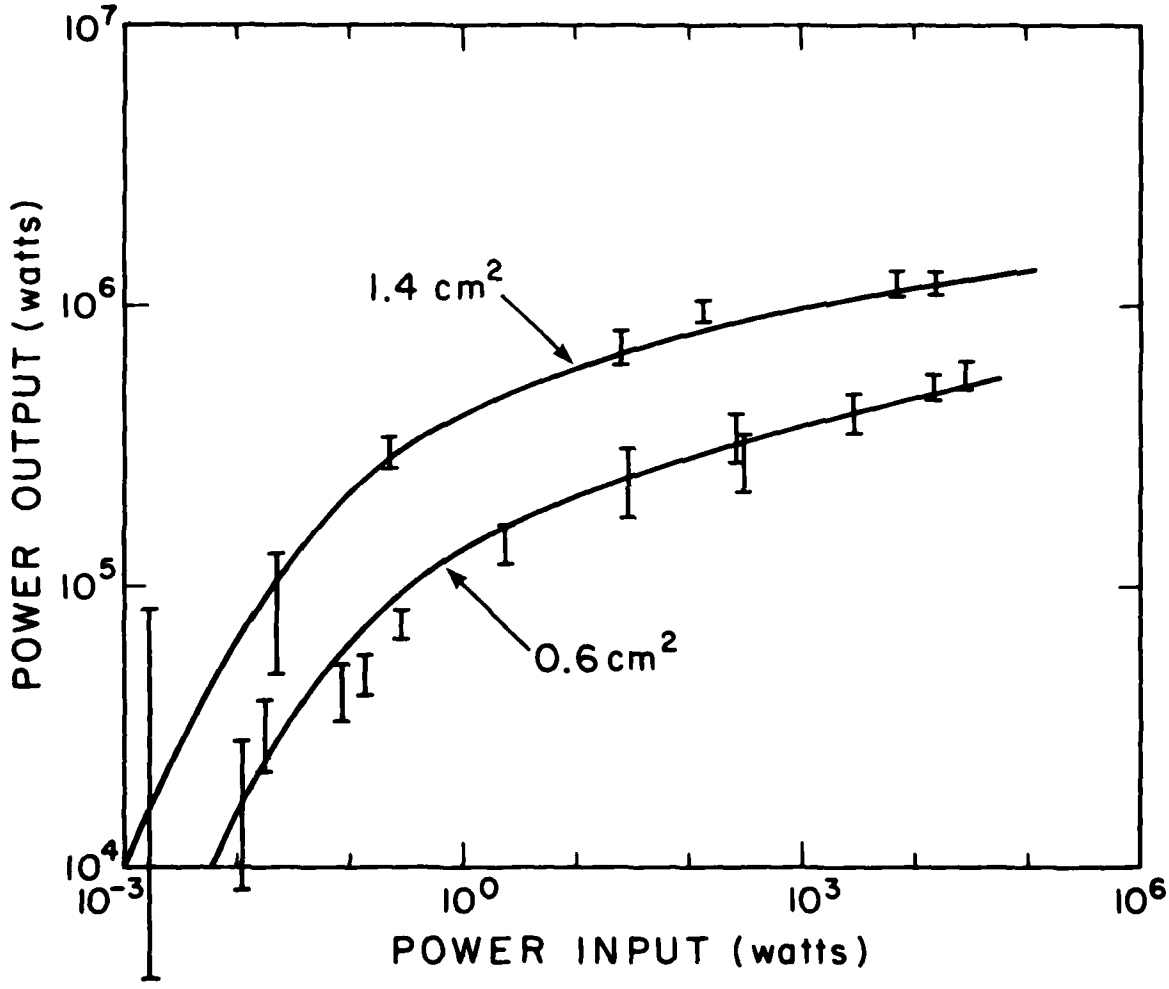
10^7
10^6
10^5
10^4
POWER OUTPUT (watts)
1.4 cm^2
0.6 cm^2
10^{-3}
10^0
10^3
10^6
POWER INPUT (watts)

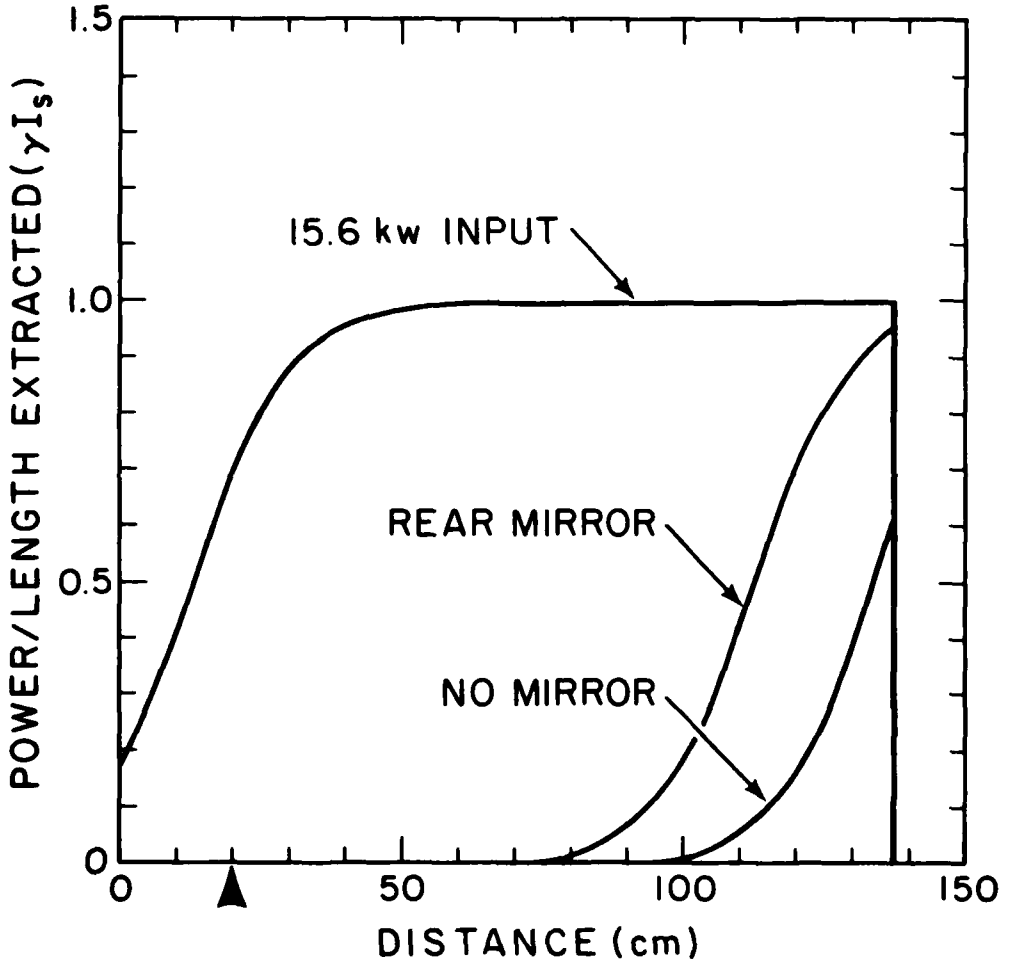
1.5
1.0
0.5
0
POWER/LENGTH EXTRACTED (γI_s)
15.6 kw INPUT
REAR MIRROR
NO MIRROR
0
50
100
150
DISTANCE (cm)

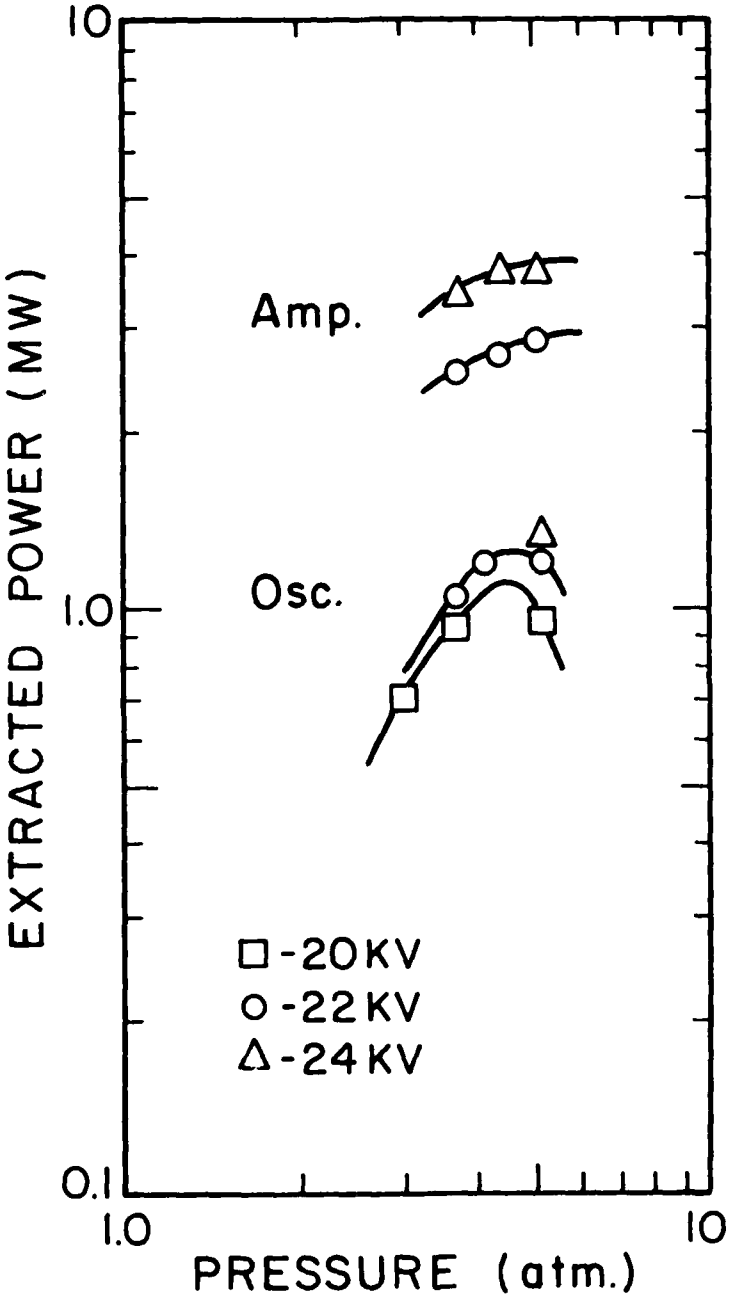
10
1.0
0.1
1.0
10
EXTRACTED POWER (MW)
PRESSURE (atm.)
Amp.
Osc.
□-20KV
o-22KV
Δ-24KV

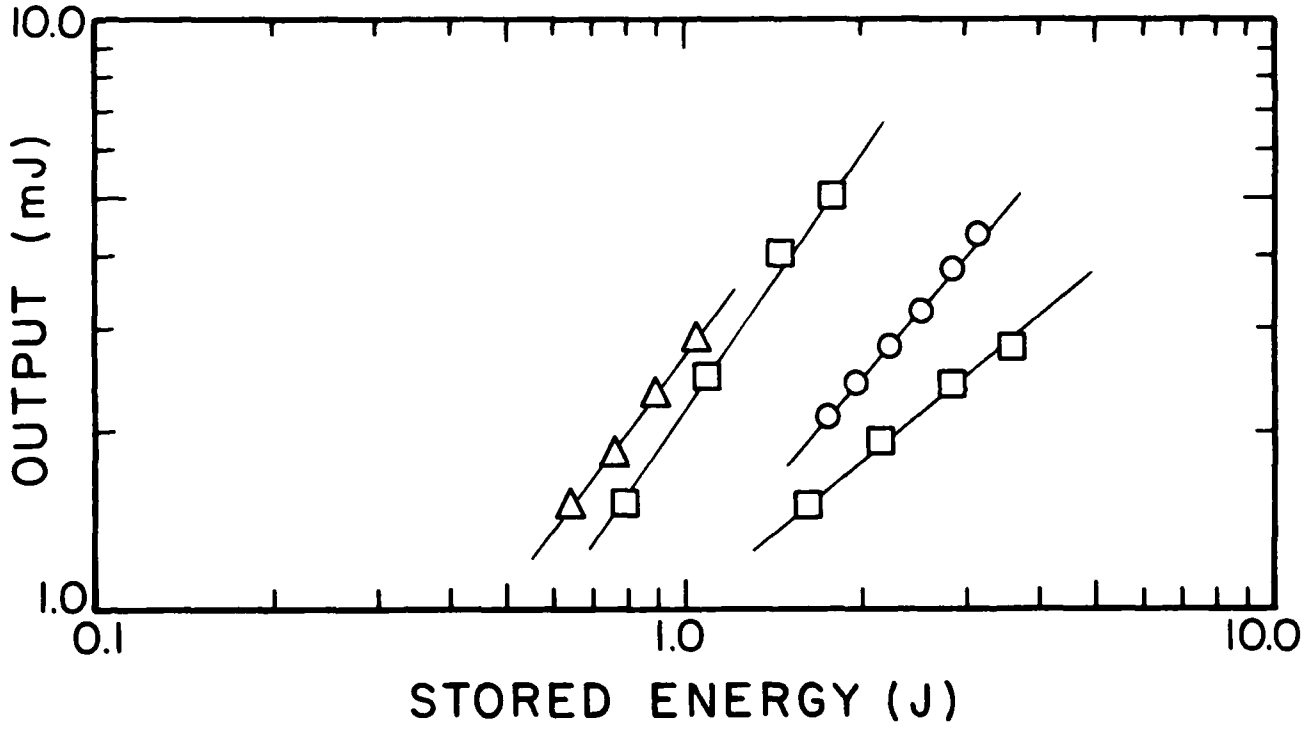
10.0
1.0
OUTPUT (mJ)
0.1
1.0
10.0
STORED ENERGY (J)

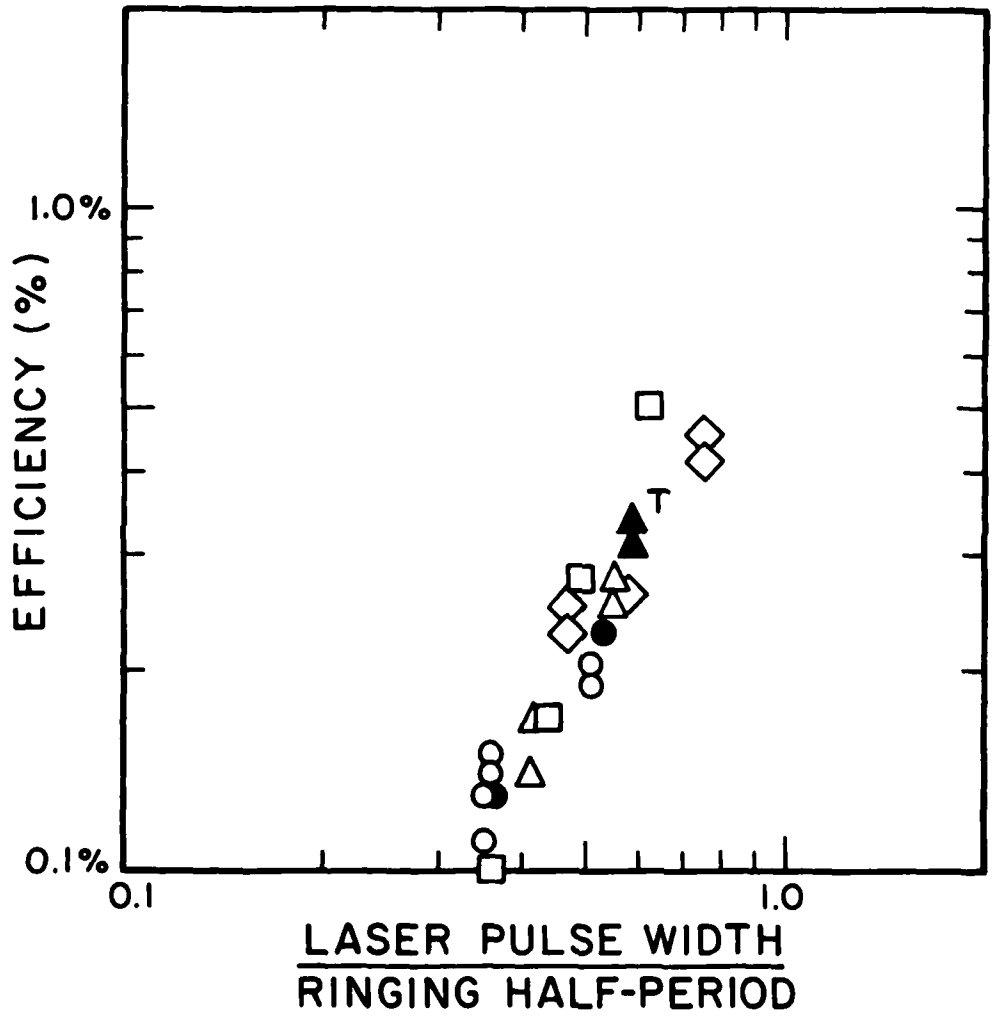
1.0%
0.1%
EFFICIENCY (%)
0.1
1.0
LASER PULSE WIDTH
RINGING HALF-PERIOD

Charge transfer pumping of the helium-nitrogen laser at atmospheric pressures in an electrical avalanche discharge[a)]

C. B. Collins, J. M. Carroll, and K. N. Taylor

Center for Quantum Electronics, The University of Texas at Dallas, Box 688, Richardson, Texas 75080
(Received 14 November 1977; accepted for publication 25 April 1978)

An atmospheric electrical avalanche (AEA) laser, stabilized by displacement current preionization, has been developed to support the study of the collisional pumping of the N_2^+, $B \rightarrow X$, electronic transition by the kinetic step $He_2^+ + N_2 + He \rightarrow N_2^+(B\,^2\Sigma_u) + 3He$. With proper preionization, the AEA laser has been operated at a pulse repetition frequency (PRF) of 1–30 Hz in an avalanche mode at 100–200 A/cm^2 and an E/p of 5 V/cm Torr. At pressures from 1 to 8 atm, an essentially uniform 30-cm^3 volume containing a high concentration of He_2^+ has been produced. Resulting laser output pumped by the charge transfer reaction has exceeded 1 MW peak power at 427.8 nm in a 4-nsec pulse. Efficiency with respect to the instantaneous power conversion has exceeded 2%, and output pulse energies have exceeded 1% of the input pulse of energy dissipated in the laser tube.

PACS numbers: 42.55.Hq, 34.70.+e, 82.30.Fi

I. INTRODUCTION

In principle, charge transfer offers a considerable advantage over other laser-pumping mechanisms because of the large cross sections[1,2] characteristic of such processes. These values lead to reaction rates which are at least an order of magnitude larger than those of other excitation transfer sequences involving neutral atomic and molecular species. As a consequence, the laser-pumping reactions can be readily arranged to be the dominant processes for loss of the ionization created in a plasma. This can be done with relatively small concentrations of the gas to be excited which, in turn, means that chemical quenching of the upper laser level should be virtually negligible in comparison to stimulated emission, as seems to be the case in the helium-nitrogen laser.[3] For example, as will be shown in this work, only 6 Torr of N_2 represents the optimum concentration in 5 atm of helium when excited in a preionized discharge.

Recently, new kinetic mechanisms have been described which further enhance the promise of the charge transfer laser. Multibody charge transfer reactions have been reported[2] which raise substantially the rates at which the principal pumping reactions can proceed. Additionally, it has been recognized[4] that the kinetic sequence involving an ion-electron capture followed by autoionization[5] offers a mechanism which is unique to molecular ions for the quenching of vibrational excitation. Thus, if the lower laser level is arranged to be a vibrationally excited state of a molecular ion, the capture-autoionization process offers a rapid kinetic channel for its depopulation. These particular features of the elementary kinetic steps contribute to the following important advantages of the charge transfer scheme of laser pumping:

(1) Since the sequence can operate as a four-level system, it should be readily adapted to a variety of excitation devices as the output should continue as long as the population of the energy storage level is replaced.

(2) Since the operating wavelength is generally longer than the photoionization and photodissociation thresholds for all of the important species in the kinetic sequence pumping the inversion, operation at high power density should be possible with no loss of efficiency.

(3) Because the laser transition occurs between bound electronic states of a molecular ion, the bandwidth of the gain is small, and, hence, the maximum gain is large. As a consequence, saturation should be reached at smaller inversion densities than in excimer transitions.

The prototype of such charge transfer systems is the helium-nitrogen laser demonstrated by Collins *et al.*[6] When excited in a plasma produced by the discharge of an intense electron beam,[7] it exhibited all of these advantages specific to this laser type. With e-beam currents of the order of 1 kA/cm^2 quasi-cw operation of the laser was achieved[4] at 427.8 nm and output power was found to accurately follow input power after the onset of threshold. A time-independent power efficiency of 3% was found and tended to confirm the operation of the laser as a four-level system.[8] As a result, no evidence of bottlenecking was found over a range of circulating intracavity intensities up to 30 MW/cm^2. Peak power densities as great as 320 MW/l showed no evidence of disturbing the kinetic sequence pumping the laser transition.[9]

Early reports[10–12] of the discharge excitation of the laser transition at lower current densities presented an output efficiency of only 0.05% of the total stored energy, and no instantaneous efficiencies were reported. Whether the lower overall values resulted from a decoupling of the plasma load from the driving circuit or whether it resulted from some failure of the kinetic mechanisms in the discharge environment was not determined. Other differences were found in the timing of the development of the laser pulse. While the results for e-beam excitation[4,7,13] had indicated a delay of 5–10 nsec between the onset of the excitation current and the initiation of the laser output, a more immediate development of the laser output was observed from these discharge plasmas having greater gain path lengths. Less than a 1-nsec delay was observed with an output pulse rise time of the order of 2 nsec. Using the accepted values of the binary rate coefficients, the lifetime against charge transfer from helium to nitrogen should have been in excess of 10 nsec at 3 atm pressures of the gas compositions generally used. This apparent inability of charge transfer to pump the laser transi-

a)Research supported by ONR Contract No. N00014-77-C-0168.

 0021-8979/78/4910-5093$01.10

TABLE I. Reaction times for charge transfer from He_2^+ as computed from traditional low-pressure rate coefficients in comparison with values computed from recently obtained coefficients describing multibody processes. Gas composition is assumed to be 0.15% N_2.

Pressure (atm)	Reaction times Bimolecular[a] (nsec)	Multibody[b] (nsec)
3	7.0	4.0
5	4.2	1.8

[a]Reference 1.
[b]Reference 2.

tion fast enough together with the lower efficiencies led early authors[10] to misidentify the principal kinetic step as being the direct collisional excitation of neutral nitrogen by hot electrons in the tail of the energy distribution and generally contributed some doubt in later work as to the similarity of the pumping mechanisms under the different conditions of excitation. However, the new multibody charge transfer reactions reported recently[2,14] now resolve this discrepancy by providing the necessarily high rates of reaction. The relevant reaction of importance in the helium-nitrogen discharge laser is termolecular charge transfer from He_2^+ to N_2, occurring with a rate coefficient of 1.6×10^{-29} cm^6 sec^{-1}. Table I summarizes the improvement in the expected speed of the reaction brought about by the inclusion of this step in the kinetic sequence. It is thus consistent with the timing of the laser outputs to attribute the operation of the helium-nitrogen laser under either e-beam or direct discharge pumping to the common excitation scheme,

Ionization

$$e + He \rightarrow He^* + 2e, \quad (1a)$$

$$He^* + 2He \rightarrow He_2^+ + He, \quad (1b)$$

Charge transfer

$$He_2^+ + N_2 \rightarrow N_2^+(B^2\Sigma_u) + 2He, \quad (2a)$$

$$He_2^+ + N_2 + He \rightarrow N_2^+(B^2\Sigma_u) + 3He, \quad (2b)$$

Stimulated emission

$$N_2^+(B^2\Sigma_u) + h\nu \rightarrow N_2^+(X^2\Sigma_g) + 2h\nu, \quad (3)$$

Capture-autoionization

$$N_2^+(X^2\Sigma_g)_{v=1} + e \rightarrow N_{2,v=1}^{**}, \quad (4a)$$

$$N_{2,v=1}^{**} \rightarrow N_2^+(X^2\Sigma_g)_{v=0} + e, \quad (4b)$$

where the double asterisk indicates an autoionizing level. The rate-limiting step in the kinetic sequence is the charge transfer step.

The work reported here concerns a reexamination of the performance of the helium-nitrogen laser excited directly in a preionized discharge. It will be shown that lowered output efficiencies generally occurred as the result of a loss of coupling between the electrical load and driving circuits caused by the time-varying impedance of the laser tube. At the E/p values of the order of 5 V cm^{-1} Torr^{-1} and the current densities of 100 A cm^{-2} employed in this work power efficiencies of 2% were found, with peak powers in excess of 1 MW. Thus, both in timing and efficiency the performance of the discharge pumped laser was found to be consistent with the results of the e-beam excitation and, hence, to be consistent with the charge transfer sequence summarized above.

II. EXPERIMENTAL METHOD

A schematic representation of the main discharge circuit together with the principal diagnostic circuitry used in the work reported here is shown in Fig. 1. The laser tube consisted of a machined Delrin pressure vessel containing 87-cm-long electrodes of 0.3-cm thickness separated by either 1.3 or 1.7 cm. The current flow in the tube was transverse to the optical axis giving computed inductances for the laser tube of 0.23 and 0.3 nH, respectively, for the two possible electrode spacings. Measured values agreed with the computed values to within experimental error. As shown in Fig. 1, the laser tube was connected in a lumped Blumlein circuit switched by an EG&G 3202 hydrogen thyratron. The capacitors marked C in Fig. 1 were constructed from a 0.08-cm-thick G-30 printed circuit board, copper clad on one side and contacted to two sheets of 0.039-cm-thick Mylar on the other. A foil electrode contacted to the outer surface of the Mylar completed the capacitors giving a value of $C = 12$ nF for each.

In operation, the electrical performance of the main discharge circuit resembled that of the neutral N_2 laser described and analyzed in detail by Fitzsimmons.[15] Because of the relatively high inductance of the thyratron, the switching circuit functioned as a lumped LCR circuit which, upon commutation of the thyratron, tended to invert the voltage across the left capacitor in Fig. 1. The ringing period of the switching circuit was of the order of 100 nsec in this arrangement.

As the voltage across that capacitor proceeded toward a full inversion, the voltage across the laser tube tended toward twice the original charging voltage. At some point, depending upon the pressure and gas composition in the laser tube, the E/p would reach a value sufficient to support the avalanche growth of the ion concentration in the gas mixture, thus initiating the kinetic chain pumping the laser transition. As the ionization increased, the conductivity increased, permitting the energy-storage capacitor to discharge through the laser tube on a time scale short compared

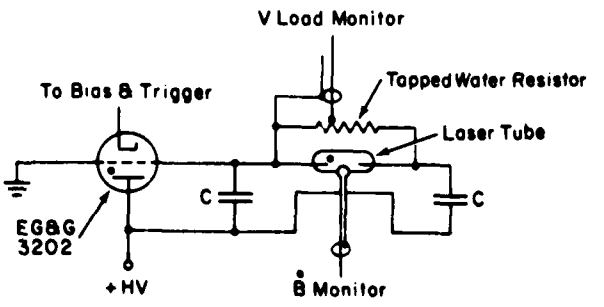

FIG. 1. Schematic diagram of the circuit of the atmospheric electrical avalanche (AEA) laser used in these experiments.

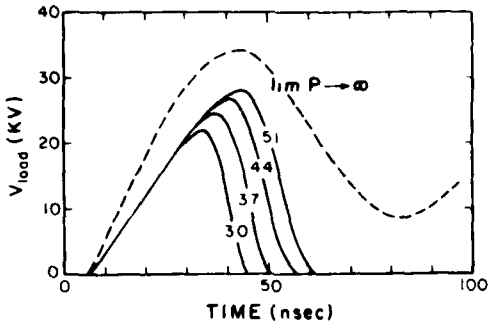

FIG. 2. Graphs of the transient voltage switched across the laser tube. The dashed curve shows the open-circuit voltage ringing across the laser tube when the electrical breakdown was inhibited. Solid curves record the voltage appearing across the laser tube when filled to the indicated pressure in atmospheres and preionized. The electrode spacing was 1.7 cm.

to the original ringing period of the switching circuit. In the atmospheric electrical avalanche (AEA) device finally realized in these experiments, discharge currents up to 30 kA could be attained with rise times of a few nanoseconds. Switched voltages approaching 50 kV could be developed across the laser tube prior to breakdown.

In operation, it was found that adequate preionization was necessary before the main discharge could develop uniform and stable plasmas. In the AEA laser developed for this work, spatial uniformity was finally achieved up to 9.3 atm pressure in discharges with transverse aspect ratios varying from 1×1 to 6×1 through the use of displacement current preionization, a technique superior to uv preionization in relatively "transparent" gases such as helium. A potential of the order of 40–50 kV was applied to an electrode outside the pressure vessel of the laser tube in a manner to create an intense electric field perpendicular to the axis of discharge current flow and perpendicular to the optical axis. The high-voltage pulse was developed by a cable transformer[16] driven by a grounded grid thyratron switching a low-inductance capacitor. A delay of the order of 0.5–1.0 μsec between the preionization pulse and the main discharge was found to be necessary. Since both the preionization and the main discharge were switched by hydrogen thyratrons, the AEA laser could be readily operated at repetition rates from 1 to 30 Hz. Because of the longitudinal gas flow, excessive heating prevented the operation of the device at higher repetition rates. It appears that a transverse gas flow would allow operation at much higher repetition rates.

III. RESULTS

As shown in Fig. 1, the electrical performance was monitored by voltage and current probes connected to the laser tube. A tapped water resistor was placed across the tube and inductively decoupled from the ground of a Tektronix 519 oscilloscope to provide the means for measuring the voltage difference applied across the laser tube. The current flowing in the discharge loop was monitored with a $\dot{B}$ loop which could be rotated through 180°. In fact, this rotation proved necessary because of the capacitive coupling between the loop and the extended capacitors. Each measurement of current was determined from the difference of two measurements of $\dot{B}$ made with the plane of the loop being rotated through 180°.

Figure 2 shows typical data obtained from the voltage probe and illustrates the interaction of the discharge load with the switching circuit. The voltage developed across the laser tube is shown for several values of pressure. In each case the charge voltage on the line was 24 kV and the electrode spacing was 1.7 cm. Shown by the dashed line is the open-circuit ringing voltage obtained at values of pressure and preionization voltage sufficiently extreme so that no discharge occurred. It agreed well with the simple model for the series LCR circuit for a switch inductance of 15 nH, a value in good agreement with the thyratron specifications. As can be seen, the peak voltage across the laser tube was found to ring to a maximum of only 1.5 times the charge voltage instead of the doubling expected for an ideal switch. The solid curves represent typical operating conditions for the pressures in atmospheres indicated in Fig. 2. It can be seen that the loading of the switching circuit caused by the conductivity of the preionized gas caused a further reduction in the voltage developed across the tube prior to the onset of the electrical avalanche. In most cases it was found that with proper preionization the voltage actually appearing across the laser tube was roughly equal to the original charging voltage. As was expected, increases in pressure in the laser tube caused progressive increases in the delay of the onset of the avalanche with corresponding increases in the voltage developed. In Fig. 2 the occurrence of the electrical avalanche can be seen to cause a rapid decrease of the voltage across the tube as the conductivity of the gas increased to meet the inverse impedance of the driving circuit. Optimal performance of the laser was found to correspond to conditions for which the duration of the avalanche spanned the maximum in the open-circuit voltage curve. For example, for a charging voltage of 24 kV, Fig. 2 indicates that the optimal performance would occur for pressures of the order of 3.7 atm, in agreement with the maximum actually observed in the laser output. Conversely, at 5.1 atm the devel-

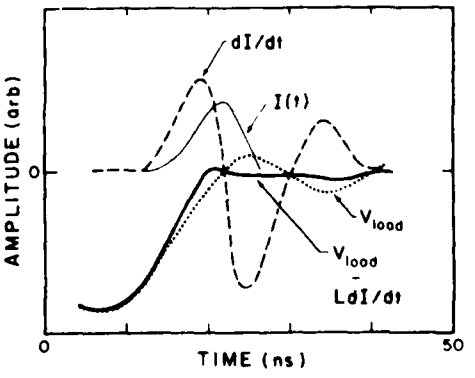

FIG. 3. Graphs of typical diagnostic data obtained from the $\dot{B}$ loop and from the voltage divider connected across the laser tube are shown by the dashed and dotted curves, respectively. The light solid curve shows the current obtained by integrating the dashed curve, and the heavy solid curve records the voltage appearing across the resistive part of the load obtained by removing the inductive component from the dotted curve. Data for both $\dot{B}$ and I have been inverted in sign for clarity of presentation.

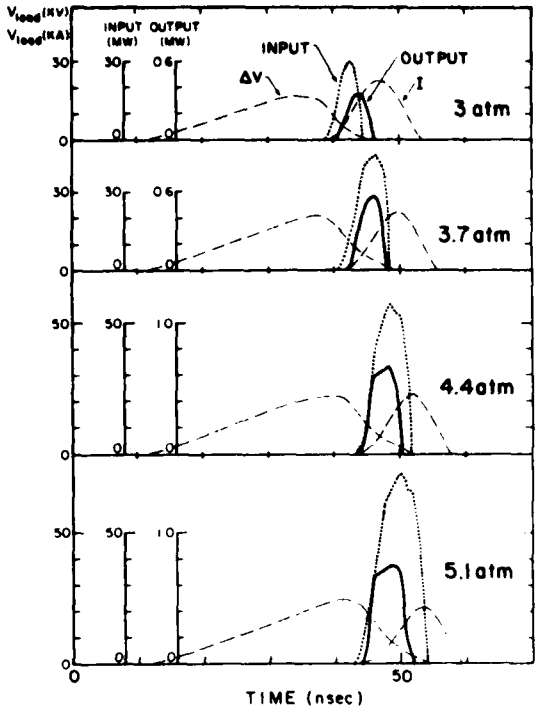

FIG. 4. Graphs comparing the electrical and optical performance of the laser tube obtained for a 1.3-cm electrode spacing and for the indicated pressures of helium containing 0.15% N_2. Dashed curves plot the voltage and current applied to the laser tube as marked and scaled to the left-most ordinate. The dotted curve records the instantaneous power dissipation in the laser tube and is scaled to the middle ordinate. The solid curve plots the output power of the laser measured at 427.8 nm and is scaled to the right-most ordinate.

oping avalanche can be seen to be competing for stored charge with the "ringing down" of the voltage in the switching circuit. A correspondingly lower laser output was observed in that case.

Figure 3 shows a comparison of typical data obtained from the voltage and current diagnostic devices. For clarity of presentation the latter data has been inverted in sign. Shown by the dashed curve is the difference obtained between successive measurements made with the $\dot{B}$ loop after rotation through 180°. It was observed that the data obtained with the two orientations generally showed the proper inversion but contained an error signal which did not change sign and which represented about 20% of the amplitude. Computing the difference of the data obtained for the two orientations effectively removed this error signal and led to the type of data for dI/dt shown in Fig. 3.

It can be seen in Fig. 3 that the successive nodes of the dI/dt curve correspond to the nodes of the direct measurement of the voltage across the load as plotted by the dotted curve. At these nodes, since $dI/dt=0$, the voltage must represent only that component which appeared across the resistive part of the load, namely, the plasma. Since that voltage was also zero at that time, it can be concluded that the avalanche had proceeded to an end point at which the resistance of the load had fallen to a small value in comparison to the driving impedance, and no further increase in ionization could occur. At later times the voltage excursions seen in Fig. 3 must represent only the voltage developed across the inductive part of the laser tube as the current continued to ring in the discharge circuit. A comparison of the relative amplitudes of the oscillations of the voltage curve and the dI/dt curve showed them to be consistent with the calculated value of tube inductance. Then, for subsequent analytical purposes the measured voltage was corrected by multiplying the value of tube inductance by the measured value of dI/dt and subtracting it from the measured voltage. A typical result for the voltage appearing across the resistive part of the load and, thus, leading to dissipation, is shown in Fig. 3 by the heavy solid curve. The time-dependent current obtained by numerically integrating the dI/dt curve is shown for comprison by the light solid curve. The absolute scale factor for the current was obtained by setting the second integral of dI/dt equal to the charge stored in the series capacitance formed from the two capacitors at the time of breakdown. The instantaneous power dissipation in the load can, then, be obtained by forming the product of the two curves.

A comparison of the time dependence of the input power to the laser output power showed that the smaller electrode spacing resulted in a better power conversion, probably because of a more-thorough saturation of the optical transition. Results for the 1.3-cm spacing of the electrodes are shown in Fig. 4 for the four values of gas pressure indicated, each containing 0.15% N_2. The charge voltage was 24 kV and the repetition rate was 10 Hz. Dashed lines show the discharge currents and the voltages which appeared across the resistive part of the load. The powers dissipated in the load are shown by the dotted curves, and the solid curves record the laser output power measured in the ($0\rightarrow1$) vibrational component of the $B\rightarrow X$ electronic transition of N_2 at 427.8 nm.

The pressure-dependent delays between the input powers applied to the plasma, and the laser outputs are consistent with the magnitude of the reaction times for the charge transfer step as shown in Table I. The scales for the power have been chosen as indicated, so that the close correlation between input and output power on the leading edge of the curves for the high-pressure plasmas corresponds to an instantaneous conversion efficiency of 2%. Integrals under the power curves shown in Fig. 4 give values for the energies of the laser pulses of 1.3, 2, 3, and 4 mJ, respectively, for the pressures varying from 3 to 5.1 atm. These results in comparison with the integrals under the input power curves yield efficiencies of 1.3, 1.0, 1.0, and 0.8%, respectively, for the conversion of the energies dissipated in the load for the cases shown in Fig. 4.

The field strengths in the plasma corresponding to the maximum observed transfer of power can also be determined from Fig. 4. At the higher pressures where the delay in the kinetic chain is minimal, the highest instantaneous power efficiency can be seen to occur on the leading edge of the pulses where the E/p is greatest. For the times at which 2% efficiency was sustained the E/p can be computed from Fig. 4 to have been decreasing from 3.5 to 2 V cm^{-1} $Torr^{-1}$. The corresponding current densities were increasing from 0 to

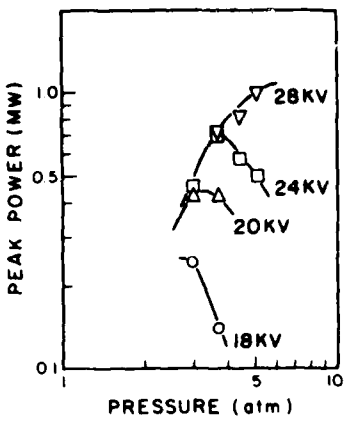

FIG. 5. Graphs showing the parameterization of the charge transfer AEA laser operating with 1.7-cm electrode spacing. Peak output power is shown as a function of helium pressure and parametrically as functions of the charge voltages shown.

160 A cm^{-2}. It can be seen that the loss of efficiencies for the conversion of the pulse energy at the higher pressures resulted from the prolonged flow of discharge current at relatively low E/p.[17]

IV. CONCLUSIONS

The parameterization of the charge transfer AEA laser is summarized in Fig. 5 for the case of the 1.7-cm electrode spacing. The peak laser power observed has been plotted as a function of gas pressure and parametrically as functions of charging voltage on the capacitors. The gross behavior is evidently dominated by the degree of the coupling of the plasma load to the electrical driving circuit. A comparison of the curve corresponding to 24 kV charging voltage with the data of Fig. 2 shows that the peak output occurred for the case in which the avalanche developed and reached completion during the period the switching circuit was ringing through the maximum in voltage, as discussed previously. Computed in terms of the maximum switched voltage, the peaks in the performance curves of Fig. 5 correspond approximately to an E/p value of 5V cm^{-1} Torr^{-1}.

In conclusion, it appears that the AEA discharge device represents a useful means for exciting the helium-nitrogen charge transfer laser, and peak powers reaching 1 MW have been demonstrated. Instantaneous power transfer efficiencies of 2% have been achieved at E/p values of the order of 3 V cm^{-1} Torr^{-1} and current densities of 100–200 A cm^{-2}. The corresponding values of efficiency for the conversion of energies dissipated in the laser tube into output pulse energies have been shown to be around 1%.

[1] D. K. Bohme, N. G. Adams, M. Mosesman, D. B. Dunkin, and E. E. Ferguson, J. Chem. Phys. **52**, 5094 (1970).
[2] F. W. Lee, C. B. Collins, and R. A. Waller, J. Chem. Phys. **65**, 1605 (1976).
[3] C. B. Collins, Seventh Semi-Annual Technical Report No. UTDP ML-94, Contract No. N00014-76-C-0174, The University of Texas at Dallas, 1975 (unpublished).
[4] C. B. Collins, Final Technical Report No. UTDP-ML-06, Contract No. N00014-76-C-0174, The University of Texas at Dallas, 1977 (unpublished).
[5] This process is the analog for molecular ions to the rapid vibrational quenching of neutral molecules by the capture of free electrons to form unstable negative ions. However, since the interaction force is Coulombic for the molecular ions in comparison with the weaker charge-induced dipole forces for the neutrals, the quenching of vibration by electron collisions should proceed even more rapidly in the case of the molecular ions. [For a detailed discussion of this process see J. Stevefelt, Phys. Rev. A **8**, 2507 (1973).]
[6] C. B. Collins, A. J. Cunningham, S. M. Curry, B. W. Johnson, and M. Stockton, Appl. Phys. Lett. **24**, 477 (1974).
[7] C. B. Collins, A. J. Cunningham, and M. Stockton, Appl. Phys. Lett. **25**, 344 (1974).
[8] A. Yariv, *Introduction to Optical Electronics* (Holt, Rinehart and Winston, New York, 1971), p. 103ff.
[9] C. B. Collins, J. M. Carroll, F. W. Lee, and A. J. Cunningham, Appl. Phys. Lett. **28**, 539 (1976).
[10] V. N. Ishchenko, V. N. Lisitsyn, A. M. Razkev, and V. N. Starinskii, JETP Lett. **19**, 233 (1974).
[11] J. B. Laudenslager and T. J. Pacala, Appl. Phys. Lett. **29**, 580 (1976).
[12] D. E. Rothe and K. O. Tan, Appl. Phys. Lett. **30**, 152 (1977).
[13] C. B. Collins and A. J. Cunningham, Appl. Phys. Lett. **27**, 127 (1975).
[14] C. B. Collins and F. W. Lee, J. Chem. Phys. (to be published).
[15] W. A. Fitzsimmons, L. W. Anderson, C. E. Riedhauser, and J. M. Vrtilek, IEEE J. Quantum Electron. **QE-12**, 624 (1976).
[16] V. N. Ishchenko, V. N. Lisitsin, and V. N. Starinskii, Opt. Technol. **41**, 155 (1974).

[17] At times following the completion of the electrical avalanche, the discharge current reaches very large values in subsequent pulses ringing through the plasma. Even though $\Delta V \sim 0$, significant power can be dissipated in it, and because of the longer times involved, significant energy as well. It is believed that this dissipative ringing in the plasma together with that through the thyratron switching circuit represents the dominant final deposition of the energy originally stored in the capacitors.

Gain and saturation of the nitrogen ion laser[a)]

C. B. Collins, J. M. Carroll, and K. N. Taylor

Center for Quantum Electronics, The University of Texas at Dallas, Box 688, Richardson, Texas 75080
(Received 22 March 1978; accepted for publication 5 May 1978)

In this work a dilute nitrogen plasma pumped by charge transfer from He_2^+ has been operated as a pulsed optical amplifier. In the experimental system used two synchronously excited plasmas were produced by preionized discharges in an atmospheric electrical avalanche device switched by hydrogen thyratrons so that repetitive operation to 30 Hz would be possible. The plasmas were electrically connected in a transverse series circuit to provide a phase delay in their excitation comparable to the optical transit time between them. Laser output at 427.8 nm from the first discharge coupled to the fields in a self-excited oscillator geometry was threaded through the second along its 85-cm longer dimension. Calibrated attenuation of the beam from the oscillator subsequently input to the amplifier provided data on the overall amplification ratio to which the two adjustable parameters of a simple model were fit. From these parameters overall small-signal gains as large as 2×10^6 were found together with saturation intensities of the order of 50 kW/cm^2. Under the same conditions a gain of about 18 was found at an output intensity of 1 MW/cm^2, conditions relatively near the ideal extraction of power at zero gain.

PACS numbers: 42.55.Hq

Since its discovery[1-3] in 1974, the nitrogen ion laser pumped by charge transfer from He_2^+ has shown several important advantages over other laser types operating at comparable wavelengths. Four-level operation with narrow line output has been demonstrated at high intensity levels for wavelengths which were not energetic enough to disturb the kinetic sequence pumping the transition. When excited in a plasma produced by the discharge of an intense electron beam with current of the order of 1 kA/cm^2 quasi-cw operation of the laser was achieved[4] at 427.8 nm and output power was found to accurately follow input power after the onset of threshold. A time-dependent power conversion efficiency of 3% was reported[4] and no evidence of bottlenecking was found over a range of circulating interacavity intensities up to 30 MW/cm^2. Peak power densities as great as 320 MW/l showed no evidence of disrupting the kinetic sequence pumping the laser transition.[5]

Although overall efficiency has been observed to degrade in preionized discharges,[6,7] recent time-resolved measurements[8] of the performance of the helium-nitrogen charge transfer laser in such environments have shown characteristics at lower excitation current densities which were similar to the e-beam results. At E/p values of the order of 5 V cm^{-1} Torr^{-1} and a current density of 100 A cm^{-2} instantaneous power conversion efficiencies of 2% were reported,[8] with peak powers in excess of 1 MW. Both in timing and efficiency the performance of the discharge pumped laser was found to be consistent with the results of the e-beam excitation and, hence, to be consistent with the charge transfer pumping sequence.

While the primary channels of the kinetic sequence responsible for the charge transfer pumping of the laser have been reasonably described,[4,8] attempts to quantitatively model this system have suffered from the paucity of rate coefficient data appropriate to atmospheric pressures. Although this can be viewed as a general problem of high-power lasers excited in high-pressure plasmas, there are specific features of the kinetics of the nitrogen ion laser that render even optimization difficult. Virtually all of the quenching rates appropriate to the $N_2^+(B^2\Sigma_u)$ upper laser level are unknown. However, the relatively small amount of fluorescence from this state under nonlasing conditions indicates that rates for such collisional quenching processes significantly exceed the relatively slow spontaneous transition probability which corresponds to a lifetime of 66 nsec. Such a circumstance immediately implies that laser oscillations would be difficult to start in a helium-nitrogen charge transfer plasma because of the absence of spontaneous radiation at the appropriate wavelengths. Conversely, such lasers should be less susceptible to uncontrolled superradiancy, as has been observed to be the case with both e-beam and pure discharge excitation. It appears, *a posteriori*, that the most efficient mode of operation for these devices is not the self-excited oscillator configuration generally employed, but rather an oscillator-amplifier combination from which the majority of the energy could be extracted at near-zero gain. Unfortunately, neither gain nor saturation intensity had been measured under lasing conditions and the viability of such a concept could not have been determined prior to the work reported here.

This paper reports the measurement of the saturation power and small-signal gain characteristic of an 85-cm helium-nitrogen plasma excited in a preionized discharge at several atmospheres pressure. Used as an amplifier the plasma exhibited an overall gain of 1.5×10^6 at 427.8 nm under small-signal conditions and a gain of 18 at extraction levels of 1 MW/cm^2. The intensity of uncontrolled superfluorescence was found to be less than two orders of magnitude below that value. Measurements of the power extracted from the amplifier for various levels of input power were found to agree with a simple model of gain saturation and yielded a value of the order of 60 kW/cm^2 for the saturation intensity.

Prior study of the discharge excitation of this system[8] in an atmospheric electrical avalanche (AEA) device had shown that power was coupled into the plasma load only for relatively short times and the majority of the energy originally stored in the capacitors persisted in ringing through the electrically shorted plasma remaining at the end of the avalanche. This suggested the use of two identical laser tubes coupled to the driving cir-

[a)]Research supported by ONR Contract No. N00014-77-C-0168.

 0003-6951/78/3302-0175$00.50

cuit in a transverse series connection, as shown schematically in Fig. 1, so that one tube could act as the switching device for the second. In this way a relatively fixed synchronization could be maintained between the plasmas and the laser output from one could be threaded back through the other after an appropriate optical delay had been introduced. The details of construction and operation of the device with a single tube have been discussed previously[8] and in this work the operation of the first tube in the series followed those results both in electrical input and laser output. Operation of the second tube was consistent with the same equivalent circuit describing the first except that the first tube played the role of the switching element in place of the thyratron. Because of the lower inductance of the first tube in comparison to the thyratron the ringing time for the inversion of the middle capacitor was shortened by about a factor of 2, giving a relative delay of about 25 nsec between the two laser plasmas. Both tubes were synchronously preionized by a pulse of the order to 40—50 kV applied to external electrodes. It was developed by a cable transformer[8,9] driven by a hydrogen thyratron switching a low-inductance capacitor. Since both the preionization and the main discharge were switched by hydrogen thyratrons the dual-AEA laser could be readily operated at repetition rates from 1 to 30 Hz.

When run as independent self-excited oscillators the two two tubes gave essentially the same laser output at 427.8 nm provided operating conditions were not excessively close to threshold. For example, at 3.7 atm of helium containing 0.15% nitrogen and at a charge voltage of 22 kV the first tube produced output pulses with peak power of 225 kW while the second tube gave 270 kW. This is somewhat below the 420 kW produced by a single tube connected between two of the capacitors. Considering the relatively wide range of operating parameters over which an instantaneous power conversion efficiency of 2% was achieved in such a single tube,[8] it is more likely that the lowered outputs from each of the two tubes in series resulted from less input electrical power being successfully coupled into the plasmas rather than from a loss of instantaneous conversion efficiency within the plasmas. Unfortunately, because of grounding problems the instantaneous electrical characteristics could not be directly measured as had been done[8] when a single tube was used.

When the mirrors were removed from the second tube under the same operating conditions the output dropped over two orders of magnitude, indicating uncontrolled superfluorescence to be of negligible importance. Then about 10% of the output from the first tube, running as a self-excited oscillator, was suitably delayed and threaded back through the second tube. Under those conditions output from the second tube was measured to be 560 kW and beam divergence was reduced by a factor of better than 2 below that which had been obtained from the same tube running as a self-excited oscillator. The insertion of calibrated neutral density filters into the beam from the oscillator input to the amplifier permitted the quantitative measurement of the amplification factor of the second laser plasma over a dynamic range of five orders of magnitude. The resulting data are shown in Fig. 2 for two of the different operating conditions which could be synchronized with the same optical delay line. The data shown correspond to operating pressures of 3 and 3.7 atm, as marked, and to charge voltages of 18.5 and 22 kV, respectively. Also shown in Fig. 2 are solid curves plotting the output powers computed from a model[10] containing two adjustable parameters,

$$I_{out} = I_s \ln\{1 + [\exp(I_{in}/I_s) - 1]\exp(\alpha_0 L)\}, \quad (1)$$

where I_{in}, I_{out}, and I_s are the input, output, and saturation intensities, respectively, α_0 is the small-signal gain in cm^{-1}, and L is gain pathlength in cm. The saturation intensity appearing in this expression differs somewhat from the textbook term[10] and is given by

$$I_s = (4\pi h\nu l_s/\lambda^2\tau)\Delta\nu, \quad (2)$$

where l_s denotes inverse transition probability for spontaneous emission at the operating wavelength, τ is the temporal FWHM of the laser pulse, λ and ν are the wavelength and frequency, respectively, of the transition, and $\Delta\nu$ is the bandwidth of transition, principally due to pressure broadening. Substitution of appropriate constants and transition probabilities into Eq. (2) gives $I_s = 11.3(\Delta\bar{\nu})$ kW/cm^2, where $\Delta\bar{\nu}$ is the linewidth in wave numbers. Thus I_s can be seen to be an essentially intrinsic parameter describing the molecular transition

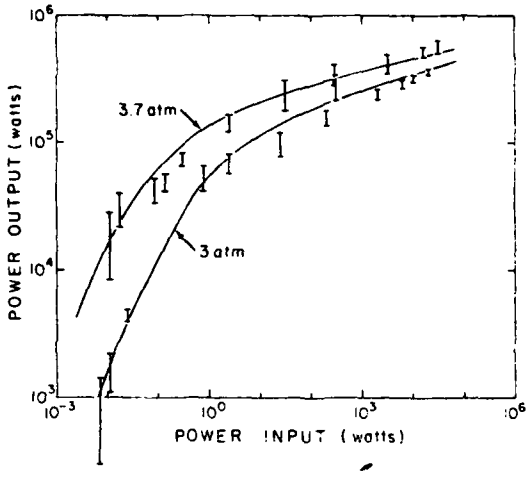

FIG. 2. Graph of the data showing peak powers output from the optical amplifier at 427.8 nm for various values of input pulse amplitudes obtained from the synchronized master oscillator. Solid curves plot output powers computed from the simple model of Eq. (1) containing the two adjustable parameters, saturation intensity, and overall logarithmic gain under small-signal conditions. The particular values used to obtain the displayed curves were 53 kW/cm^2 and 12.0, respectively, for the curve fit to the 3-atm data and 58 kW/cm^2 and 14.5, respectively, for the curve fit to the 3.7-atm data.

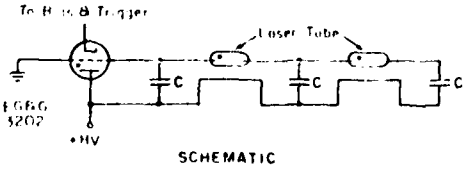

FIG. 1. Schematic diagram of the circuit of the particular version of AEA discharge system used in these experiments.

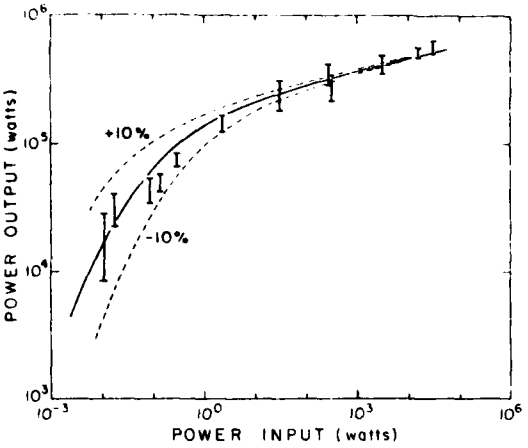

FIG. 3. Graph of the data obtained at a pressure of 3.7 atm for peak power outputs from the optical amplifier for various values of input pulse amplitudes obtained as in Fig. 2. The solid curve plots values computed from Eq. (1) using a saturation intensity of 58 kW/cm^2 and an overall logarithmic gain of 14.5. Dashed curves show the sensitivity of the model to the changes of overall logarithmic gain indicated on the graph.

in N_2^*, whereas the other adjustable parameter ($\alpha_0 L$) is an extrinsic parameter depending on the strength of the kinetics pumping the inversion.

Adjustments of the two parameters needed to obtain the agreement seen in Fig. 2 between the model given in Eq. (1) and the experimental data gave values for the saturation intensity, I_s of 53 and 58 kW/cm^2 for the 3- and 3.7-atm data, respectively. The sensitivity of the model to this adjustable parameter is greatest at the higher input powers where Eq. (1) reduces approximately to $I_s\alpha_0 L + I_{in}$, the expression for the extraction of power from the inversion under the fully saturated conditions of zero gain. Thus, at the limits of high input power the uncertainty in the product $I_s\alpha_0 L$ is linearly dependent upon the uncertainty in the measurement of the output intensity. As seen in Fig. 2, this was about $\pm 15\%$. The sensitivity of the model to $\alpha_0 L$ is greatest under small-signal conditions as shown in Fig. 3 where the effect of varying the gain by $\pm 10\%$ is illustrated in comparison with the 3.7-atm data. Even the poorly resolved data obtained from the amplification of 10-mW input pulses were sufficient to determine the overall gain parameter ($\alpha_0 L$) to within 10%. The values corresponding to the solid curves approximating the 3- and 3.7-atm data in Fig. 2 were 12 and 14.5, respectively. It is interesting to note that in these particular cases the overall gain which depends upon the inversion density scaled in a manner directly proportional to the pressure. The saturation intensities, while not resolved significantly, appeared to scale more slowly with pressure and a dependence on $P^{1/2}$ might be indicated. As discussed above, since I_s is essentially an intrinsic parameter, only a very slow variation through changes in the bandwidth of the gain with operating conditions would be expected. The two values of I_s obtained in this work correspond to linewidths centered around 4.9 cm^{-1}, a reasonable value for pressure broadening at 3 to 4 atm.

Thus, the work reported here has shown that N_2^* plasmas pumped by charge transfer from He_2^* can be effectively used as optical amplifiers at 427.8 nm at intensities nearing full saturation of the transition. Under the highest gain conditions examined a small-signal gain along the 85-cm path of 1.5×10^6 was observed with little uncontrolled superfluorescence. Fitting of the input-output data to a simple model indicated the corresponding zero-signal gain was $\exp(14.5) \sim 2\times10^6$. Under the same operating conditions a gain of about 18 was found at output intensities of 1 MW/cm^2, conditions relatively near the ideal extraction of power at zero gain. At input intensity levels of the order of I_s, 50–60 kW/cm^2, the power extracted from the amplifier was over twice that obtained from the same plasma coupled to the fields in a self-excited oscillator. Since the latter configuration generally operates with an instantaneous power conversion efficiency around 2% at these pressures, it appears that the amplifier operates at an efficiency of 4% relative to the instantaneous power coupled into the plasma.

Evidently the relatively narrow bandwidth realized from this laser transition between bound electronic states of N_2^* compensates the high rate of collisional quenching of the upper laser level and thus brings the saturation intensity down to values which can be reasonably attained in master oscillators. Since the quenching channel can be bypassed if laser intensities in the plasma significantly exceed the relatively modest saturation intensity, the strong collisional quenching becomes an advantage because it suppresses uncontrolled superfluorescence. Thus, it appears that as an optical amplifier, the helium nitrogen laser holds the potential for efficient high-power operation at several visible wavelengths.

[1]C. B. Collins, A. J. Cunningham, S. M. Curry, B. W. Johnson, and M. Stockton, Appl. Phys. Lett. **24**, 477 (1974).
[2]C. B. Collins, A. J. Cunningham, and M. Stockton, Appl. Phys. Lett. **25**, 344 (1974).
[3]V. N. Ishchenko, V. N. Lisitsyn, A. M. Razkev, and V. N. Starinskii, JETP Lett. **19**, 233 (1974).
[4]C. B. Collins, The University of Texas at Dallas Final Technical Report No. UTDP-ML-06, Contract No. N00014-76-C-0714, (unpublished).
[5]C. B. Collins, J. M. Carroll, F. W. Lee, and A. J. Cunningham, Appl. Phys. Lett. **28**, 539 (1976).
[6]J. B. Laudenslager and T. J. Pacala, Appl. Phys. Lett. **29**, 580 (1976).
[7]D. E. Rothe and K. O. Tan, Appl. Phys. Lett. **30**, 152 (1977).
[8]C. B. Collins, J. M. Carroll, and K. N. Taylor, J. Appl. Phys. (to be published).
[9]V. N. Ishchenko, V. N. Lisitsin, and V. N. Starinskii, Opt. Technol. **41**, 155 (1974).
[10]Expression (1) has been taken from an equivalent expression used to described the integrated pulse energy extracted from an optical amplifier operating on a transition showing homogeneous broadening. See F. Hopf, in *High Energy Lasers and Their Applications*, edited by S. Jacobs, M. Sargent III, and M. O. Scully (Addison-Wesley, Reading, Mass., 1974), p. 96. The conversion from pulse energy in the atomic units of the above reference to intensities results in Eq. (1) where I_s is a factor of $t_2/2\tau$ larger than the textbook saturation intensity, as described in A. Yariv, *Introduction to Optical Electronics*, 2nd ed. (Holt, Reinhart, and Winston, New York, 1976), p. 108. The characteristic times t_2 and τ denote the lifetime of the upper laser level and the temporal FWHM of the output pulse, respectively.

DYES PUMPED BY THE NITROGEN ION LASER *

C.B. COLLINS, K.N. TAYLOR and F.W. LEE
Center for Quantum Electronics, The University of Texas at Dallas, Box 688, Richardson, Texas 75080, USA

Received 24 March 1978

Coumarin derivatives, 6, 30, and 102, were excited in a simple dye laser by the output at 427.8 nm from a nitrogen ion laser pumped by charge transfer from He_2^+. Tuning ranges and stabilities of the dyes are reported.

The effective substitution of amino and hydroxyl groups into coumarin dye molecules resulted several years ago [1,2] in a family of coumarin derivatives which spanned the otherwise difficult blue-green region of the spectrum accessible to dye lasers. Because of the limited absorptivity of these coumarins at 337.1 nm and their relative fragility, these dyes found their principal usage in cw laser pumped systems employing longer pumping wavelengths or in flashlamp-pumped devices. More recently, however, fluorination [3] of the various coumarin derivatives has yielded greatly improved stability against photochemical decomposition, as well as lowering the wavelengths at which peak absorption occurs. As a result most N_2-laser manufacturers now routinely list the blue-green spectral ranges to be covered by these fluorinated coumarins operating in dye lasers pumped by their most powerful nitrogens lasers. Generally, at megawatt levels of input power, even at the reduced absorptivities found at 337.1 nm, satisfactory saturation of the laser transition can be accomplished so that high conversion efficiencies are approached [4,5]. However, little apparent success has been found in further attempts to pump the unfluorinated courmarin derivatives with pulsed lasers of high peak power.

This paper reports an examination of the excitation of a selection of coumarin derivatives in a simple dye laser excited by the pulsed output at 427.8 nm from a nitrogen ion laser [6]. The pump laser, itself, was excited in an Atmospheric Electrical Avalanche (AEA) device, stabilized by displacement current preionization. The output at 427.8 nm was derived from the (0,1) vibrational component of the $B \rightarrow X$ electronic transition of N_2^+ pumped by charge transfer from He_2^+. As reported previously [6], since both preionization and discharge circuitry were switched by hydrogen thyratrons, stable operation could be achieved at a PRF varying from 1 to 30 Hz with megawatt level outputs in a 4 ns pulse. For the purpose of the experiments reported here the AEA pump laser was operated at a reduced voltage to give 1 mJ pulses at 427.8 nm with 250 kW peak power.

The dye laser consisted of an 1800 l/mm grating, a 2 ml dye cell, and an output coupler having 60% reflectivity over the blue-green region of the spectrum. These elements were mounted colinearly and pumped transversely with the output from the nitrogen ion laser. No circulation of the dyes was attempted. Three dyes were used, coumarins 6, 30, and 102, each dissolved in ethanol in molar concentrations of 10^{-2}. The depth of penetration of the pumping radiation into the dye was very small and in the case of coumarin 30, excessively so, rendering alignment difficult. In that particular case a concentration of 10^{-3} molar was also used for convenience but with otherwise similar results.

Table 1 lists the resulting tuning ranges obtained. It can be seen that the tuning range for coumarin 102 was greater than that suggested as being typical of N_2 laser pumping at 337.1 nm and compared favorably with flashlamp pumping [7]. For each dye examined output intensities compared favorably to, or exceeded,

* Research supported by ONR Contract No. N00014-77-C-0168.

Table 1
Summary of tuning ranges obtained by pumping the coumarin derivatives listed with 1 mJ pulses at 427.8 nm obtained from a helium-nitrogen charge transfer laser operating at 10 Hz with 250 kW peak power

Dye	Tuning range (nm)
Coumarin 6	507–529
Coumarin 30	482–507
Coumarin 102	453–510

that obtained from coumarin 1 when pumped with 337.1 nm in a similar geometry at comparable power levels, to the extent similar geometries could be arranged. The general impression was that these coumarin derivatives, 6, 30, and 102, were very intense when pumped with 1 mJ pulses at 427.8 nm in the simple dye laser geometry. However, no effort was made to arrange critical output coupling and optimum pumping geometry in order to determine the absolute conversion efficiencies of the dyes.

The lifetimes of the dyes were surprising in view of their fragility when flashlamp-pumped. Even without forced circulation of the dye solution, operation for periods of 10 to 30 min at 10 Hz failed to show appreciable degradation of either of the three dyes when pumped with the 427.8 nm radiation. It is interesting to compute that 10 min operation corresponded to the average absorption of one pump photon per dye molecule in the case of the 10^{-2} molar concentrations, thus indicating that the lifetime of the molecule is in excess of several absorption-emission cycles. In the case of the coumarin 30 at the 10^{-3} concentration the lifetime was indicated to be in excess of 30 photons per molecule.

It is, thus, indicated that the monochromatic pumping of the simple derivatives of coumarin dye at a wavelength more near to their absorption maxima results in not only efficient, but also non-destructive excitation of these laser dyes. Considering the moderately high, 1–4% instantaneous power conversion efficiency of the pump laser, it may be that the dyes examined in this work offer an effective means of downconversion of the pump radiation into the blue-green spectral region with reasonable efficiency.

The authors gratefully acknowledge stimulating discussions and the loan of a spectrometer from their colleague, Dr. G. Marowsky of the Max-Planck-Institute, Gottingen.

References

[1] S.A. Tuccio, K.H. Drexhage and G.A. Reynolds, Opt. Commun. 7 (1973) 248.
[2] K.H. Drexhage, in: Topics in applied physics, Vol. 1, Dye lasers, ed. F.P. Schafer (Springer-Verlag, New York, 1977) p. 161 ff.
[3] E.L. Schimitschek, J.A. Trias, P.A. Hammond, R.A. Henry and R.L. Atkins, Opt. Commun. 16 (1976) 313.
[4] Molectron Corp., 177 N. Wolfe Rd., Sunyvale, CA 94086.
[5] Lambda Physik, Wagensteig 8, D-3400 Gottingen, Germany.
[6] C.B. Collins, J.M. Carroll and K.N. Taylor, J. Appl. Phys., to be published.
[7] Laser dyes (Exciton Chemical Co., 5760 Burkhardt Rd., Dayton, Ohio 45431).

A regenerative power amplifier operating on the blue-green line of the nitrogen ion laser[a)]

C. B. Collins, J. M. Carroll, K. N. Taylor, and F. W. Lee

Center for Quantum Electronics, The University of Texas at Dallas, Box 688, Richardson, Texas 75080
(Received 29 May 1978; accepted for publication 18 July 1978)

Operation of the nitrogen ion laser as an optical regenerative amplifier driven by a master oscillator allows the output to be effectively switched into the blue-green region of the spectrum. In this work an amplifier containing a dilute plasma of nitrogen ions was pumped by termolecular charge transfer from He_2^+ produced by an intense e-beam propagating through several atmospheres pressure of gas mixture. The injection of relatively broadband output from a dye laser oscillator caused the output from the amplifier to switch entirely into the (0,2) vibrational component of the $B \rightarrow X$ electronic transition of N_2^+ at 470.9 nm. An output linewidth of 0.007 nm was achieved together with the early saturation of the laser transition needed for the extraction of power from the amplifier at optimal efficiency.

PACS numbers: 42.60.Cz

It has been shown recently that an N_2^+ plasma pumped by charge transfer from He_2^+ can be used more effectively as an optical amplifier than as a self-excited oscillator.[1] The relatively weak spontaneous emission resulting from rather strong collisional quenching has been generally observed to make laser oscillations difficult to start in this system.[2-6] However, since the quenching channel can be bypassed if the optical intensities in the plasma exceed the saturation intensity, strong collisional quenching can be an asset by suppressing uncontrolled superfluorescence, provided the saturation intensity is not too great to achieve with practical devices. The saturation intensity of a laser transition depends directly upon the bandwidths of the gain and recent measurements have shown that the narrow bandwidth realized from the $B \rightarrow X$ transition between the bound electronic states of N_2^+ does sufficiently compensate the high rate of collisional quenching to bring the saturation intensity down to values[1] of the order of 50 kW/cm^2. In fact, in that work operation of the nitrogen ion laser was reported under conditions very near the ideal of maximum power extraction at zero gain.

Attempts to tune or shift the spectral band on which the charge-transfer laser operates are necessarily affected most critically by these considerations. The normal output of the laser is in the (0,1) vibrational component of the $B \rightarrow X$ transition of N_2^+, although some shifting into the (0,0) and (0,2) components has been reported.[3] The latter lies at a wavelength of 470.9 nm which is nearly optimal for applications involving underwater propagation. Unfortunately for that context, the relative transition probabilities for stimulated emission of the (0,2) and (0,1) components are in the ratio of 1 to 3.6, rendering both the gain and the difficulty in starting oscillations from spontaneous emission even more severe. The consequence of this can be seen in the relatively weak output reported[3] from self-excited oscillators operating on the blue-green component, even with high levels of excitation. However, the weak (0,2) component was reported to have been the only output under those conditions indicating that uncontrolled superfluorescence in the (0,1) band was effectively suppressed even at high powers. These considerations have suggested *a posteriori* that spectral shifting of the output from the nitrogen ion laser could be accomplished best in an oscillator-amplifier configuration.

This paper reports the construction and demonstration of an optical regenerative amplifier operated successfully on a component of the blue-green (0,2) band of N_2^+. It was pumped by the termolecular charge transfer[7,8] of energy from He_2^+ produced in the discharge of an intense electron beam into several atmospheres pressure of helium containing 50 Torr of nitrogen. The optical cavity used in these experiments consisted of one plane and one concave mirror separated by 12.5 cm and arranged on an axis perpendicular to the direction of e-beam propagation. Dielectric coatings were obtained to give a mean photon lifetime in the cavity of 20 nsec at 470.9 nm and only 0.8 nsec at the 427.8-nm wavelength corresponding to the (0,1) component.

A maser oscillator was constructed from a pulsed dye laser using coumarin 1 dye pumped by a conventional nitrogen laser with a peak power of several hundred kilowatts. An intracavity telescope together with an 1800-line/mm grating in the dye laser cavity gave an oscillator bandwidth corresponding to about 0.07 nm at 470.9 nm. Peak powers of the order of 1 kW were obtained within this bandwidth.

Output from the master oscillator was coupled into the cavity of the regenerative amplifier through the partial transparency of the plane mirror. Unfortunately the relatively long photon lifetime in the cavity together with the rather short duration of the oscillator pulse combined to render the coupling of the oscillator to the amplifier comparatively weak. Most of the illumination incident upon the amplifier cavity was rejected and the intracavity fields could not in single pulses build to values much in excess of the external fields. As a result, it was estimated that the peak oscillator power actually coupled into the amplifier was of the order of a few hundred watts at best.

Synchronization of the dye laser oscillator with the

[a)]Research supported by ONR Contract No. N00014-77-C-0168.

 0003-6951/78/3307-0624$00.50

e-beam was accomplished by delaying a synchronization pulse from the e-beam command circuit with a variable delay generator and then using it to trigger the thyratron switching the nitrogen laser pumping the dye. Overall system jitter was of the order of 50 nsec and was observed to be quite random. This required an undesirably large number of e-beam discharges be made in order to obtain a few in which synchronization occurred to an accuracy comparable to the mean lifetime of an oscillator photon in the amplifier cavity.

Figure 1 shows typical data obtained when adequate synchronization was achieved. The intensity of the amplifier output at 470.9 nm is shown as a function of time following the onset of the e-beam current. Under these conditions the amplifier plasma was being pumped by an e-beam sheet reaching a peak current of the order of 22 kA with transverse dimensions of 1×10 cm. The dotted lines in Fig. 1 bound the variance in the time at which the e-beam current had decayed to $1/e$ of the peak value. This variance itself was contributed by an auxiliary crowbar electrode in the e-beam diode envelope which served to clip the low-energy tail of the pulse in order to improve the foil lifetime.

Data from two separate discharges are shown in Fig. 1 together with the individual oscillator pulses injected into the amplifier cavity. In order to render both signals visible on the same scale the pulse from the oscillator was obtained from the dye laser beam rejected by the amplifier cavity. Being of low divergence it passed completely through the apertures providing geometric attenuation of the more divergent beam subsequently emitted from the cavity. Thus, although the sensitivity scales were the same between the successive discharges shown in Fig. 1, the oscillator pulses were not on the same scale having bypassed a total of several orders of magnitude of attenuation.

The upper trace in Fig. 1 can be seen to correspond to nearly optimal occurrence of the oscillator timing. The lower occurred too early by about two mean photon

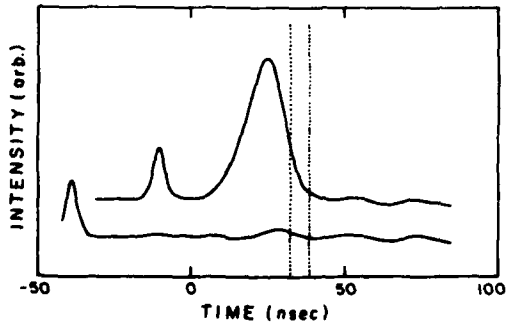

FIG. 1. Plot of the output intensities at 470.9 nm from the regenerative amplifier excited by the oscillator pulses seen on the leading edges of the waveforms. Intensities are plotted as functions of time following the onset of the e-beam current. Dotted lines bound variation in the times at which the e-beam current had fallen to e^{-1} of the peak value. Data from two separate discharges with different delays in the arrival of the oscillator pulses are shown with the zeros of intensity offset for clarity.

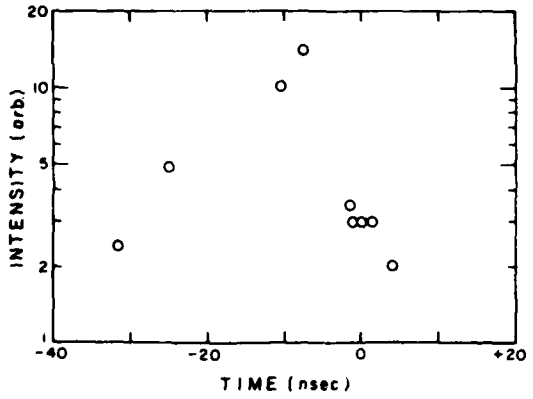

FIG. 2. Peak intensities of the 470.9-nm output from the regenerative amplifier plotted as a function of the delay following the onset of the e-beam current, in the time of arrival at the amplifier of the pulses from the oscillator.

lifetimes in the cavity implying that the oscillator intensities circulating within the amplifier cavity were down by more than a factor of 7 at the start of the e-beam discharge. Nevertheless, even this reduced level of injected energy resulted in some output as the power emitted from self-excited oscillations in the amplifier was generally inadequate to record on the oscilloscope and could only be dimly seen as a very diffuse pattern on a screen in a darkened room. In contrast the output corresponding to the upper trace was visibly both intense and compact as expected from the appearance of the pattern of the oscillator power reemitted from the amplifier cavity in the absence of e-beam excitation.

Figure 2 shows the dependence of the amplifier output on the time delay between the onset of e-beam current pumping the amplifier and the arrival of the optical pulse from the oscillator. This delay could not be controlled on the time scale shown and the points plotted represent the random delays resulting from the system jitter. The data from the lower trace in Fig. 1 is not shown as it would have plotted both to the left and below the coordinates chosen. The decrease in output with the increasingly early arrival of the oscillator pulse is roughly consistent with the inferred lifetime of those photons in the amplifier cavity.

Somewhat surprising is the apparent occurrence of the peak in Fig. 2 at small negative times. This may have resulted from nonoptimal coupling of the oscillator fields into the cavity. The mean photon lifetime in the cavity quoted earlier as 20 nsec corresponded to purely axial propagation. However, since it represented fewer than 50 cavity transits, the excitation of stable cavity modes could not be necessarily expected. If the amplifier cavity is considered to have been an optical waveguide folded upon itself, the stably propagating modes must have consisted of bundles of rays periodically converaging and diverging upon reflection at the cavity mirrors.[9] For nonideal bundles of rays initially incident upon such a structure the divergence is great after several reflections and the fraction of propagating photons walking-off the mirror on the next reflection is

large. However, once the maximum divergence has been passed the subsequent pattern of focusing and defocusing is simply periodic and the remaining photons stay in the cavity until they are transmitted through the mirrors. It can be reasonably expected that the energy finally emitted into the output beam would be greater if the maximum divergence of the circulating intensity, with its high loss of photons, had passed before amplification ensued. This would require an early arrival of the incident pulse from the oscillator and could explain the peak performance seen in Fig. 2 at small negative times.

Interferometric measurement of the amplifier output showed the laser line to be considerably narrowed. An FWHM of 0.007 nm was found in contrast to the 0.07-nm bandwidth of the oscillator pulse originally injected into the cavity. Thus it appears the system described here was not working as a conventional injection-locked oscillator in which a narrow-band input serves to frequency lock a broadband amplifier. This was confirmed by the inability of the amplifier to track the oscillator as it was tuned by more than one FWHM to either side of the output line. Rather the system seemed to operate as an optical regenerative amplifier in which the useful portion of the bandwidth of the input excited growing oscillations in the amplifier cavity. In any case it appears that the injection of broadband illumination near 470.9 nm into an amplifier cavity offers a means not only of switching the nitrogen ion laser output into the blue-green but also provides the radiation needed to reach an early saturation of this low-gain transition so that optimal efficiency may be achieved.

[1]C. B. Collins, J. M. Carroll, and K. N. Taylor, Appl. Phys. Lett. **33**, 175 (1978).
[2]C. B. Collins, A. J. Cunningham, and M. Stockton, Appl. Phys. Lett. **25**, 344 (1974).
[3]C. B. Collins and A. J. Cunningham, Appl. Phys. Lett. **27**, 127 (1975).
[4]J. B. Laudenslager and T. J. Pacala, Appl. Phys. Lett. **29**, 580 (1976).
[5]D. F. Rothe and K. O. Tan, Appl. Phys. Lett. **30**, 152 (1977).
[6]C. B. Collins, J. M. Carroll, and K. N. Taylor, J. Appl. Phys. **49** (1978).
[7]F. W. Lee, C. B. Collins, and R. A. Waller, J. Chem. Phys. **65**, 1605 (1976).
[8]C. B. Collins and F. W. Lee, J. Chem. Phys. **68**, 1391 (1978).
[9]A. Yariv, *Introduction to Optical Electronics*, 2nd ed. (Holt, Rinehart, and Winston, New York, 1976), p. 18.

REPRINTED FROM PROCEEDINGS OF THE INTERNATIONAL CONFERENCE ON LASERS '78, DECEMBER 11-15, 1978
PRINTED IN USA

GAIN AND SATURATION OF THE NITROGEN ION LASER*

C. B. Collins, J. M. Carroll, and K. N. Taylor
Center for Quantum Electronics, MS/NB1
The University of Texas at Dallas
Box 688, Richardson, Texas 75080

Abstract

In this work a dilute nitrogen plasma pumped by charge transfer from He_2^+ has been operated as a pulsed optical amplifier. In the experimental system used two synchronously excited plasmas were produced by preionized discharges in Atmospheric Electrical Avalanche (AEA) devices switched by hydrogen thyratrons so that repetitive operation to 30 Hz would be possible. In a departure from previous work, the plasmas were arranged to be electrically independent except for triggering adjustments to provide a phase delay in their excitation comparable to the optical transit time between them. Laser output at 427.8 nm from the first discharge coupled to the fields in a self-excited oscillator geometry was threaded through the second along its 137 cm, longer dimension. Calibrated attenuation of the beam from the oscillator subsequently input to the amplifier provided data on the overall amplification ratio to which the two adjustable parameters of a simple model were fit. From these parameters overall small signal gains as large as 10^7 were found together with saturation intensities of the order of 50 KW/cm^2 which confirmed preliminary values reported earlier that had been obtained from a substantially different geometry. Under the same conditions a gain of about 76 was found at an output intensity of 0.85 MW/cm^2, conditions relatively near the ideal extraction of power at zero gain.

Introduction

Since its discovery[1,2,3] in 1974, the nitrogen ion laser pumped by charge transfer from He_2^+ has shown several important advantages over other laser types operating at comparable wavelengths. Four-level operation with linewidth as narrow as .007 nm was demonstrated at high intensity levels for wavelengths which were not energetic enough to disturb the kinetic sequence pumping the transition. When excited by an intense electron beam with currents of the order of 1 KA/cm^2, quasi-cw operation of the laser was achieved[4] at 427.8 nm and output power was found to accurately follow input power after the onset of threshold. A time-dependent power conversion efficiency of 3% was reported[4] and no evidence of bottlenecking was found over a range of circulating intracavity intensities up to 30 MW/cm^2. Extracted power densities as great as 320 MW/ℓ gave no evidence of disrupting the kinetic sequence pumping the laser transition.[5]

In preionized discharges[6,7] the overall efficiency had been initially observed to degrade, but more recent time-resolved measurements[8] of the performance of the helium nitrogen charge transfer laser in such environments have shown characteristics at lower excitation current densities which were similar to the e-beam results. At E/p values of the order of 5 Vcm^{-1}torr^{-1} and a current density of 100 Acm^{-2} instantaneous power conversion efficiencies of 2% were reported,[8] with peak powers in excess of 1 MW. The most recent scaling studies have brought output powers to 2.8 MW and the corresponding efficiencies for the utilization of the energy stored on the final discharge capacitor to 0.3%. Both in timing and efficiency the performance of the discharge pumped laser is consistent with the results of the e-beam excitation and, hence, consistent with the charge transfer pumping sequence.

In some respects, such as in the ability of the kinetic channels and intermediate species to withstand very high circulating powers without disruption, in the transparency of the laser medium to the output line, and in the relative freedom of the laser transition from runaway superfluorescence, the potentials of the charge transfer laser exceed those of the rare-gas halide systems. However, other aspects resulting primarily from the fact that the laser transition connects highly excited states of an ion have caused the realization of the potential benefits of this system to lag considerably behind the development of the excimer devices.

The first of these problems is that the output scales with ionization but the laser medium contains no attaching gases so that efforts to reach higher output energy densities have necessarily resulted in electrical avalanches to successively lower values of discharge impedance. With direct e-beam, ion-beam, or nuclear pumping this presents no conceptual difficulty, but with direct discharge pumping the growing impedance mismatch with the driving circuit has limited the useful duration of the pumping pulse to a time

* Research supported by ONR Contract No. N00014-77-C-0168.

comparable to that required for the avalanche to develop in the laser medium. Thus a dominant factor controlling the overall efficiency of such a discharge device is the extent to which the stored energy can be completely discharged through the laser medium in a time comparable to the relatively few nanoseconds required for the electrical avalanche. This has transformed the problem of optimizing the charge transfer laser into an effort in technology development and progress is being made in that direction.

The second difficulty specific to this system has resulted from the relatively small amount of fluorescence emitted from the upper laser level under non-lasing conditions. This clearly suggests that rates for collisional quenching processes significantly exceed the relatively slow spontaneous transition probability corresponding to a lifetime of 66 nsec. Such a circumstance immediately implies that laser oscillations would be difficult to start in a helium nitrogen charge transfer plasma because of the absence of spontaneous radiation at the appropriate wavelengths. However this is the same effect that makes such lasers less susceptible to uncontrolled superradiancy, as has been observed to be the case with both e-beam and pure discharge excitation.

Lest it be prematurely concluded that such a high rate of quenching precludes effective operation of a charge transfer device, it must be recalled that the probability of extracting one photon per inversion is given by the ratio $I/(I + I_s)$, where I and I_s are the circulating intracavity intensity and the saturation intensity, respectively. The fact that the transition occurs between bound molecular levels has been recently shown[9] to lead to a bandwidth of the gain of only 5 cm^{-1} and thus, to bring the saturation intensity down to a reasonable value of the order of 50 KW/cm^2. This value can be readily attained in a small discharge oscillator and immediately suggests that the nitrogen ion laser would show its best performance when coupled to the fields in an oscillator-amplifier configuration. In fact, used as an amplifier, a charge transfer plasma excited in a preionized transverse discharge, 85 cm in length exhibited[9] an overall gain of 18 at extraction levels of 1 MW/cm^2, conditions relatively near the ideal extraction of power at zero gain. The intensity of uncontrolled superfluorescence was found to be less than two orders of magnitude below that value. Measurements of the power extracted from the amplifier for various levels of input power were found to agree with a simple model of gain saturation and yielded a value of the order of 58 KW/cm^2 for the saturation intensity.

The work reported here attempts to extend this modelling to a larger single-pass amplifier excited by a preionized discharge. It was the intent to assimilate the results obtained with this system together with past results into a comprehensive kinetic model which could guide the technologic advances necessary to overcome the problems pecular to this system.

Kinetic Background

Past attempts to quantitatively model the kinetic sequence pumping the nitrogen ion laser have suffered from the paucity of rate coefficient data appropriate to atmospheric pressures. Although this can be viewed as a general problem of high-power lasers excited in high pressure plasmas, it is interesting to note that the existence of the type of charge transfer reaction pumping this system was unsuspected prior to the development of the laser. In fact prior to the work of Lee and Collins,[10] it was generally assumed that the extensive literature on charge and excitation transfer reactions derived from low pressure experiments could be used to adequately model the high pressure laser environment. Unfortunately, it has been recently shown that many bimolecular reactions studied at low pressures have their termolecular analogs which dominate at pressures around one atmosphere because of the importance of multibody collisions.[11,12] A semi-classical model of such reactive collisions has been reported[11,12] which now provides guidance in estimating these new reaction channels which may be of importance to a variety of lasers operating in high pressure plasmas.

A revision of the kinetic scheme descriptive of the nitrogen ion laser pumped by charge transfer from He_2^+ has been made in order to include the multibody processes. The resulting sequence shown in Table 1 together with rate coefficients and branching ratios has served to explain all of the elements in the existing data base comprising the results of measurements on devices pumped by both e-beams and preionized discharges.

The rate limiting step in the growth of the inversion leading to cavity oscillation is the charge transfer step which scales with the concentrations of both helium and nitrogen. At helium pressures compatable with the experimental apparatus generally used, once the laser transition is saturated the probability of extracting one photon per ion initially produced is determined primarily by the competition between the reaction channels of He^+. The branching ratio between those channels should asymptotically approach unity as the partial pressure of nitrogen is reduced, thus posing a requirement inconsistent with those needed to attain threshold. As a consequence, this together with the generally small spontaneous fluorescence emitted confirms the indications that the nitrogen ion laser must be expected to operate most efficiently as an optical amplifier.

Table 1

Dominant Reaction Channels
in Helium Nitrogen Plasmas Supporting
Stimulated Emission from the B $\rightarrow$ X
Transition of N_2^+

Reaction rate coefficients are shown in parentheses in units of 10^{-10} cm^3sec^{-1} and 10^{-30} cm^6sec^{-1} for those component bimolecular and termolecular reactions, respectively, which dominate the evolution of the reactive species of importance. Branching information is shown as a multiplicative factor preceeding the rate coefficient.

Pumping Channels		Competing Losses	
Ionization			
$He^+ + 2He \rightarrow He_2^+ + He$	$(.065)^a$	$He^+ + N_2 \rightarrow$ Products	$(12)^b$
		$He^+ + N_2 + He \rightarrow$ Products	$(22)^c$
Charge Transfer			
$He_2^+ + N_2 \rightarrow N_2^+(B) + 2He$	$.75(11)^d$	$He_2^+ + N_2 \rightarrow$ Other Products	$.25(11)^d$
$He_2^+ + N_2 + He \rightarrow N_2^+(B) + 3He$	$.75(16)^d$	$He_2^+ + N_2 + He \rightarrow$ Other Products	$.25(16)^d$
		$He_2^+ + e + X \rightarrow$ Recombination	$(\ )^e$
Stimulated Emission			
$N_2^+(B) + h\nu \rightarrow N_2^+(X,v=1) + 2h\nu$	$(\ )^f$	$N_2^+(B) + e \rightarrow$ Neutrals	$(600)^c$
		$N_2^+(B) + N_2 \rightarrow N_4^+$	$(4)^g$
Lower State Quenching			
$N_2^+(X,v=1) + e \rightarrow N_2^{**}(v=1)$	$(10,000)^h$		
$N_2^{**}(v=1) \rightarrow N_2^+(X,v=0) + e$			
$N_2^+(X,v=1) + N_2 \rightarrow N_2(v=1) + N_2^+(X,v=0)$	$(\ )^i$		

a. Ref. 13.
b. Ref. 14.
c. Ref. 15.
d. Rate coefficients from Ref. 10, branching ratios from Ref. 15.
e. This depends strongly on electron temperature and is difficult to estimate meaningfully.
f. $\sigma = 14P^{-0.6}$ Å^2 where P is the pressure in atmospheres, Ref. 15.
g. Apparently this is a 3-body process which effectively occurs as a bimolecular reaction because of saturation, Ref. 15.
h. Estimated, Ref. 4 and Ref. 15.
i. Private communication, F. C. Fehsenfeld, NOAA. A value in excess of Langevin, 8×10^{-10}, is expected.

Fortunately the situation is relatively favorable for the realization of an efficient single-pass amplifier pumped by the kinetic sequence summarized in Table 1 when excited by a preionized discharge. The growth of an optical pulse in an amplifying medium has been shown theoretically* and confirmed experimentally in the helium nitrogen system[9] to be described by the expression,

* Equation (1) has been taken from an equivalent expression used in Ref. 16 to describe the integrated pulse energy extracted from an optical amplifier operating on a transition showing homogeneous broadening. The conversion from pulse energy in the atomic units of the above reference to intensities results in Equation (1) where I_s is a factor of $t_2/2\tau$ larger than the textbook saturation intensity, as described in A. Yariv, Introduction to Optical Electronics (2nd Ed., Holt, Rinehart, and Winston, New York, N.Y., (1976), p. 108. The characteristic times t_2, and τ denote the lifetime of the upper laser level and the temporal FWHM of the output pulse, respectively.

$$I_{out} + I_s \ln[1 + (e^{I_{in}/I_s} - 1)\, e^{\gamma L}] \qquad (1)$$

where γ is the gain, L is the length of the plasma, and I_{in} and I_s are the input and saturation intensities, respectively.[16] In the limit of an input intensity from an external oscillator which is large compared to the saturation intensity, the expression takes a particularly simple form

$$I_{out} = I_{in} + \gamma L I_s \qquad (2)$$

This is the ideal limiting case of the extraction of power at zero gain and corresponds to the removal of an optical power of γI_s from the plasma per unit length. The intensity, I_s, is an intrinsic parameter depending little upon experimental conditions and γ is an extrinsic variable directly related to the strength of the pumping. While the simple expression for kinetic branching $I/(I + I_s)$ predicts 50% extraction when $I_{in} = I_s$, the growth of the intensity increases this amount.

It is interesting to note that under the experimental conditions for which data has been reported for the excitation of a nitrogen ion device with a preionized discharge,[8,9] the model described above would predict a kinetic efficiency of the order of 0.5 and a saturation intensity of the order of 50 KW/cm^2. Thus an optical amplifier should be capable of operating at an instantaneous power conversion efficiency of the order of one-half the quantum efficiency relative to the ion cost, or about 3% provided the transition was rapidly saturated so that unit extraction efficiency could be achieved. This is in quite good agreement, not only with the discharge results recently reported,[9] but also with the general experience obtained with the e-beam devices.[4]

Method and Results

Since the actual outputs achieved from nitrogen ion lasers have been generally dominated by the photon extraction parameters, it was the intent of this work to confirm the recent measurements of gain and saturation intensity[9] in several different amplifier geometries. The only results reported previously had been obtained from an 85 cm discharge plasma connected electrically in series with the optical oscillator used to provide the input pulses to the amplifier.

For the measurements reported here two completely independent, atmospheric electrical avalanche (AEA) devices were constructed as described in Ref. 8, and synchronized to discharge with a reasonably constant phase delay. The smaller of the two was coupled to the fields in the geometry of an oscillator and its output was threaded through the 137 cm length of the larger device after undergoing a suitable optical delay. The cross sectional area of the plasma in the amplifier described here was 1.4 cm^2 in contrast to the 0.6 cm^2 used to obtain the data reported previously.[9]

When operated at a charge voltage of only 22 KV, discharges into 4.3 atmospheres of helium containing 0.15% N_2 resulted in the extraction of 2.8 megawatts in a 14 mJ pulse with an input from the oscillator of only 16 KW. For consistency with previous work, the measurements of the gain and saturation were performed at 3.7 atm pressure. A charge voltage of 20 KV provided a reasonable level of excitation.

Calibrated neutral density filters were used to attenuate the oscillator power input to the amplifier permitting the quantitative measurement of the amplification factor of the second laser plasma over a dynamic range of six orders of magnitude. The resulting data are shown in Figure 1 for two of the different operating geometries, each being identified by the cross sectional area of the amplifying plasma. The corresponding lengths to the 0.6 and 1.4 cm^2 cross sections were 85 cm and 137 cm, respectively and the charge voltages were 22 and 20 KV, respectively. Common parameters were maintained in the operating media which were 3.7 atm of helium containing 0.15% N_2.

Also shown in Figure 1 are solid curves plotting the output powers computed from the model summarized by Equation (1), containing the two adjustable parameters, I_s and γL. As discussed earlier these represent the saturation intensity and logarithmic gain describing the amplifying medium. The adjustment of these two parameters needed to obtain the agreement shown in Figure 1 between the model given in Equation (1) and the experimental data was made while maintaining the value reported previously[9] for I_s of 58 KW/cm^2. The sensitivity of the model to γL is greatest under small signal conditions and even the poorly resolved data obtained from the amplification of 10 mW input pulses were sufficient to determine this overall gain parameter to within 10%. The values used to obtain the solid curves approximating the data from the larger and smaller devices were 16.2 and 14.5, respectively.

Since γ is simply proportional to the inversion density reached, it is significant that products of γL and cross sectional area from the two systems correspond to within 10% to the inverse ratio of the source impedances driving them. This is quite consistent

with the approximation that the useful power density delivered to the discharge load at constant charge voltage and discharge pressure is simply proportional to the peak current density which in turn is correlated with the inverse source impedance. Thus it appears that not only do the values of saturation intensity agree, but that the differences measured in the logarithmic gains are completely consistent with the changes in discharge geometry made in the amplifiers.

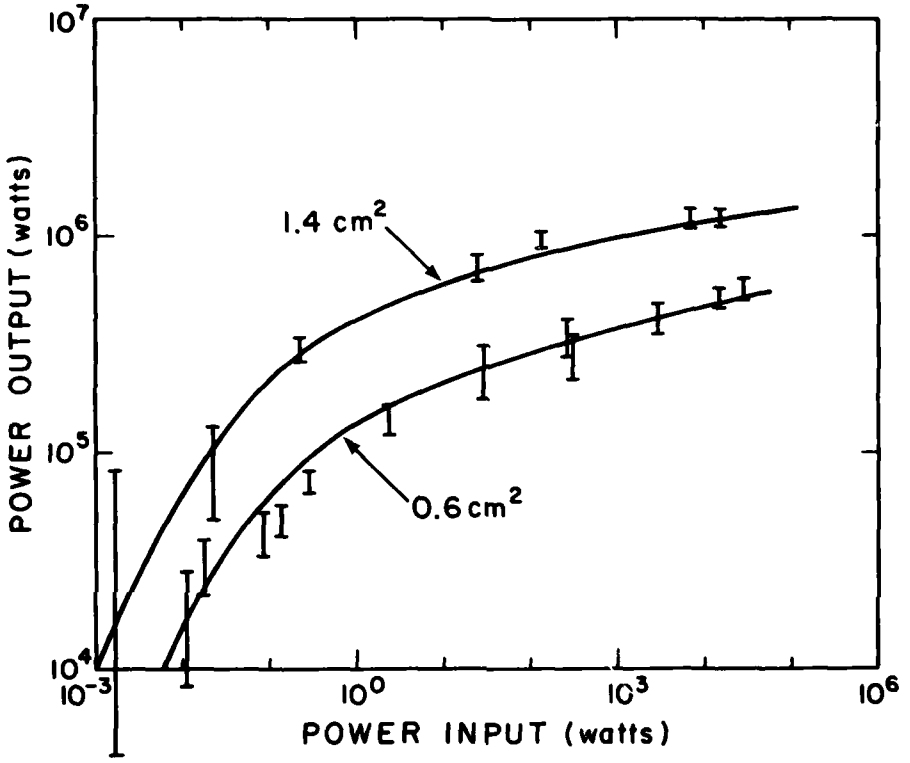

Fig. 1. Graph of the data showing peak powers output from the optical amplifier at 427.8 nm for various values of input pulse amplitudes obtained from the synchronized master oscillator. Solid curves plot output powers computed from the simple model of Equation (1) containing the two parameters, the saturation intensity of 58 KW/cm^2 and the overall logarithmic gain which was adjusted to fit the data. The particular values used to obtain the displayed curves were 16.2 and 14.5 for the amplifiers with the 1.4 and 0.6 cm^2 apertures, respectively.

The extent to which a unit extraction efficiency was achieved in the larger system is shown in Figure 2. Plotted there are calculations of the derivative of Equation (1) evaluated for the different conditions indicated using the values of γL and I_s determined above. As mentioned in the previous section, a unit extraction efficiency, and hence, unity in Figure 2, corresponds to the removal of an intensity of γI_s per unit length from the amplifying medium. It can be seen that an input from the oscillator of 15.6 KW served to saturate the power extraction from the final 87 cm of the amplifier. The overall loss of efficiency resulting from the failure to saturate the first 50 cm of the length of the amplifier can be readily seen from the areas under the curves shown in Figure 2 which give the actual powers that appeared in the output beams in units of $\gamma I_s LA$, where A is the cross sectional area. Then the maximum intensity which might have been extracted under ideal conditions corresponds to the rectangular area of unit height and having the width of $L = 137$ cm. It can be seen that the area under the curve resulting from 15.6 KW input represents most of the area of the ideal rectangle and computation shows the extraction efficiency under those conditions to have been 90%. It is interesting to compare that value with the extraction efficiencies computed for the other two cases shown in Figure 2. The relatively small extraction achieved by superfluorescence amounts to only 5% of the

ideal value and the effect of a rear mirror added to form a self-excited oscillator raised this only to 18%. In fact, because of the finite duration of the avalanche the effect of the mirror was only to make the plasma appear to be a longer superfluorescent device. For that case the virtual source of the superfluorescence is indicated on the abscissa of Figure 2 by the triangle and the direction of propagation and growth was first toward mirror located at zero and then back to L centimeters.

It can be clearly seen that the power input from the 15.6 KW oscillator is much more effective at these levels of pumping than superfluorescence or mirrors in extracting most of the energy stored in the inversion. Evidentually, it was this problem with extraction efficiency rather than kinetics that led to the requirement for a high level of pumping in order to achieve the efficient operation that had been reported previously.[8] At those levels of pumping γ apparently became great enough that the onset of efficient extraction occured earlier during the transit of a photon through the plasma and a reasonable fraction of the stored energy was extracted with the use of a single rear mirror.

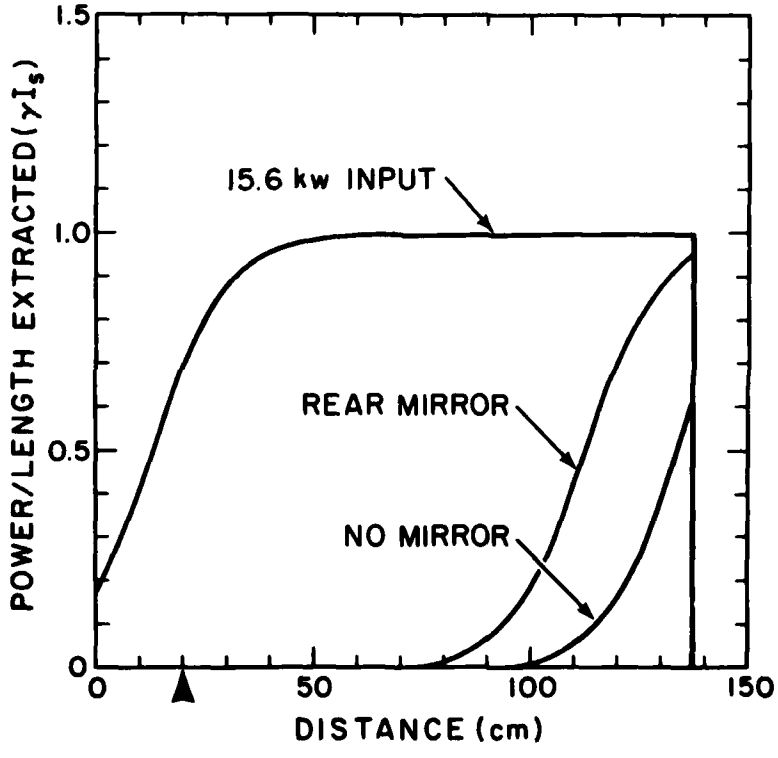

Fig. 2. Plot of the derivatives of the power extracted from the 1.4 cm^2 amplifier plotted as functions of the length of the optical path travelled by a photon from the oscillator, as calculated from Equation (1) using the extraction parameters determined from Figure 1. Units are γI_s so that unity implies full saturation of the transition at the corresponding point in the plasma. The three different means of coupling the plasma to the fields are identified by the label adjacent to the corresponding curve. In the case of the single rear mirror the position of the virtual photon source is indicated by the filled triangle on the abscissa and propagation is assumed to proceed from the source to the mirror located at the origin and then reflect back to give the values of extraction plotted by the corresponding curve.

Conclusions

The importance of the results inferred from this work lies in the decoupling of the kinetics pumping the inversion from the efficiency of extracting the photons. As mentioned previously the two requirements are not optimized by the same adjustments of

experimental parameters and it is essential to be able to extract the energy efficiently when operating under conditions optimizing the power flow in the kinetics. The work reported here has shown that N_2^+ plasmas pumped by charge transfer from He_2^+ can be effectively used as optical amplifiers at 427.8 nm at intensities nearing full saturation of the transition over most of the volume of the device. Under the highest gain conditions examined a small signal gain along the 137 cm path of 10^7 was observed with little uncontrolled superfluorescence. Under the same operating conditions a gain of about 75 was found at output intensities of 0.85 MW/cm^2, conditions relatively near the ideal extraction of power at zero gain. At input intensity levels of 15 KW the power extracted from the amplifier was five times that obtained from the same plasma coupled to the fields in a self-excited oscillator.

Evidently the relatively narrow bandwidth realized from this laser transition between bound electronic states of N_2^+ compensates the high rate of collisional quenching of the upper laser level and thus brings the saturation intensity down to values which can be reasonably attained in master oscillators. Since the quenching channel can be bypassed if laser intensities in the plasma significantly exceed the relatively modest saturation intensity, the strong collisional quenching becomes an advantage because it suppresses uncontrolled superfluorescence. Thus, it appears that as an optical amplifier, the helium nitrogen laser holds the potential for efficient, high power operation at several visible wavelengths.

References

1. Collins, C. B., Cunningham, A. J., Curry, S. M., Johnson, B. W., and Stockton, M., Appl. Phys. Lett., Vol. 24, p. 477. 1974.
2. Collins, C. B., Cunningham, A. J., and Stockton, M., Appl. Phys. Lett., Vol. 25, p. 344. 1974.
3. Ishchenko, V. N., Lisitsyn, V. N., Razkev, A. M., and Starinskii, V. N., JETP Lett., Vol. 19, p. 233. 1974.
4. Collins, C. B., Final Technical Report No. UTDP-ML-06, Contract No. N00014-76-C-0174, The University of Texas at Dallas (March, 1977).
5. Collins, C. B., Carroll, J. M., Lee, F. W., and Cunningham, A. J., Appl. Phys. Lett., Vol. 28, p. 539. 1976.
6. Laudenslager, J. B., and Pacala, T. J., Appl. Phys. Lett., Vol. 29, p. 580. 1976.
7. Rothe, D. E., and Tan, K. O., Appl. Phys. Lett., Vol. 30, p. 152. 1977.
8. Collins, C. B., Carroll, J. M., and Taylor, K. N., J. Appl. Phys., Vol. 49, p. 5093. 1978.
9. Collins, C. B., Carroll, J. M., and Taylor, K. N., Appl. Phys. Lett., Vol. 33, p. 175. 1978.
10. Lee, F. W., Collins, C. B., and Waller, R. A., J. Chem. Phys., Vol. 65, p. 1605. 1976.
11. Collins, C. B., and Lee, F. W., J. Chem. Phys., Vol. 68, p. 1391. 1978.
12. Collins, C. B., and Lee, F. W., J. Chem Phys. (pending).
13. Deloche, R., Monchicourt, P., Cheret, M., and Lambert, F., Phys. Rev., Vol. A 13, p. 1140. 1976.
14. Dunkin, D. B., Fehsenfeld, F. C., Schmeltekopf, A. L., and Ferguson, E. E., J. Chem. Phys., Vol. 49, p. 1365. 1968.
15. Petersen, J. V., Theoretical Modelling of Charge Transfer Lasers, Ph.D. Dissertation, The University of Texas at Dallas. 1977.
16. Hopf, F., in: High Energy Lasers and Their Applications (ed. S. Jacobs, M. Sargent III, and M. O. Scully, Addison-Wesley Publishing Co., Reading, Mass., 1974), p. 96.

REPRINTED FROM PROCEEDINGS OF THE INTERNATIONAL CONFERENCE ON LASERS '79, DECEMBER 17-21, 1979
PRINTED IN USA

TRAVELING WAVE EXCITATION OF THE NITROGEN ION LASER*

C. B. Collins and J. M. Carroll
Center for Quantum Electronics
The University of Texas at Dallas
Box 688, Richardson, Texas 75080

Abstract

A repetitively pulsed, traveling wave laser has been operated with a front-to-back ratio exceeding 200 to 1 when producing peak powers at megawatt levels. When run as a traveling wave amplifier over 3 MW were obtained in 6 nsec pulses.

Introduction

Since its discovery[1,2,3] in 1974, the nitrogen ion laser pumped by charge transfer from He_2^+ has excelled in the production of high output power densities at visible wavelengths. With e-beam excitation outputs as great as 320 MW/ℓ have been obtained[4,5] at 428 nm with a time-independent power conversion efficiency of 3%. A recent review[6] has shown that even the inert-gas halide lasers have apparently not operated at this level of power density. In preionized discharges, the comparison is similar if results are considered at comparable efficiencies. Over 44 MW/ℓ at 428 nm have been obtained[7] with charge transfer pumping of the usual N_2^+ (B→X) transition. While the record for an excimer device has been reported[6] to have been 220 MW/ℓ obtained for KrF, this was achieved at a value of overall efficiency four times less than that which characterized the charge transfer result.

The kinetic model which has been developed[8] for the helium-nitrogen variant of the charge transfer laser explains this facility for sustaining high powers of illumination in terms of a very high transparency of the active medium at the wavelength of the laser line. In this and related respects, such as in the ability of the kinetic channels and intermediate species to withstand very high circulating powers without disruption, and in the relative freedom of the laser transition from runaway superfluorescence, the potentials of the charge transfer laser exceed those of the rare-gas halide systems. However, other aspects resulting primarily from the fact that the laser transition connects highly excited states of an ion have caused the realization of the potential benefits of this system to lag considerably behind the development of the excimer devices.

Although exceptional power densities have been extracted from a charge transfer laser with discharge excitation, the scaling of such devices can be severely limited by the relatively short time, τ_a, during which the impedance of the medium is high enough to permit the efficient deposition of the electrical input power. This is not a problem that is unique to the charge-transfer system but one which occurs with more severity in this device because of the absence of any significant constituent which might be able to stabilize the discharge through electron attachment. Measurements have shown[7] that in an avalanche discharge in a plasma of typical composition used for the nitrogen ion laser the impedance collapses to its short-circuited value in a time of the order of a few nanoseconds. Thus, in simple transverse discharge geometries[7,9] physical dimensions must be limited to values small in comparison to $c\tau_a$, where c is the speed of light in the medium, if the relatively high values of power transfer efficiency occurring during the early parts of the avalanche are to be utilized. In the charge transfer laser this means dimensions small in comparison to a meter.

In principle, this restriction on the scale of a charge transfer laser can be removed by arranging for traveling wave excitation of the discharge plasma.[10,11] In such a system the active medium would consist of an assembly of short segments arranged end to end and individually excited by preionized transverse discharges. Each segment would be electrically phased so that its discharge would start at a time which would become successively later for segments farther down the sequence. Then, if the relative electrical phases were properly adjusted to match the speed of light propagating down the length of the assembly, the leading edge of the output wave traveling through it could be arranged to be always passing through successive plasma segments at the moment of electrical breakdown. Finally if the length of an individual segment were too short to allow for the growth of the intensity of a counterpropagating wave to reach appreciable proportions after traversing a single section, any possibility that counterpropagating output could start from spontaneous emission would be eliminated. Thus, the use of traveling wave excitation would provide for the maximum overall efficiency for the extraction of the energy stored in the inversions of populations in very short-lived plasmas and for the minimum possibility for the development of uncontrolled superfluorescence.

*Research supported by ONR Contract No. N00014-77-C-0168

Excitation of the conventional N_2 laser in a traveling wave geometry has been previously arranged[10,11] through the use of commutation switches characterized by very fast rise times. In the usual configuration either individual single-shot switches[10] or shaped transmission lines driven by spark gaps[11] have been used to initiate breakdown waves that had rise times which were short in comparison to the longitudinal transit times of the media. However, this seemed to preclude the operation of these devices at any significant repetition rate. Nevertheless, directionalities as great as 10 to 1 were achieved. Recently an improvement of these devices has been described[12] in which commutation is effected by a conventional hydrogen thyratron connected to a stripline in a grounded-grid configuration. Such a system is capable of operation at pulse repetition frequencies limited only by the recovery time of the thyratron and the heating of the working medium.

In the work reported here a dilute nitrogen plasma pumped by charge transfer from He_2^+ has been operated as a traveling wave laser. The active medium has been coupled to the propagating fields both in the geometry of an optical amplifier and in the geometry of a unidirectional, single-pass laser. With a proper arrangement of experimental variables, at pressures ranging from 2 to 4 atm synchronization was obtained between the breakdown wave propagating between successive electrode segments and the speed of light in the laser medium contained between the electrodes. Under those conditions and with no need of mirrors or optical elements the device functioned as a unidirectional superfluorescent laser. Peak output powers of 1.5 MW at 428 nm were measured in an 6 nsec pulse in the forward direction. Ratios between the outputs from the front and back of the traveling wave laser routinely exceeded 200 to 1 with the counterpropagating output consisting primarily of highly divergent rays scattered from physical irregularities in the electrode structures.

Experimental Method

The experimental system employed in this work differed from that described previously[12] in that preionization was required in order to uniformly excite the helium nitrogen plasmas at atmospheric pressures. As in the AEA laser developed earlier,[7] displacement current preionization was used. A potential of the order of 40 - 50 kV was applied to an electrode mounted outside the pressure vessel of the laser tube in a manner to create an intense electric field perpendicular to the axis of current flow in the main discharge and perpendicular to the optical axis. A delay of the order of 0.5 - 1.0 μsec between the preionization pulse and the main discharge was found to be necessary. However, the exact amount of delay was not a critical parameter so a single preionization pulse was applied simultaneously to all discharge segments.

To excite the main discharge, low impedance striplines were transversely connected to the electrode segments. Each individual segment operated as an electrical avalanche discharge of the type described previously,[7] with the exception that commutation of the switching sides of each of the discharges was effected by a common thyratron. Since commutation of the preionization circuit was also provided by a hydrogen thyratron, repetitively pulsed operation of the system was facilitated. Operation at pulse repetition frequencies as great as 40 Hz was observed in this work with the average output power being limited at the higher values by gas heating.

The relatively rapid development of the avalanche breakdown in each individual segment tended to sharpen the rise time of the switching wavefront as perceived down the longitudinal axis and provided better definition of the relative phase of each segment than would have been obtained from the slower rise time characteristic of the thyratron alone. It was found by experimentation that an electrode length of 17 cm proved to be short enough to suppress bidirectional output from a single segment, while being long enough to correspond to a nearly discernable change of phase. In actual practice the phase was constant over an individual segment and successive segments were set to phases differing by time of 17/c.

In this work a nominal 1.5 meter device containing 7 discharge segments was constructed. Although some variations of phasing were observed when operating pressures and voltages were changed, the degree of this variability was acceptable over the working pressure and voltage ranges. These variations were detected in the growth of the duration of the output pulses as the propagating fields tended to "outrun" the breakdown wave or in the inverse effect. The latter type of dephasing tended to be the most serious as the plasma was found to become absorptive at the laser wavelength during the later afterglow period, in agreement with previous measurements.[1] To avoid this possibility for the reabsorption of a "slow" output pulse the phasing of the discharge segments was adjusted so that in normal operation the leading edge of the output gradually outran the breakdown wave. If not done excessively, the trailing edge of the output contained enough intensity to saturate the transition in the farther segments and in this way the output pulse was gradually stretched by an amount proportional to the number of segments traversed. As generally employed, this technique led to output pulses from the 1.5 m device which were 6 nsec in duration.

Results

For the characterization of the performance of the traveling wave nitrogen ion laser, a calibrated ITT F-4000 vacuum photodiode connected to a Tektronix 7912 waveform digitizer was used to measure the time resolved output power. Calibrated neutral density filters

the worst case in Fig. 1. It is interesting to note that the divergences of the beams obtained from the TWA mode of operation were reduced to the 2 mR value characteristic of the oscillator input.

It appears that as a consequence of this work, the use of traveling wave excitation of larger aperture amplifiers offers an attractive means for overcoming the natural limitations on the scale of short pulse lasers.

References

1. C. B. Collins, A. J. Cunningham, S. M. Curry, B. W. Johnson, and M. Stockton, Appl. Phys. Lett. 24, 477 (1974).
2. C. B. Collins, A. J. Cunningham, and M. Stockton, Appl. Phys. Lett. 25, 344 (1974).
3. V. N. Ishchenko, V. N. Lisitsyn, A. M. Razkev, and V. N. Starinskii, JETP Lett. 19, 233 (1974).
4. C. B. Collins, Final Technical Report No. UTDP-ML-06, Contract No. N00014-76-C-0174, The University of Texas at Dallas (March, 1977).
5. C. B. Collins, J. M. Carroll, F. W. Lee, and A. J. Cunningham, Appl. Phys. Lett. 28, 539 (1976).
6. C. A. Brau in Excimer Lasers, ed. by C. K. Rhodes, Springer Series on Topics in Applied Physics, Vol. 30 (Springer-Verlag, Berlin, Heidelberg, N. Y. 1979) pp. 110-126.
7. C. B. Collins, J. M. Carroll, and K. N. Taylor, J. Appl. Phys. 49, S093 (1978).
8. C. B. Collins, J. M. Carroll, and K. N. Taylor, Proc. of the Int. Conf. on Lasers '79, SPIE, 168, 363 (1979).
9. C. B. Collins, J. M. Carroll, and K. N. Taylor, Appl. Phys. Lett. 33, 175 (1978).
10. J. D. Shipman, Appl. Phys. Lett. 10, 3 (1967).
11. B. Godard, IEEE J. Quantum Electron., QE-10, 147 (1974).
12. C. B. Collins, U.S. Patent #4,053,853 (1977).

compensated the large dynamic range of intensities encountered in this experiment. System linearity and the rejection of spurious reflections were given considerable attention. The resulting measurements of the output at 428 nm from the device operating as a single pass laser, optically self-excited from spontaneous radiation are shown in Fig. 1. The aperture was 1.5 cm^2 and the output beam divergence was about 6 mR. No optics of any kind were present in the system and the output windows were anti-reflection coated to avoid any spurious directionality which might have been introduced by possibly fortuitous reflections.

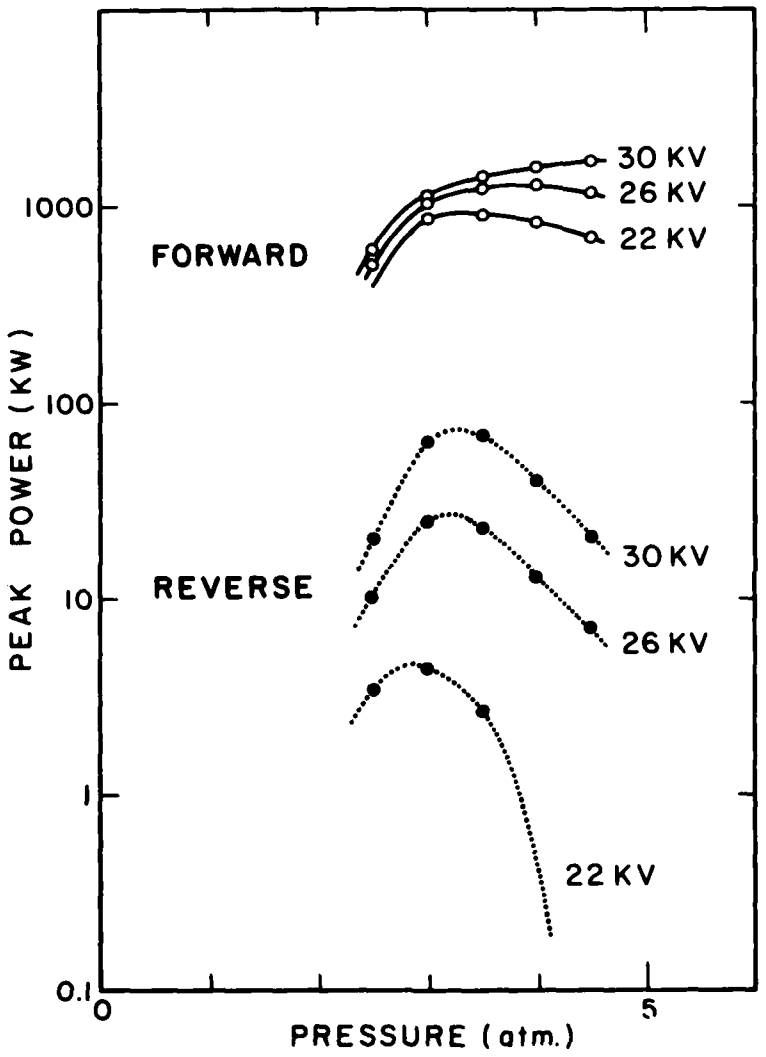

Fig. 1. Peak power output at 428 nm emitted from the single pass traveling wave laser containing 7 electrode segments. Measurements are plotted as functions of the pressure of the helium mixture containing 0.15% N_2 and excited at the charge voltages shown. Output from the forward and reverse directions as shown by solid and dotted curves, respectively.

The data presented in Fig. 1 shows both the output detected in the direction of propagation, denoted as "forward" with respect to the direction of travel of the breakdown wave, and the counterpropagating output labeled as "reverse." Directionalities at megawatt levels of output can be seen to have been of the order of 200 to 1. At the highest levels of excitation attempted with this device directionalities are shown to have dropped to about 20 to 1. It is interesting to estimate the gain of a single section under these conditions under which the directionality was degraded. The saturation intensity has been reported to have been I_s = 58 kW cm^{-2}, under similar conditions.[9] If reasonably early saturation were assumed, the output intensity would be expected to be $I = I_s e^{\gamma L}$ where γ is the small signal gain for the transition and L is the length of the active discharge. In this case a solution for (γL) would give 17.2, which, when divided by the number of

segments, would imply a logarithmic gain of about 2.5 per segment. This seemed inconsistent with the 60 kW level of power detected in the reverse case under the worst conditions shown in Fig. 1 and suggested that the assumption of an early saturation of the transition might have been optimistic. This in turn suggested the use of the same laser plasma as a traveling wave amplifier (TWA).

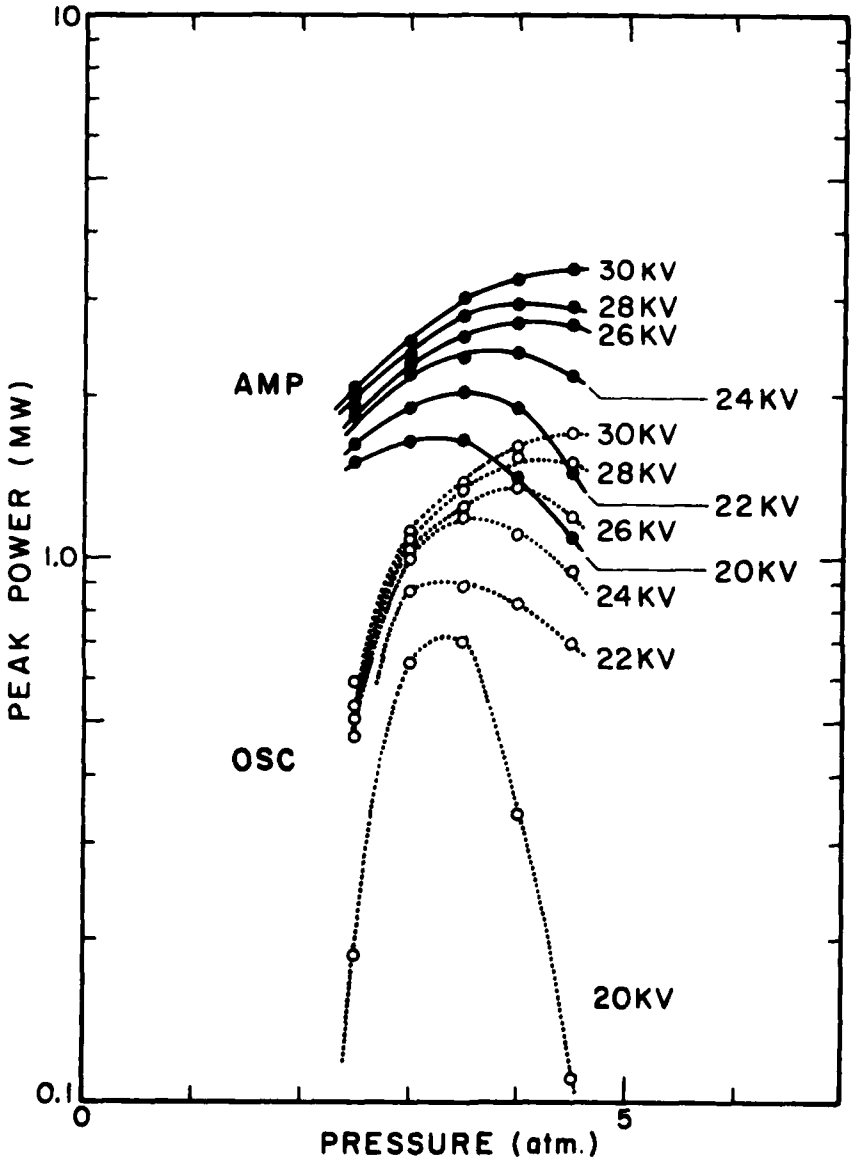

Fig. 2. Peak power outputs at 428 nm emitted from the helium-nitrogen plasma excited by the 7 segment traveling wave discharge device plotted as functions of the pressure of the helium mixture containing 0.15% N_2. Outputs in the forward direction are shown by dotted curves for the use of the device as a single pass laser and by solid curves for its use as an optical amplifier excited by the injection of 100 kW cm^{-2} peak input power.

Figure 2 shows the increase in output power obtained from the use of the 1.5 m system as a TWA excited by the injection into the appropriate end of the device of 100 kW cm^{-2} at 428 nm obtained from another nitrogen ion laser. These outputs were not sensitive to small changes in the input power, thus implying that under these conditions the optical transition was indeed saturated throughout the length of the amplifier. This higher value of output is consistent with a gain per section of $\sim\exp(4.1)$, a value more nearly in agreement with the magnitude needed to explain the relatively large counterpropagating output seen in

the worst case in Fig. 1. It is interesting to note that the divergences of the beams obtained from the TWA mode of operation were reduced to the 2 mR value characteristic of the oscillator input.

It appears that as a consequence of this work, the use of traveling wave excitation of larger aperture amplifiers offers an attractive means for overcoming the natural limitations on the scale of short pulse lasers.

References

1. C. B. Collins, A. J. Cunningham, S. M. Curry, B. W. Johnson, and M. Stockton, Appl. Phys. Lett. 24, 477 (1974).
2. C. B. Collins, A. J. Cunningham, and M. Stockton, Appl. Phys. Lett. 25, 344 (1974).
3. V. N. Ishchenko, V. N. Lisitsyn, A. M. Razkev, and V. N. Starinskii, JETP Lett. 19, 233 (1974).
4. C. B. Collins, Final Technical Report No. UTDP-ML-06, Contract No. N00014-76-C-0174, The University of Texas at Dallas (March, 1977).
5. C. B. Collins, J. M. Carroll, F. W. Lee, and A. J. Cunningham, Appl. Phys. Lett. 28, 539 (1976).
6. C. A. Brau in Excimer Lasers, ed. by C. K. Rhodes, Springer Series on Topics in Applied Physics, Vol. 30 (Springer-Verlag, Berlin, Heidelberg, N. Y. 1979) pp. 110-126.
7. C. B. Collins, J. M. Carroll, and K. N. Taylor, J. Appl. Phys. 49, 5093 (1978).
8. C. B. Collins, J. M. Carroll, and K. N. Taylor, Proc. of the Int. Conf. on Lasers '79, SPIE, 168, 363 (1979).
9. C. B. Collins, J. M. Carroll, and K. N. Taylor, Appl. Phys. Lett. 33, 175 (1978).
10. J. D. Shipman, Appl. Phys. Lett. 10, 3 (1967).
11. B. Godard, IEEE J. Quantum Electron., QE-10, 147 (1974).
12. C. B. Collins, U.S. Patent #4,053,853 (1977).

Traveling wave excitation of the nitrogen ion laser

C. B. Collins and J. M. Carroll
Center for Quantum Electronics, The University of Texas at Dallas, Box 688, Richardson, Texas 75080

(Received 10 December 1979; accepted for publication 26 February 1980)

A repetitively pulsed, traveling-wave laser has been operated with a front-to-back ratio exceeding 1000 : 1 when producing peak powers in excess of 3 MW.

PACS numbers: 42.55.Hq

Since its discovery[1-3] in 1974, the nitrogen ion laser pumped by charge transfer from He_2^+ has excelled in the production of high-output power densities at visible wavelengths. With *e*-beam excitation, outputs as great as 320 MW/*l* have been obtained[4,5] at 428 nm with a time-independent power conversion efficiency of 3%. With preionized discharges, over 44 MW/*l* have been achieved at 2% efficiency.[6,7] A recent review[8] has shown that even the inert-gas halide lasers have apparently not operated at the highest of these levels of power density.

Unfortunately, the scaling of such devices can be severely limited at such power densities by the relatively short time τ during which the impedance of the medium is high enough to permit the efficient deposition of the electrical input power. This is not a problem that is unique to the charge transfer system, but one which occurs with more severity in this device because of the absence of any significant constituent which might be able to stabilize the discharge through electron attachment. Measurements have shown[6] that in an avalanche discharge in a typical nitrogen ion laser plasma the impedance collapses to its short-circuited value in a few nanoseconds. Thus in simple transverse-discharge geometries,[9] physical dimensions must be limited to values small in comparison to $c\tau$, where c is the speed of light in the medium, if the relatively high values of power transfer efficiency occurring during the early parts of the avalanche are to be utilized. In the charge transfer laser this means dimensions small in comparison to a meter.

In principle, this restriction on the scale of a charge transfer laser can be removed by arranging for traveling-wave excitation of the discharge plasma.[10,11] In such a system the active medium would consist of an assembly of short segments arranged end-to-end and individually excited by preionized transverse discharges. Each segment would be electrically phased so that initiation would start at a time which would become successively later for segments farther down the sequence. Then, if the relative electrical phases were properly adjusted to match the speed of light propagating down the length of the assembly, the leading edge of the output wave traveling through it could be arranged to be always passing through successive plasma segments at the optimal moment of electrical breakdown. Finally, if the length of an individual segment were too short to allow for the growth of the intensity of a counterpropagating wave to reach appreciable proportions after traversing a single section, any possibility that counterpropagating output could start from spontaneous emission would be eliminated.

Excitation of the conventional N_2 laser in a traveling-wave geometry has been previously arranged[10,11] through the use of commutation switches characterized by very fast rise times. In the usual configuration either individual single-shot switches[10] or shaped transmission lines driven by spark gaps[11] were used to initiate breakdown waves that had rise times which were short in comparison to the longitudinal transit times of the media. However, this seemed to preclude the operation of these devices at any significant repetition rate. Nevertheless, directionalities as great as 10 : 1 were achieved. Recently, an improvement of these devices has been described[12] in which commutation is effected by a conventional hydrogen thyratron connected to a stripline in a grounded-grid configuration. Such a system is capable of operation at pulse repetition frequencies limited only by the recovery time of the thyratron and the heating of the working medium.

In the work reported here, a dilute nitrogen plasma pumped by charge transfer from He_2^+ has been operated as a traveling-wave laser. The experimental system actually employed differed from that described previously[12] in that preionization was required in order to uniformly excite the helium nitrogen plasmas at atmospheric pressures. As in the avalanche laser developed earlier,[6] displacement current preionization was used. However, as the exact amount of delay was not found to be a critical parameter, a single preionization pulse was applied simultaneously to all discharge segments.

To excite the main discharges, low impedance striplines were transversely connected to the electrode segments. Each individual segment operated as an electrical avalanche discharge of the type described previously,[6] with the exception that commutation of the switching sides of each of the discharges was effected by a common thyratron. Since commutation of the preionization circuit was also provided by a hydrogen thyratron, repetitively pulsed operation of the system was facilitated. Operation at pulse repetition frequencies as great as 40 Hz was observed in this work with the average output power being limited at the higher values by gas heating.

The relatively rapid development of the avalanche breakdown in each individual segment tended to sharpen the rise time of the switching wave front as perceived down the longitudinal axis and provided better definition of the relative phase of each segment than would have been obtained from the slower rise-time characteristic of the thyratron alone. It was found by experimentation that an electrode

 0021-8979/80/063017-03$01.10

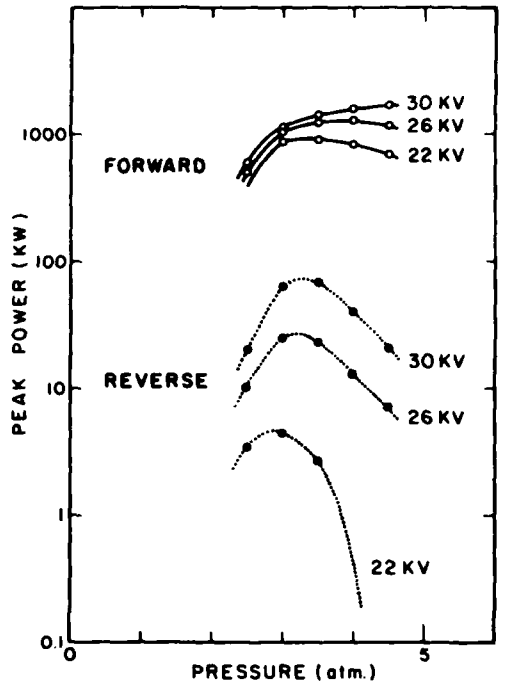

FIG. 1. Pressure and voltage dependence of the peak power output at 428 nm emitted from the single-pass traveling-wave laser containing 7 electrode segments. Forward and reverse directions are shown by the solid and dotted curves, respectively.

length of 17 cm proved to be short enough to suppress bidirectional output from a single segment, while being long enough to correspond to a nearly discernable change of phase. In actual practice the phase was constant over an individual segment, and successive segments were set to phases differing by times of 17/c.

Both a nominal 1.5-m device containing 7 discharge segments and a 5-m device containing 21 segments were constructed in the course of this work. Although some variations of phasing were observed in both devices when operating pressures and voltages were changed, the degree of this variability was acceptable over the working pressure range of 2–4 atm of helium containing 0.15% N_2. These variations were detected in the growth of the duration of the output pulses, as the propagating fields tended to "outrun" the breakdown wave, or in the inverse effect. The latter type of dephasing tended to be the most serious, as the plasma was found to become absorptive at the laser wavelength during the later afterglow period in agreement with previous measurements.[1] To avoid this possibility for the reabsorption of a "slow" output pulse, the phasing of the discharge segments was adjusted so that in normal operation the leading edge of the output gradually outran the breakdown wave. If not done excessively, the trailing edge of the output contained enough intensity to saturate the transition in the farther segments and in this way the output pulse was gradually stretched by an amount proportional to the number of segments traversed. This technique led to output pulses from the 1.5-m device which were 6 nsec in duration between half-power points, and which were 7–8 nsec for the 5-m system. However as a test of the extent to which the duration of the output pulse could be controlled in this manner, the 5-m laser was phased to give 15-nsec pulses with no loss of integrated pulse energy by adjusting only the spacings of the electrodes in successive segments.

For the characterization of the performance of the traveling-wave nitrogen ion lasers, a calibrated ITT F-4000 vacuum photodiode connected to a Tektronix 7912 waveform digitizer was used to measure the time resolved output power. Calibrated neutral density filters compensated the large dynamic range of intensities encountered in this experiment. System linearity and the rejection of spurious reflections were given considerable attention. The resulting measurements of the output at 428 nm from the 1.5-m device operating as a single-pass laser, optically self-excited from spontaneous radiation, are shown in Fig. 1. The device aperture was 1.5 cm^2 and the output beam divergence was about 6 mrad. No optics of any kind were present in the system and the output windows were antireflection coated to avoid any spurious directionality which might have been introduced by possibly fortuitous reflections.

The data present in Fig. 1 show both the output detected in the direction of propagation, denoted as "forward" with respect to the direction of travel of the breakdown

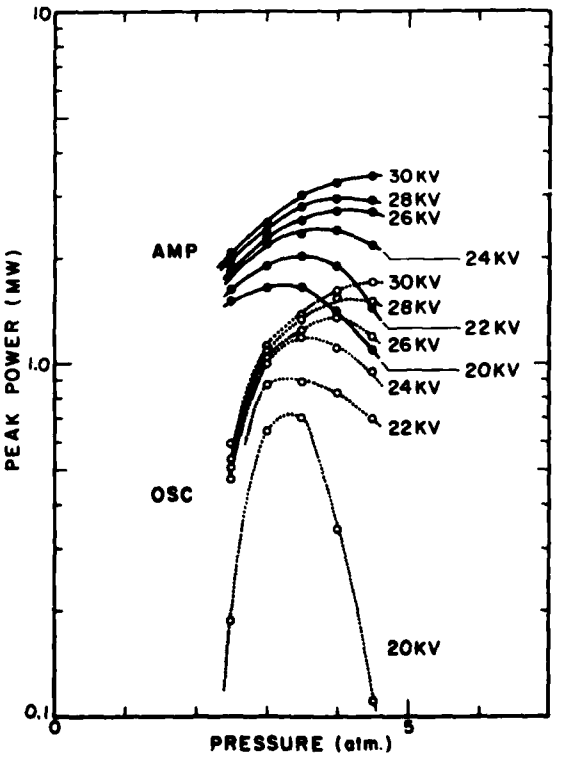

FIG. 2. Peak power outputs at 428 nm emitted from the helium-nitrogen plasma excited by the 7-segment traveling-wave discharge device plotted as functions of the pressure of the helium mixture containing 0.15% N_2. Outputs in the forward direction are shown by dotted curves for the use of the device as a single-pass laser and by solid curves for its use as an optical amplifier excited by the injection of 100 kW cm^{-2} peak input power.

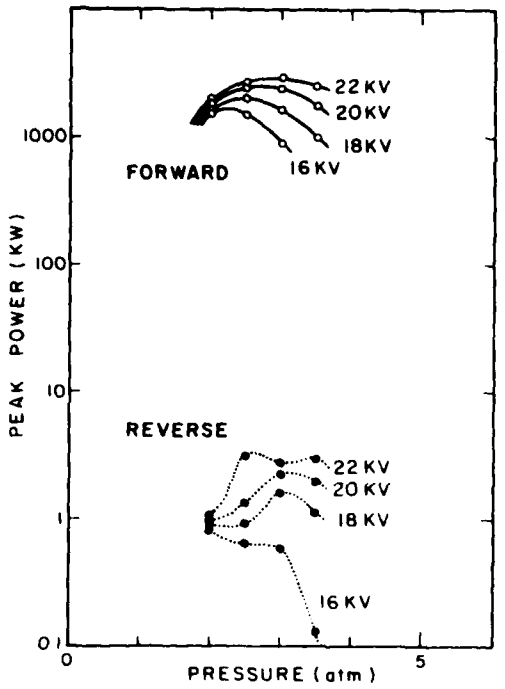

FIG. 3. Data from the 21-segment device presented as in Fig. 1.

wave, and the counterpropagating output labeled as "reverse." Directionalities at megawatt levels of output can be seen to have been of the order of 200 : 1. At the highest levels of excitation attempted with this device directionalities are shown to have dropped to about 20 : 1. It is interesting to estimate the gain of a single section under these conditions under which the directionality was degraded. The saturation intensity has been reported to have been $I_s = 58$ kW cm^{-2} under similar conditions.[9] If reasonably early saturation were assumed, the output intensity would be expected to be $I = I_s \gamma L$, where γ is the small signal gain for the transition and L is the length of the active discharge. In this case a solution for γL would give 17.2, which, when divided by the number of segments, would imply a logarithmic gain of about 2.5 per segment. This seemed inconsistent with the 60-kW level of power detected in the reverse case under the worst conditions shown in Fig. 1, and suggested that the assumption of an early saturation of the transition might have been optimistic. This is turn suggested the use of the 1.5-m plasma as a traveling-wave amplifier (TWA).

Figure 2 shows the increase in output power obtained from the use of the same 1.5-m system as a TWA excited by the injection, into the appropriate end of the device, of 100 kW cm^{-2} at 428 nm obtained from another nitrogen ion laser. These outputs were not sensitive to small changes in the input power, thus implying that under these conditions the optical transition was indeed saturated throughout the length of the amplifier. This higher value of output is consistent with a gain per section of $\sim \exp(4.1)$, a value more nearly in agreement with the magnitude needed to explain the relatively large counterpropagating output seen in the worst case in Fig. 1. It is interesting to note that the divergences of the beams obtained from the TWA mode of operation were reduced to the 2-mrad. value characteristic of the oscillator input.

Figure 3 presents the results obtained with the 5-m system operated under conditions of insufficient excitation to permit any single segment to amplify significantly in the reverse direction. As in the case of the data shown in Fig. 1, the device was run as a single pass, self-excited laser. Because of the greater length, the beam divergence was of the order of 2 mR. It can be seen that front-to-back ratios exceeding 1000 : 1 were achieved over a variety of operating conditions. In terms of pulse energy the directionalities were much greater than seen in Fig. 3, because the pulses in the reverse direction were of the order of 1 nsec or less in duration in comparison to the forwardly propagating outputs of 7–8-nsec duration.

It appears that as a consequence of this work, the use of traveling-wave excitation of larger aperture amplifiers offers an attractive means for overcoming the natural limitations on the scale of short pulse lasers. In addition, the same approach provides the facility for tailoring the temporal shape of the output pulse to meet specific requirements should they arise.

ACKNOWLEDGMENT

The authors wish to gratefully acknowledge the support provided by ONR Contract No. N00014-77-C-0168.

[1]C.B. Collins, A.J. Cunningham, S.M. Curry, B.W. Johnson, and M. Stockton, Appl. Phys. Lett. **24**, 477 (1974).
[2]C.B. Collins, A.J. Cunningham, and M. Stockton, Appl. Phys. Lett. **25**, 344 (1974).
[3]V.N. Ishchenko, V.N. Lisitsyn, A.M. Razkev, and V.N. Starinskii, JETP Lett. **19**, 233 (1974).
[4]C.B. Collins, Final Technical Report No. UTDP-ML-06, Contract No. N00014-76-C-0174 (The University of Texas at Dallas, March, 1977).
[5]C.B. Collins, J.M. Carroll, F.W. Lee, and A.J. Cunningham, Appl. Phys. Lett. **28**, 535 (1976).
[6]C.B. Collins, J.M. Carroll, and K.N. Taylor, J. Appl. Phys. **49**, 5093 (1978).
[7]C.B. Collins, J.M. Carroll, and K.N. Taylor, SPIE J. **168**, 363 (1979).
[8]C.A. Brau, in *Excimer Lasers*, edited by C.K. Rhodes (Springer, Berlin, 1979), Springer Series on Topics in Applied Physics, Vol. 30, pp. 110–126.
[9]C.B. Collins, J.M. Carroll, and K.N. Taylor, Appl. Phys. Lett. **33**, 175 (1978).
[10]J.D. Shipman, Appl. Phys. Lett. **10**, 3 (1967).
[11]B. Godard, IEEE J. Quantum Electron. **QE-10**, 147 (1974).
[12]C.B. Collins, U.S. Patent No. 4 053 853 (Oct. 11, 1977).

An atomic-fluorine laser pumped by charge transfer from He_2^+ at high pressures

C. B. Collins, F. W. Lee, and J. M. Carroll
Center for Quantum Electronics, The University of Texas at Dallas, Box 688, Richardson, Texas 75080

(Received 10 April 1980; accepted for publication 2 September 1980)

Scalable laser output at high powers has been obtained from the quartet system of atomic fluorine when excited by charge transfer from He_2^+ in a traveling-wave discharge.

PACS numbers: 42.55.Fn, 42.60.By

The discovery of a new charge transfer laser system is described in this report. Ever since the first successful demonstration[1-3] of the nitrogen ion laser pumped by charge transfer from He_2^+, it had been realized that other similar systems offered the possibilities of higher efficiencies and broader selections of wavelengths. Stimulated emission had been demonstrated[1,4,5] almost simultaneously from N_2^+, CO^+, and He_2^* as a result of collisional pumping from He_2^+ in about equivalent amounts, but only the N_2^+ was made to lase successfully,[6-11] although the systems appeared kinetically equivalent. This inability to realize a straightforward extension of proven techniques to analogous systems finally motivated a detailed study of the kinetics of charge transfer from[12,13] He_2^+, from[14] Ar_2^+, and from[15] Ne_2^+, with a wide variety of others species present in atmospheric pressures of diluents.

In the course of the extension of these studies to the reactions with electronegative gases, strong selective excitation of the quartet system of atomic fluorine was observed to result from a charge transfer reaction of He_2^+ with species traceable to F_2. The spectral lines excited in this way were completely different from the doublet lines which had been excited in atomic-fluorine lasers previously operated at relatively low pressures. For these quartet species a direct application of the nitrogen ion laser techniques at diluent pressures of several atmospheres did succeed in achieving laser outputs at levels of power and efficiency comparable to those obtained in the analogous N_2^+ system. Those efforts and results lie at focus of the work reported here.

The strong correlation between the populations of He_2^+ and the intensities of the spontaneous emission of components of the quartet system of atomic fluorine produced in plasmas of fluorine diluted in atmospheric pressures of helium were initially observed with *e*-beam excitation. From experimental measurements of the time dependence of the He_2^+ ions in the early afterglow period following the termination of the *e*-beam discharge, the destruction frequencies ν, of the populations were determined directly from the relationship

$$\nu \equiv [He_2^+]^{-1} \frac{d}{dt}[He_2^+] = \frac{d}{dt}(\ln [He_2^+]), \qquad (1)$$

as described previously.[12,13] Generally such destruction frequencies were constant over a time interval sufficient for the loss of about one order of magnitude of the population of ions. The open circles in Fig. 1 show the values obtained experimentally as functions of the diluent pressure for various partial pressures of fluorine. The results for 0 mTorr of reactant were obtained from Refs. 12 and 13. The linear approximations to these data shown in Fig. 1 are consistent with the parameterization

$$\nu = \nu_0 + 1.0\times10^{-9}[F_2] + 5.9\times10^{-29}[F_2][He], \qquad (2)$$

where brackets denote concentrations and ν_0 is the rate at which intrinsic losses of He_2^+ occurred that were not related to reactions with the added species. According to the usual interpretation[12,13] the remaining terms describe the bimolecular and termolecular reactions of He_2^+ with F_2.

Also plotted in Fig. 1 by the + symbols are the destruction frequencies obtained in the same way as in Eq. (1) from the fluorescence measured in the red region of the spec-

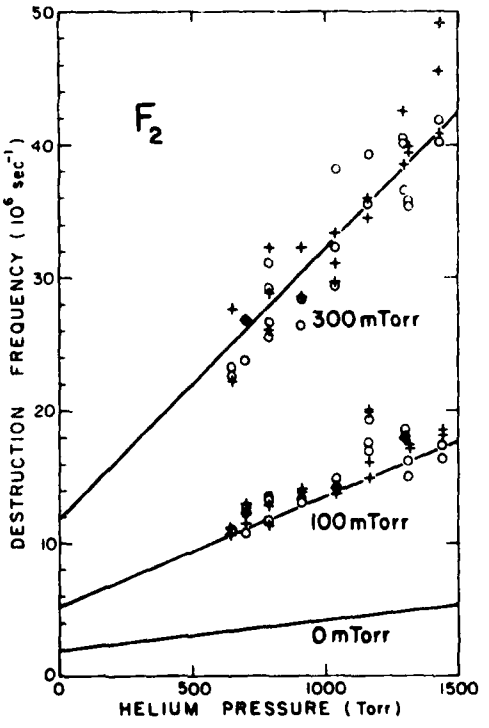

FIG. 1. Destruction frequencies measured for the important populations as functions of the pressure of the helium diluent and parametrically as functions of the partial pressures of the F_2 reactant: O, He_2^+ populations; +, $F^*(3p\,^4P^0_{5/2})$ populations as determined from fluorescence at 740 nm.

 0003-6951/80/220857-03$00.50

trum from transitions in the quartet system of F. The particular data shown in Fig. 1 corresponds to the transition $3p\ ^4P^o_{5/2} \rightarrow 3s\ ^4P_{3/2}$ at 739.9 nm. Because of rapid quenching of the upper level, these apparent destruction frequencies should have described the occurrence of the rate-limiting step in the kinetic sequence populating the $3p\ ^4P^o_{5/2}$ upper level. The strong correlation between the fluorescent intensity at 740 nm and the He_2^* population can be clearly seen to persist over a fairly wide range of variations of the experimental parameters, and this seems to imply a persistent causitive relationship rather than fortuitous coincidence. For example, the inverse lifetimes for the other potential energy donors,[16,17] He* and[18,19] He_2^*, in similar plasmas involving other reactants have been shown to be quite distinct and uncorrelated with each other and with the destruction frequency of He_2^*.

The fact that the principal fluorescence observed at visible wavelengths radiated from a transition in neutral atomic fluorine attests to the presence of a charge neutralization step in the pumping sequence, but one which did not lead to the production of energy storing species with lifetimes differing perceptably from those of He_2^*. This seemingly narrows the field of kinetic sequences to a few relatively straightforward possibilities. One could invoke the ion-ion recombination of F_2^* with F , but this reaction is endothermic for the production of the observed quartet state by 2.0–2.1 eV. Dissociative recombination of F_2^* with electrons would seem to be a minor channel because of the relatively small ratio $[e]/[F\ ]$ which might be expected in such a plasma. Almost by elimination, the most plausible kinetic scheme appears to be

$$F_2 + e \rightarrow F\ + F, \tag{3a}$$

$$He_2^* + F\ \rightarrow F^*(3p) + 2He, \tag{3b}$$

where the upper radiative level is directly pumped by the ion-ion recombination of He_2^* and F . Such a process may be considered to be a charge transfer reaction between He_2^* and the negative ion F . A two-electron process is implied by (3b) with one $2p$ electron of F being transferred to the He_2^* and another being promoted to the $3p$ orbital by the excess energy. This is quite similar to the type of two-electron jump required in any charge transfer process and does not violate the Wigner spin rule because of the mixed coupling schemes involved. Not only is the thermochemistry of this reaction sequence more favorable than for other alternatives, but reaction (3b) is essentially resonant if the total internal energy of the reactants on the left is reduced by the Coulomb energy of attraction along the reaction coordinate that is unavailable for rearrangement as internal energy at large internuclear separations. The transitions at 740 and 755 nm that were strongly enhanced in the e-beam afterglows originated on the common $F(3p\ ^4P^o_{5/2})$ state which is the lowest-energy state of F having an excited $3p$ electron. A resonance for the direct excitation of that level would correspond to a reduction of the internal energy of the reactants equivalent to the Coulombic energy at a separation of the order of 0.65 nm. The direct excitation of the highest-energy quartet $3p$ state $^4S^o_{3/2}$ would occur resonantly at 0.76 nm.

These considerations would imply that reaction (3b) proceeded through a pseudocrossing occurring at the order of distance which is of a plausible size.

It is not unreasonable to assume that in these experiments the concentraiton [F] was simply proportional to the product of electron density and fluorine concentration $[F_2]$. Because of the pressure-dependent stopping power of helium for the e beam, $[e] \propto [He]$. Then the concentration of F might be expected to have been $[F\ ] \propto [F_2]\,[He]$. In that case the reaction frequency for the loss of He_2^* due to the production of F would take the form $k_{3b}[F\ ] = k_{eff}[F_2]\,[He]$ in agreement with the termolecular part of the destruction frequency expressed empirically in Eq. (2). A bimolecular part could have been contributed by other concurrent reactions of He_2^* with F_2 that would represent loss processes in the pumping sequence. Thus the kinetic efficiency would be expected to have been no greater than the ratio of the rate for the occurrences of the termolecular part of Eq. (2) to the bimolecular part. This would give a kinetic efficiency of the order of 70% at pressures around 2 atm.

Much weaker fluorescence was observed from the high-energy $3p$ doublet states. From Eq. (1) much slower lifetimes, which were suggestive of He*, were found for the sources of these populations. The same slow lifetimes were also seen in the quartet intensities at very late times following the disappearance of the strong initial source interpreted as being the reaction of Eq. (3b). This seems to imply that both doublet and quartet states were excited rather weakly by He*, while only the quartet lines benefitted from the faster, more intense pumping obtained from He_2^* at early times. A possible anomaly was found in the line near 731 nm, which showed the quartet behavior but which could have been either a doublet line at 731 or a quartet line at 733 nm.

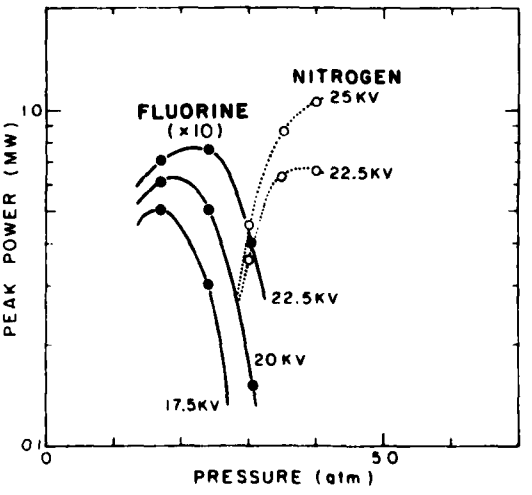

FIG. 2. Pressure and voltage dependence of the peak power outputs emitted from a 1.5-m-long traveling-wave laser pumped by charge transfer from He_2^*: ●, red lines emitted from quartet $3p$ states of F^* excited in helium containing 0.2% F_2. Output powers have been multiplied by a factor of 10 for convenience in presentation. O. The 428-nm line emitted from N_2^* excited in helium containing 0.15% N_2.

Laser output has been reported previously[20-22] from only the doublet transitions. Peak powers of 10 W were reported[21] and operation seemed limited to low pressures of tens of Torr. Scaling studies at very high levels of excitation[20] for pressures near 100 Torr produced some success, raising peak powers to ~70 kW from the doublet lines. The principal step pumping those doublet transitions was inferred[22] to be predissociation of HeF* produced from He*. Because the latter species does not tend to predominate at high pressures, the possibilities for successfully scaling that system to high powers and efficiencies seemed remote.

Charge transfer pumping of the quartet system presents a completely different prospect. The general similarity of the kinetics to those of the nitrogen ion laser suggested immediately that similar successes could be achieved with the quartet fluorine system, through the use of the same type of devices already optimized for the N_2^+ laser. Figure 2 shows the results obtained by exciting atmospheric pressures of helium containing 0.2% F_2 in a preionized, traveling-wave discharge device similar to one developed[11] for the nitrogen ion laser. Comparative results were obtained from helium-nitrogen mixtures containing 0.15% N_2. The pulse widths were generally about 8 nsec for the fluorine lines and 5 nsec for the N_2^+ output at 428 nm. No optics were used in obtaining these outputs, and the powers measured from the fluorine system were divided between at least five major lines of the quartet system. The 740- and 755-nm quartet transitions were the most intense, emitting about 70% of the power, which was divided between them in roughly equal proposition. The majority of the remaining power was found in transitions from the other quartet $3p$ states, $^4S^0$ and $^4D^0$. The line at 634.8 nm, corresponding to the transition $3p\ ^4S^0_{3/2} \rightarrow 3s\ ^4P_{3/2}$, contained about 27% of the power, and the remaining 3% was distributed within the $3p\ ^4D^0 \rightarrow 3p\ ^4P$ complex near 686 nm that was difficult to examine in detail because of the insensitivity of the detector in that wavelength region. Lesser fractions of the output were found in the lines near 730, 713, and 697 nm. Since the timing of the traveling-wave discharge had been optimized for the N_2^+ output, the directionality obtained in helium-fluorine mixtures was only 10:1, in contrast to the much greater front-to-back ratios usually obtained with the nitrogen mixture.[11]

Although these first outputs obtained from the quartet fluorine system are an order of magnitude lower than those characteristic of the N_2^+ system, their distribution between competing transitions implies that they are far from saturated. It seems that the actual potential of this system can be determined only through the use of an oscillator-amplifier configuration, so that a single transition can be saturated. Since the possible transitions from the $3p$ quartet states comprise 18 lines spanning a range of wavelengths from 624 to 757 nm, such an approach would also offer a wide selection of output wavelengths.

From the kinetics it appears that the quartet atomic-fluorine laser pumped by charge transfer from He_2^+ holds an even greater potential than the analogous N_2^+ laser for the development of scalable high-power output at high efficiency. Already this pumping channel has improved output efficiencies available in this wavelength region over those obtained previously from the doublet atomic-fluorine laser excited by He*. If the potentially high kinetic pumping efficiency can be demonstrate in large systems operated as pulse amplifiers, then the development of fluorine charge transfer lasers with overall efficiencies of 1–2% should be possible.

The authors gratefully acknowledge the support of this work provided by NSF Grant ENG-7816930 and the equipment provided by ONR Contract No. N00014-77-C-0168.

[1]C. B. Collins, A. J. Cunningham, S. M. Curry, B. W. Johnson, and M. Stockton, Appl. Phys. Lett. **24**, 477 (1974).
[2]C. B. Collins, A. J. Cunningham, and M. Stockton, Appl. Phys. Lett. **25**, 344 (1974).
[3]V. N. Ishchenko, V. N. Lisitsyn, A. M. Razkev, and V. N. Starinskii, JETP Lett. **19**, 233 (1974).
[4]R. A. Waller, C. B. Collins, and A. J. Cunningham, Appl. Phys. Lett. **27**, 323 (1975).
[5]C. B. Collins, A. J. Cunningham, S. M. Curry, B. W. Johnson, and M. Stockton, Appl. Phys. Lett. **24**, 245 (1974).
[6]C. B. Collins, University of Texas at Dallas Final Technical Report No. UTDP-ML-06 (unpublished, 1977).
[7]C. B. Collins, J. M. Carroll, F. W. Lee, and A. J. Cunningham, Appl. Phys. Lett. **28**, 535 (1976).
[8]C. B. Collins, J. M. Carroll, and K. N. Taylor, J. Appl. Phys. Phys. **49**, 5093 (1978).
[9]C. B. Collins, J. M. Carroll, and K. N. Taylor, in Proceedings International Conference on Lasers, 1979 [SPIE J. **168**, 363 (1979)].
[10]C. B. Collins, U. S. Patent No. 4,053,853 (1977).
[11]C. B. Collins and J. M. Carroll, J. Appl. Phys. **51**, 3017 (1980).
[12]F. W. Lee, C. B. Collins, and R. A. Waller, J. Chem. Phys. **65**, 1605 (1976).
[13]C. B. Collins and F. W. Lee, J. Chem. Phys. **68**, 1391 (1978).
[14]C. B. Collins and F. W. Lee, J. Chem. Phys. **71**, 184 (1979).
[15]C. B. Clllins and F. W. Lee, J. Chem. Phys. **72**, 5381 (1980).
[16]F. W. Lee and C. B. Collins, J. Chem. Phys. **65**, 5189 (1976).
[17]C. B. Collins and F. W. Lee, J. Chem. Phys. **70**, 1275 (1979).
[18]F. W. Lee and C. B. Collins, J. Chem. Phys. **67**, 2798 (1977).
[19]F. W. Lee, C. B. Collins, L. C. Pitchford, and R. Deloche, J. Chem. Phys. **68**, 3025 (1978).
[20]I. J. Bigio and R. F. Begley, Appl. Phys. Lett. **28**, 263 (1976).
[21]L. O. Hocker and T. B. Phi, Appl. Phys. **29**, 493 (1976).
[22]L. O. Hocker, J. Opt. Soc. Am. **68**, 262 (1978).


FILMED
4-8